RADIATION EFFECTS IN PHOTONIC MODULATOR STRUCTURES

Charles Barnes

Jet Propulsion Laboratory
California Institute of Technology
Pasadena, CA 91109

and

Roger Greenwell

Science & Engineering Associates, Inc.
San Diego, CA 92108

ABSTRACT

A review is given of the effects of radiation on various photonic modulator materials and devices including polymer-based structures, insulator-based devices, semiconductor-based devices and spatial light modulators. We conclude by providing recommendations for further work in the area of radiation effects in photonic modulators.

2. INTRODUCTION

Our purpose in this paper is to assess the technology of active photonic modulators from the point of view of radiation hardness assurance (RI-IA). We will briefly review photonic modulators by examining the characteristics of four categories of devices: polymer-based modulators, insulator-based modulators, semiconductor-based modulators and spatial light modulators (SLMs). For each of the first three categories we will begin by listing the advantages and disadvantages, without regard to RHA, then very briefly examine operating characteristics, and finally focus on the issue of RHA for each class of modulator. In the case of SLMS, because there is such a wide variety of these devices, we employ the basic feature of spatial light modulation as a common characteristic, irrespective of the material type, and examine a sampling of such device types, and then consider the issue of radiation effects *in* SLMS.

A basic requirement of all active modulator types is the necessity for modulating an information-containing light beam using some controllable external parameter. This may be the light beam itself, a second control light beam, an acoustic wave, *or*, most commonly at this point in time, an electric field, all of which are used to modify the refractive index and/or the absorption spectrum of the material. Thus, one of the most important properties of a potential modulator material is the strength of the electro-optic (EO) effect. In Table 1 below, we summarize EO coefficients for various materials used to construct modulators.

Table 1. Electro-optic coefficients of various materials used for modulators.

Material	Electro-optic coefficient, r... pm/V
GaAs	$r_{41} = -1.5$
InP	$r_{41} = -1.4$
KDP	$r_{41} = 8$, $r_{63} = 11$
$LiNbO_3$	$r_{33} = 30.8$, $r_{51} = 28$, $r_{13} = 8.6$, $r_{22} = 3.4$
2-methyl-4 -nitroaniline	$r_{11} = 67$
SiO_2	$r_{41} = 1.4$, $r_{11} = 0.6$
Monoazo nitroamine diepoxide- 1 and amino benzylamine-2 in tetrohydrofuran	$r_{33} = 32$
Polyimide-containing dye, DCM	$r_{33} = 4.1$
4-nitrophenol in photolime gel	$r_{33} = 10$ to 40

3. POLYMER-BASED MODULATORS

Introduction

Polymers represent a particularly exciting material class for the manufacture of waveguides and electro-optic (EO) modulators. In addition to having attractive EO properties, polymers possess a demonstrated compatibility with many types of other material technologies, including III-V semiconductors [1–3] and Si [1,3--8]. These attractive features, along with the general dramatic growth in work on optical systems and modulators, noted by Jabr [9], have led to a wide variety of demonstrations and research accomplishments in the use of polymers as waveguides and EO modulators [1–1 9].

The important features of polymers that result in this class of materials being well-suited to waveguide and EO modulator applications include the following:

1. Compatibility with a variety of substrate materials including Si, GaAs, glass, metals and plastics [1].
2. Polymer waveguide fabrication compatible with Si VLSI process fabrication technology [5].
3. Various waveguide shapes easily defined with standard photolithographic techniques [1-3,5,8].
4. Polymer waveguide layers easily stacked on top of one another [5].
5. Very low dielectric constant which allows for very high speed operation [1-5].
6. Easily defined large area multiple guiding regions [3].
7. High waveguide packing densities [3,5].
8. Low waveguide propagation losses (<0.1 dB/cm) [3].
9. Low, CMOS-compatible drive voltages [5].
10. Refractive indices at optical and RF frequencies are comparable allowing good velocity matching in microwave-optical modulators [4,6].
11. Low cost, low temperature fabrication [3,5,8].

While there are many advantages to polymer EO modulators, at the present time there are also disadvantages which include the following:

1. Polymer EO modulator technology is very new and is changing and evolving rapidly.
2. Commercial off-the-shelf polymer EO modulators are not yet available.
3. Structural and optical properties of polymers can be sensitive to the external environment.
4. For EO modulators, the poling of the polymer, necessary to establish strong EO properties, is sensitive to environmental effects, especially high temperature [3,6,8, 13, 19-22].

Materials/Operating Characteristics

A variety of polymers have been used to fabricate thin film waveguide and EO modulator materials and devices. In the case of waveguides where electro-optic modulation is not required, the fabt ication consists of deposition, patterning and waveguide definition through implementation of appropriate refractive index variations. Deposition can be done in a variety of ways including dipping, roller coating, spraying or most frequently, spin coating onto a variety of substrates [1]. Patterning and area definition of waveguides are easily accomplished with standard photolithographic techniques. Some of the more successful recent polymer waveguide fabrication techniques include photolime gel polymers used to construct complex structures, such as channel waveguide arrays that allow wavelength division multiplexing (WDM) at 12 different wavelengths [2,3], as shown below in Figure 1; polyamides of various types [7,23-29]; polyphenylene [17]; and crosslinked liquid acrylate monomers [21].

Similar materials have been used to construct polymer electro-optic devices with the additional requirement of inducing a large enough EO effect to allow the resulting structure to function as an EO modulator. Strong second order nonlinear electro-optic effects (Pockels effect) are usually achieved by doping the host polymer with an appropriate dipolar molecule, and poling the polymer so that it is noncentrosymmetric with the molecules aligned to form a uniaxial, EO active material, [1,3-6,8,10,13,15,19,20,26,30]. The poling process is conceptually simple [31], but it is often difficult to achieve stable, optimum results in practice. The temperature of the doped polymer is raised to near the glass transition temperature, T_g, of the polymer and a DC electric field is applied to the film. The dipolar dopant molecules then align themselves in the direction of the electric field rendering the polymer noncentrosymmetric. The polymer is then cooled while still applying the electric field.

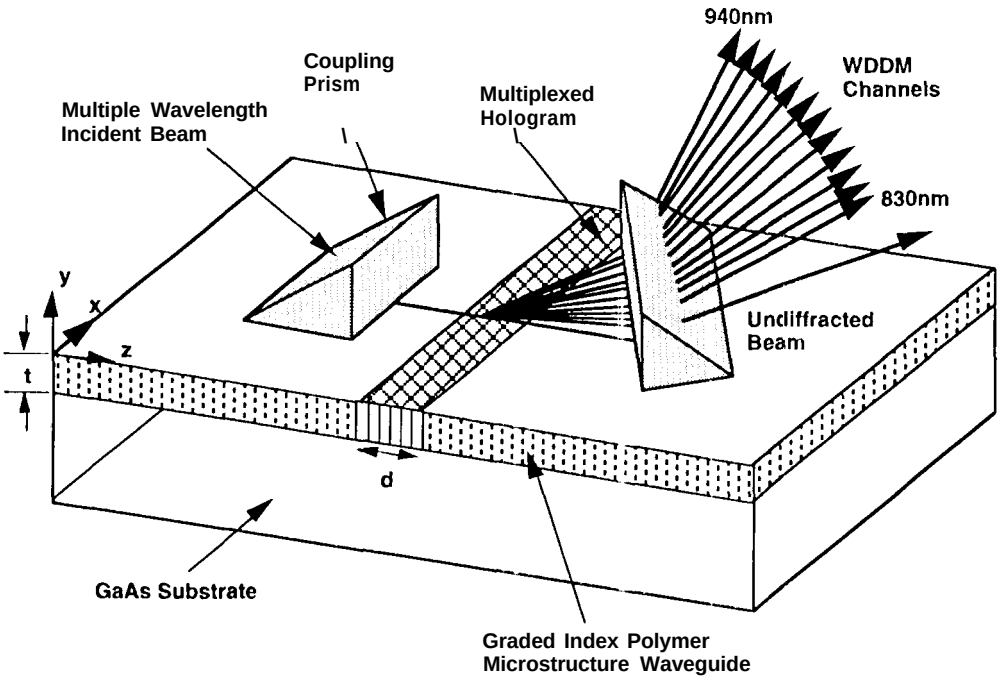

Figure 1. Implementation of a 12-channel single mode polymer waveguide wavelength division demultiplexing device on a semi-insulating GaAs substrate [3].

The dopant molecules used to achieve electro-optic effects must have appropriate characteristics which include the following:

1. The electronic structure and bonding must be such that the mole.cule is capable of responding to the electric field to achieve a preferred alignment.
2. The molecule must be physically and chemically compatible with the host polymer.
3. The molecule must not induce significant absorption at the operating wavelength of the polymer EO device/waveguide.
4. The poling field and temperature that are used must not damage the host polymer.
5. The molecule must be stable and maintain its electric field-induced alignment characteristics at the operating temperature of the EO device.

A review [19] of attractive dipolar dopant molecules that have been studied indicates a wide variety of useful molecules, many of which are quite exotic and specialized, Of the desirable characteristics listed above, the fifth is the most difficult to achieve and is responsible for impeding the development of practically useful polymer EO devices. With many combinations of polymer host/dopant guest molecules, the dopant molecules begin to lose their alignment and the material gradually returns to its pre-poled centrosymmetric state after some period of time. The closer the operating temperature is to the poling temperature, approximately equal to T_g, the more rapidly the EO effect decays away. The stability of the material system is dependent on exactly how the dopant is incorporated in the polymer and how the poling is done. Several techniques [32-38] have been tried to increase the stability of the poled material including choice of a polymer with a high T_g (the polyamides are attractive for this reason) [8]; maintenance of field and temperature for extended periods [32]; use of proper poling field polarity and gas ambient [20]; and use of cross-linking [3,6,35,36,38] or main chain incorporation of dopants [34,37].

Following waveguide formation and poling of EO-sensitive dopants in the polymer, light modulation can be achieved with either the second order EO effect (Pockels effect) using applied electric fields, or with the third order Kerr effect using high intensity light beams. In the first case, the applied electric field alters the refractive index which, in turn, causes a phase shift of the carrier light beam. For the Kerr effect, modulation is achieved by optical intensity-induced changes in the refractive index.

One of the more common types of modulators is the Mach-Zender (MZ) interferometer in which an incoming light beam is split between two branches and then recombined at the output of the device.. Schematic diagrams of the formation of a

nonlinear optical (NIX)), simple polymer-based MZ device are shown in Figure 2. At the top of Figure 2, we show the critical poling step with application of a large electric field at high temperature. As implied by the diagram, in many cases poling also serves to form the waveguide since the poled dopants induce a refractive index change. As shown at the bottom and right, an electrode is placed over one branch so that an electric field can be applied to cause a phase shift of the light beam in one of the branches. The phase shift in one beam then results in a modulation when the two beams arc recombined due to the interference between the beams. The voltage, $V_{a\pi}$, required to produce a phase change of π over the length of the electrode arm is given by

$$V_{a\pi} = \frac{\lambda}{n_z^3 r}\frac{g}{L} \tag{1}$$

where λ is the wavelength of the light, g is the distance between the electrodes, r is the EO coefficient and L is the length of the active region (see Figure 2) [39,40]. For a typical polymer, the approximate value of $\lambda/n_z^3 r$ at $\lambda = 1\mu m$ is

$$\frac{\lambda}{n_z^3 r} \approx \frac{1x10^{-6} m}{1.6^3 x30x10^{-12}\frac{m}{V}} \approx 8.1x10^3 \quad \text{volt s} \tag{2}$$

which results in an acceptable value of $V_{a\pi}$ if g/L is of the order of 10^{-3} or less, a thickness to length ratio that is easily achieved. The material properties of polymers, which easily allow the formation of very thin films, arc particularly well-suited to minimizing the g/L ratio.

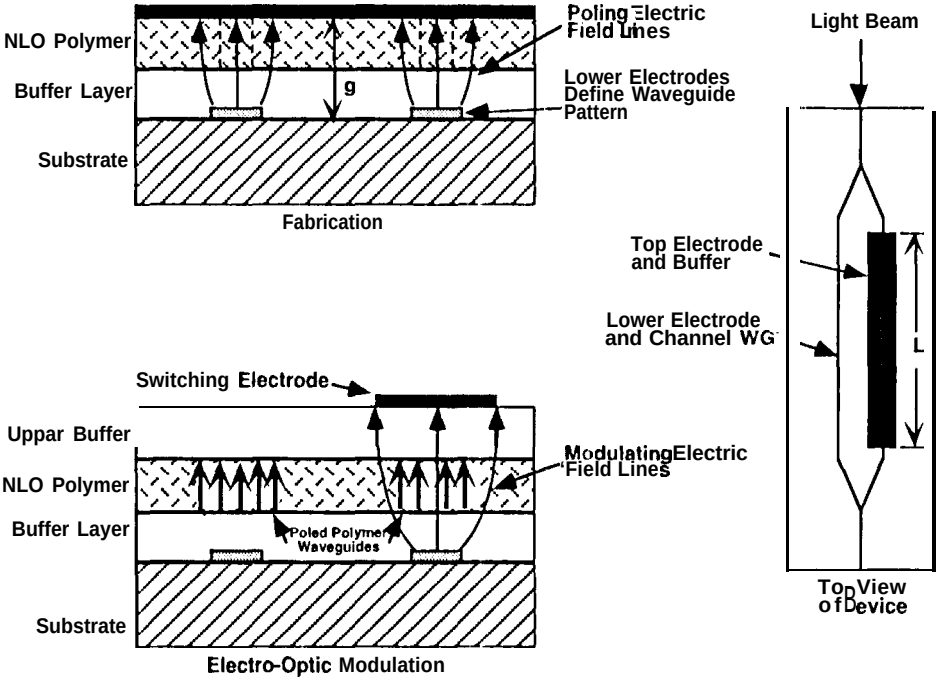

Figure 2. Fabrication of a simple Mach-Zender interferometer using poled polymer active wave guides [10].

Mach-Zender-like modulator structures have been fabricated with polymers by various workers [1,3-6,10,1 9]. An all-polyimide Mach-Zender modulator was constructed with an electrode length of 1.7 cm and operated at 200 MHz [5]. Because of the ease with which polyimide layers can be stacked, the authors successfully demonstrated a 3-level stack of MZ devices. Paul, et al [6] used thermosetting epoxies as a polymer host to fabricate phase modulators on Si substrates. Under the poling conditions used, the epoxy experienced additional curing resulting in a stable poled condition at room temperature. No change was observed in poled EO activity for more than a 1000 hrs at 85*C. Because the poling was effective and produced a large r_{33} value of approximately 32 pm/V, the value of V_π was less than 5 V and compatible with CMOS integrated circuits. in addition, the modulator was capable of operation at 18 GHz. In a similar modulator development effort, Teng, et al [4] were able to demonstrate device operation at 40 GHz. Other work [1] has also focused on the development of high bandwidth (20 GHz) modulators using poled polymer structures. Compared with $LiNbO_3$, polymer modulators are superior at the high bandwidths required for microwave modulation due to the fact that polymers have an optical refractive index equal to their microwave frequency refractive index, so that velocity (phase) matching in traveling wave microwave modulators can be nearly lossless in polymers.

General Radiation Effects in Polymers

Prior to specifically examining the work that has been done on radiation effects in polymer EO devices, we briefly review the more general subject of radiation effects of all types on polymer materials. One reason for this is that we wish to establish in general the susceptibility of polymers to these effects. This is necessary because to date, only limited work [41 ,42] has been done directly on the effects of radiation on polymer EO devices.

An extensive body of work in the literature [41-77] has established that the physical, chemical, electrical and optical properties of a wide variety of polymers are susceptible to radiation effects. Here the term "radiation" is intended to include not only particles, gamma rays and x-rays, but also UV and laser light. These effects range from major macroscopic effects such as laser-induced surface ablation [43-47] to the effects of ion bombardment on the electrical conductivity of polymers [48].

Much of the work on radiation effects is concerned with the use of radiation as a tool to modify the properties of a particular polymer. For example, UV light has been used to attach the EO-active dopant to the polymer matrix [5 1], and to create refractive index patterns in polyimide films doped with UV-sensitive benzoin type photosensitizers [52]. Other recently reported examples of radiation-induced modification processes include crosslinking of poly(tetrafluoroethylene) by x-rays and electrons [53], radiation-induced formation of diene, triene and tetraene from polyethylene in the presence of acetylene [54], electron irradiation-induced polymerization of fullerene (C_{60}) films grown on GaAs [55], electron irradiation-induced gelation of blends of polystyrene - polyvinyl methyl ether) [56], and gamma ray ir radiation and Xe and O ion implantation-induced grafting of styrene in poly(vinylidene fluoride) films [57]. Other studies [61-64] have shown that radiation can also alter the electrical conductivity of a polymer.

A variety of effects have also been observed in polymers as the result of ion bombardment [65-68]. Ion implantation with a variety of ions into poly(p-phenylene vinylene) films resulted in changes in both the electrical and optical properties of this material [65]. The absorption edge was found to shift from the UV toward the visible, an effect attributed to the narrowing of the band gap of the material. A doping effect on the conductivity was observed for low energy implants, but the magnitude was much smaller than the damage-induced increase in the conductivity. In a study [66] particularly relevant to this assessment, it was shown that ion implantation with H, Li and B caused an increase in the refractive index of polyallyldiglycol carbonate polymers. Typical results are shown in Figure 3. Thus, optical waveguides can be made by selective ion implantation into films of this material. The radiation damage-induced increase in refractive index was attributed to structural changes that were proportional to the amount of deposited energy. It has also been shown [68] that radiation damage can enhance the diffusion of heavy ions like Xe in a polymer film, thus also substantiating the radiation- nduced rearrangement of chemical species that can lead to structural modifications of polymers.

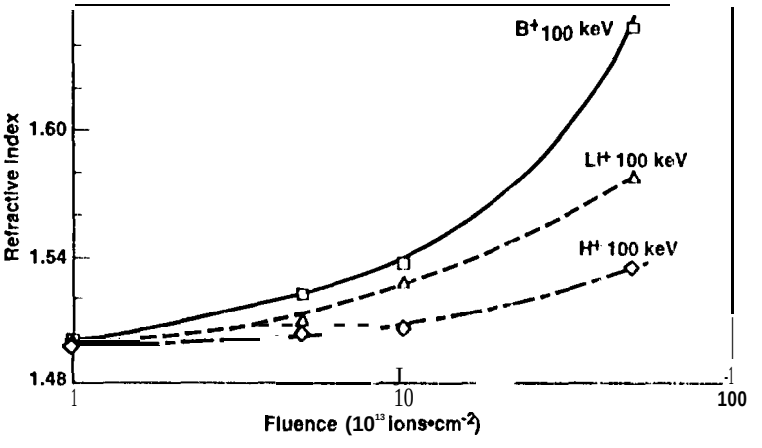

Figure 3. Refractive index variation induced by various ions implanted in polyallyldiglycol carbonate [66].

Several other studies [69-73] have emphasized the effects of radiation under natural space environment-like conditions and have shown that significant changes occur in the properties of polymers. For example, it was shown that exposure of poly(arylene ether)s to 1 MeV electrons while under high vacuum caused changes in molecular weight, solvent volubility and tensile strength [72]. Similar effects were observed after exposure of poly(methyl methacrylate) to x-rays in a vacuum *[73].*

Finally, we note that there also have been recent studies of the combined effects of radiation and other types of stress such as thermal heating [74-77]. Studies [74] have shown that combined heating and irradiation affect the refractive index of poly(p-xylyene) films, while exposure to visible light and heating causes phase transitions to occur in poly(N-isopropylacrylamide-co-chlorophyllin) gels [75]. In an interesting study [76], it was demonstrated that electron irradiation reversed the effects of physical aging of glassy polymers such as polystyrene, poly(methyl methacrylate) (PMM A) and polycarbonate. The extent of this "deaging" was proportional to dose and it was suggested that this phenomenon was due to radiation-induced internal gas evolution that produces an increase in free volume within the polymers.

These recent examples, together with a large body of work in the earlier literature, clearly attest to the general sensitivity of polymers to various types of radiation. Often the effects are positive as in the case of radiation-induced stabilization of a poled EO polymer. It is important to note, however, that in contrast with ionizing radiation effects in commercial Si MOS-based devices, relatively large radiation doses are required to cause significant effects in polymers. In spite of this, however, the use of these attractive materials in modulator applications in radiation environments must be accompanied by characterization studies which establish radiation hardness assurance guidelines for these materials and devices.

Radiation Effects in Polymer Modulator Materials

in the only studies [41,42] specifically y intended to determine the effects of radiat ion on electro-optic (EO) polymers, two types of EO polymers were examined before and after 3 MeV electron irradiation to a rnaximurn dose of 44 Mrad. The first type of polymer studied was a PMMA host doped with a guest chromophor e, Disperse Red 1 (DR 1) dye, while the second was a syndioregic cinnamarnide main chain polymer in which the EO active material is incorporated in the polymer main chain. Both polymers were poled near T_g, which was 95°C for the PMMA and 208°C for the main chain material.

In the first study [41], detection of the effects of electron irradiation was complicated by the fact that the temperature at which the samples were held was high enough to cause significant decay of the EO activit y over a period of days, especially for the PMMA samples. Thus, the poled state of the samples was not very stable. Following irradiation of the PMMA, additional decreases in the EO activity were observed. In the case of the main chain polymer, no effects of irradiation were seen at the maximum dose of 44 Mrads.

In subsequent work [42], accelerated aging of the EO activity was studied in unirradiated and electron irradiated PMMA/DR 1. At 94°C significant decay of the EO activity was observed in less than an hour, whereas in the first study similar changes required several days at room temperature. As shown in Figure 4, the rate of decay of EO activity at 94°C was observed to increase with electron dose. The authors suggested that this reduced stability after in adiation may be due to a lower glass transition temperature which results from polymer chain breakage since chain scission in PMMA under irradiation has been observed previously. We note, however, that our review of recent work has shown that radiation-induced crosslinking is widely observed, and in fact has been used to further stabilize the poled state rather than making it less stable. Thus, other types of polymers may behave differently than the PMMA/DR1. We also note that the doses required to cause significant changes in the behavior of the PM MA/DR1 were generally well above typical close requirements for most applications.

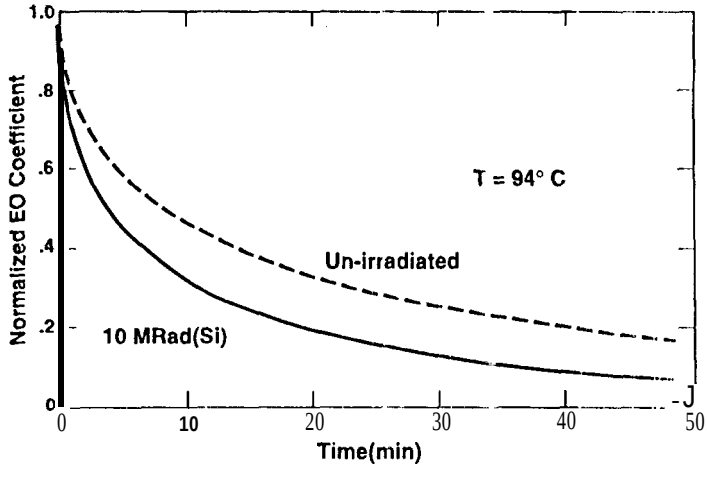

Figure 4. Decay of EO activity in PMMA/DR1 at 94°C for unirradiated and electron irradiated material [after 42].

4. INSULATOR-BASED MODULATORS

introduction

Although the Section heading is general, this Section is essentially devoted to an assessment of ferroelectric $LiNbO_3$ and $LiTaO_3$ materials and devices. Clearly, the development of optical modulators has been dominated until recently by $LiNbO_3$ in terms of both the longevity of research and development, and the variety of commercially available devices. However, there are still problems with this technology, and challenges to be met by continuing research. As recently as 1993, with regard to $LiNbO_3$, it was stated that "predictable and reproducible performance has been difficult to achieve and maintain, in spite of the fact that $LiNbO_3$ research goes back nearly 20 years" [78]. It is not a highly controversial statement to say that $LiNbO_3$ process technology will probably never reach the level of precision and control that has been achieved already by semiconductor process technologies. This, of course, is one reason why we suspect that ultimately the high level of recent research activity on semiconductor modulator structures will lead to a dominance over $LiNbO_3$ by these materials, especially in integrated devices where electronic digital functions are placed on the same chip as photonic functions. At the present time, however, $LiNbO_3$-based modulators have several advantages including:

1. Long history of research and development.
2. Commercially available devices.
3. Well-established electro-optic (EO) $LiNbO_3$ material processing techniques: Ti in-diffusion and proton exchange.
4. Large refractive indices and EO coefficients.
5. Refractive index easily increased with dopants facilitating waveguide definition.
6. Waveguide width, effective depth and peak refractive index change can be independently controlled with processing parameters.
7. Availability of large, optical quality Czochralski-pulled single crystal boules.
8. Highly stable poled ferroelectric single crystal domains in as-received boules. The high Curie temperature (1150°C) of $LiNbO_3$ means that the poled state of $LiNbO_3$ is more stable than that of the polymers discussed in the previous Section.
9. Minimum power usage when voltages are applied due to insulating nature of $LiNbO_3$ and $LiTaO_3$.

As we have noted, the $LiNbO_3$/$LiTaO_3$ EO technologies also have significant disadvantages, including the following:

1. Process technologies not as well-controlled as those for semiconductors.
2. Critical, unexplained materials issues, in spite of many years of research [78].
3. Difficult to grow thin films of proper quality for EO devices.
4. Incompatibility with semiconductor process technologies and digital/photonic integration with semiconductor devices on a single chip.
5. Device instabilities, especially for fabrication by the proton exchange process.
6. Detrimental pyroelectric and photorefractive effects. (These effects can be used to advantage, however, as in $LiNbO_3$ holograms [79].)

Materials/Operating Characteristics

We begin by briefly reviewing the pertinent characteristics of $LiNbO_3$ and $LiTaO_3$ materials and devices. More extensive discussions can be found in the literature [78,80,81]. Of the various metals that can be diffused into $LiNbO_3$ to form waveguides, Ti is the metal of choice, and Ti-diffused waveguides are found in the majority of $LiNbO_3$ EO devices. The advantages of Ti are as follows:

1. Ti can be patterned into any geometry using standard photolithographic methods,
2. Ti produces fairly large and approximately equal index changes for both the ordinary index, no, and extraordinary index, n_e [82]. At a wavelength of 0.63 μm, the change in n_e is nearly linear and varies as $\Delta n_e \approx 6 \times 10^{-3}$ for each % change in Ti weight concentration. The Ti-induced index change exhibits a small inverse dependence on wavelength [83].
3. Ti does not cause additional absorption of light in the visible or near IR [84].
4. The diffusion coefficient of Ti is large enough to allow the formation of tightly confining waveguides at reasonable diffusion temperatures and times, and does not depend on crystal orientation.

As one might expect with complex materials like $LiNbO_3$ and $LiTaO_3$, problems are encountered with Ti indiffusion and the resulting structures. The more prominent ones are as follows:

1. In z-cut (the "cut" refers to the direction perpendicular to the surface) $LiNbO_3$, domain inversion of the ferroelectric domains can occur requiring repoling of the material.
2. The pyroelectric effect is strong in $LiNbO_3$ resulting, in electric fields across the waveguides when temperature differentials are present [78].
3. During Ti diffusion, Li_2O outdiffusion can occur altering the optical properties of the waveguide [85].
4. Ti indiffused waveguides exhibit a strong photorefractive effect due to the presence of Fe impurities. This can be mitigated to some extent by MgO doping [86].
S. As a result of the high temperatures required to produce significant diffusion in reasonable times, Ti indiffusion cannot be used in $LiTaO_3$ because of its low Curie temperature (620°C) at which depoling of the domains can occur.

The high temperature, long diffusion time requirements for Ti indiffusion have provided considerable impetus to develop the low temperature proton exchange (PE) technique as a second method for producing tightly confining, high index waveguides. [87]. The basic chemical process for PE is the exchange of hydrogen ions and lithium ions between the source material and the Li(Nb or Ta)O_3. A variety of organic and inorganic acids have been used as H' sources, with benzoic acid being the preferred choice. The patterned substrate is immersed in an acid melt held at the temperature required to produce sufficient exchange in a short time, 150°C to 300°C for 5 minutes to an hour. The important advantages of the PE method are as follows:

1. Very large index changes.
2. Low temperature(150"C to 300°C) process.
3. Short waveguide formation times, of the order of minutes.
4. High resistance to the photorefractive effect.
S. Selectable polarization because only the extraordinary index, n_e, is increased.
6. Useful for $LiTaO_3$ whose low Curie temperature (620°C) precludes using a diffusion process.
7. Compatibility with standard clean room and semiconductor processing steps.

As is usually the case, these advantages are offset to some degree by the following disadvantages:

1. High propagation loss.
2. Significantly lower electro-optic (r_{33}) [88], acousto-optic [89], and frequency doubling [90] coefficients.
3. Instability in the refractive indices due to continuing movement of H^+ ions after waveguide fabrication [91].

These detrimental effects of the PE process can be partially or completely removed by annealing the crystal subsequent to proton exchange at 300C to 400C for a few hours [92]. Two undesirable effects of annealing are a minor reduction in the increase in extraordinary index, Ant, and a somewhat increased sensitivity to the photorefractive effect [93]. The generally positive effects of annealing on PE $LiNbO_3$ make it a contender for many applications where the properties of Ti:$LiNbO_3$ are not as appropriate.

Whether formed by Ti indiffusion or the PE process, the characteristics of the resulting waveguides determine the properties of the guided mode. For example, a compromise is often necessary between efficient fiber-waveguide coupling (large guided mode size), and minimum drive voltage (small mode size). In addition, fiber-waveguide insertion loss is a function of Ti metal thickness (Ti dopant concentration), as are the waveguide refractive index properties. The supported waveguide mode size exhibits a minimum as a function of the waveguide strip width. At a wavelength of 1.3 μm, the optimum waveguide strip width is approximately 5 to 7 μm.

The choice of electrode characteristics, including placement relative to the waveguides, is critical for the successful and efficient operation of $LiNbO_3$ devices. This is particularly true for high speed applications because, unlike the polymers, there is a large difference in refractive indices at microwave and optical frequencies for $LiNbO_3$ and $LiTaO_3$. Placement of the electrodes over or near the waveguides depends on the crystal orientation and the required bandwidth. As shown in Figure 5, in the case of z-cut devices the electric field must be perpendicular to the planar surface (in the z axis direction) in order to take advantage of the largest electro-optic coefficient, r_{33}. Direct placement over the waveguide necessitates the use of a buffer layer, usually $Si0_2$, between the electrode and the waveguide. For x- or y-cut $LiNbO_3$, shown at the bottom of Figure 5 for a single waveguide structure, the EO-sensitive z axis is parallel to the planar surface of the. device. Thus, the electrodes are placed on either side of the waveguide so that the fringing field is horizontal (parallel to z axis) as it passes through the waveguide.

The choice of electrode metal depends on the specific application, For most applications, aluminum electrodes are appropriate. However, for high bandwidth or microwave applications, gold has been the preferred electrode metal. Note, however, that for those radiation environment applications where there is a high prompt dose rate requirement, the high absorption cross section of Au for x-rays must be taken into considerate ion.

In addition to the electrode metal type, other stringent conditions must be imposed on electrodes for microwave applications of $LiNbO_3$ devices because of the difference in optical and microwave refractive indices. Generally, two types of electrodes are used for $LiNbO_3$ modulators and switches: lumped electrodes and traveling wave electrodes. The lumped electrode is simpler, but is restricted to a relatively low high-frequency cutoff because the device is limited by the KC time constant of the capacitance of the electrode configuration and the terminating resistor used to match the impedance of the source. The bandwidth-length product, AfL, for lumped electrodes is typically 2 GHz-cm [80]. Significant improvement in the bandwidth can be achieved by using traveling wave electrodes rather than lumped electrodes. The traveling wave. electrode is basically an extension of the microwave transmission line that is terminated in the same characteristic impedance as the microwave source line. In this case, the modulator bandwidth is limited by the difference in velocity between the microwave and optical signals. If the velocities are matched the optical signal experiences the same voltage over the length of the electrode. The dependence on velocity matching and hence on refractive index equivalence, has been shown [94] to be given by

$$\Delta fL = \frac{?C}{\pi(n_m - no)} \qquad (3)$$

where n_m is the microwave refractive index. For typical values of $n_o = 2.2$ and $n_m = 4.2$, $\Delta fL \approx 9.4$ GHz-cm. Note that as $(n_m - n_o)$ becomes small, the bandwidth-length product becomes large. An important issue for radiation applications will be whether or not radiation affects the two different refractive indices in the same manner.

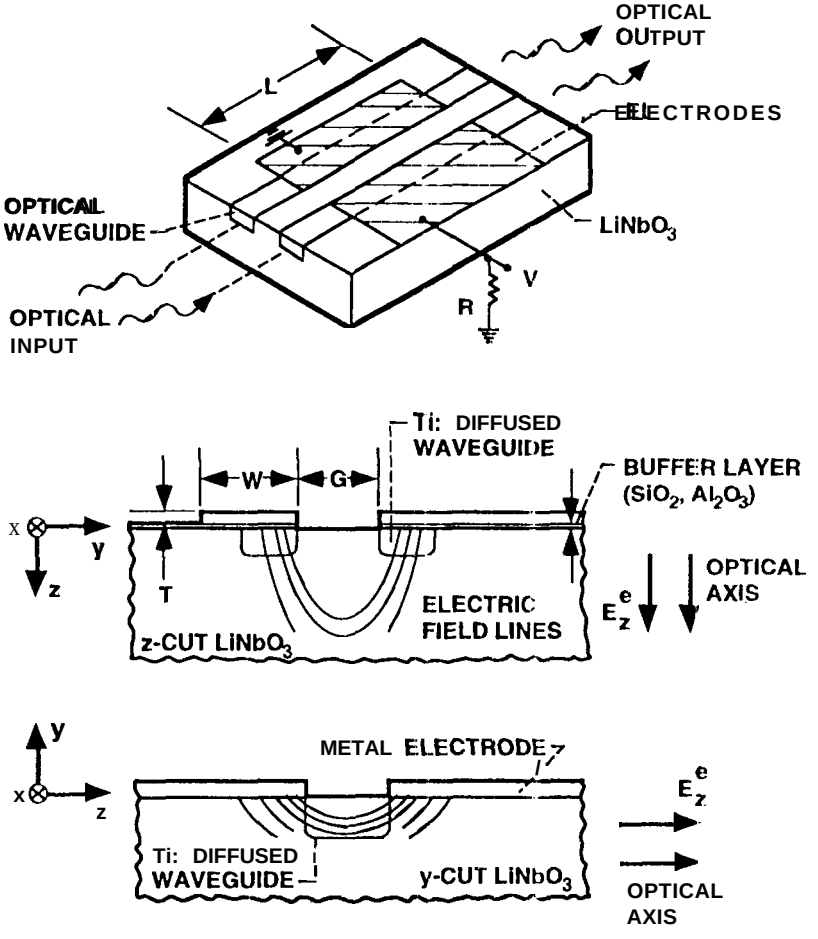

Figure 5. Top and middle: a simple dual waveguide coupler structure in z-cut $LiNbO_3$. Bottom: A single waveguide in y-cut material showing electric field parallel to optic axis that allows control by largest EO coefficient, r_{33} [9S].

We now wish to briefl y review representative types of lithium niobate modulator devices. From the point of view of this assessment, an important and basic $LiNbO_3$ device type is the directional coupler, because this device has been used as the vehicle for most radiation effects studies of $LiNbO_3$ modulator structures. A simple coupler structure is shown at the top of Figure 5. An important characteristic of a coupler is the strength of the coupling between the waveguides in the coupler. The coupling efficiency per unit length (coupling strength), κ, varies exponentially with waveguide gap size, G (see Figure 5):

$$\kappa(z) = \kappa_0(z)e^{-G/\gamma} \tag{4}$$

where κ_0 and γ both depend on waveguide parameters, such as Ti metal thickness, and γ is a measure of tbe evanescent decay length of the fundamental mode of the waveguide [78]. The coupling efficiency for the entire waveguide, that is, the fraction of the power transferred from the power input guide to the second, crossover waveguide, η, is given by [80,81]

$$\eta = \sin^2\left[\int_0^L \kappa(z)dz\right] = \sin^2(\kappa L), \text{ for } \kappa \text{ independent of z,} \tag{5}$$

where L is the length of the coupling region as shown in Figure 5. This equation applies to the synchronous case where there is no difference in propagation constant, β, (proportional to refractive index) for the two guides: $\Delta\beta$ = O; that is, where there is no application of an electric field to one of the guides to intentionally induce a phase shift. For the case of a nonzero $\Delta\beta$, such as a switched directional coupler, the coupling efficiency has the form

$$\eta = \frac{1}{1 + (\Delta\beta / 2K)^2}\sin^2 KL[1+(A\sim/2K)2]]'2 \tag{6}$$

Note that equation (6) reduces to the simpler form of equation (5) when $\Delta\beta$ = O. The form of equations (5) and (6) indicates that the coupling efficiency, η, is periodic in nature so that the power coupled into the second guide can vary periodically between zero and approximate y 100%. Complete coupling is achieved when $kL = n\pi/2$, where n is an odd integer. The smallest length for complete coupling, $L_{\pi/2} = \pi/2k$, has been shown to vary between approximately 200 μm and 1 cm for $Ti:LiNbO_3$ [96].

Operation of a directional coupler as a switch requires the application of a bias such that the electric field in one of the guides causes a $\Delta\beta$ that results in zero coupling, that is, η = O. The required change in propagation constant is given by [81]:

$$\Delta\beta = 2\sqrt{3}\kappa \tag{7}$$

Thus, as one might expect, the stronger the coupling efficiency between the guides, that is, the larger κ is, the greater change that is required in β to reduce the coupling from η = 1 to O through electric field-induced phase mismatch between the guides.

Because of the difficulties associated with matching up active coupler length, 1.., with $L_{\pi/2}$, and predicting the value of K in couplers fabricated in a production environment, it is best to design the switch so that both the on and off states are electrically controlled, and L does not have to precisely equal $L_{\pi/2}$. This is achieved in the reverse-$\Delta\beta$ directional coupler switch by splitting the electrodes into t wo pairs of electrodes with the opposite bias applied to the second pair [80] so that $\Delta\beta$ of the first pair = $-\Delta\beta$ of the second pair. Analysis of the coupling coefficients that apply to this case shows that for a given value of L not equal to an integer multiple of $L_{\pi/2}$, two values of $\Delta\beta$ can be found that will result in no crossover and in complete crossover between the waveguides [97]. This technique has been used successfully to fabricate switches with extremely low crosstalk [98], and in combination with traveling wave electrodes, high speed, low crosstalk switches [99].

Additional types of $LiNbO_3$ modulator structures which are important include the following:

1. Mach-Zender (MZ) interferometric switches and modulators. These well-developed, popular device types have already been mentioned in the previous Section. In contrast with the couplers discussed above, the arms are spaced wide enough apart so that there is no evanescent coupling between them. Although Figure 2 shows only a single electrode over one arm, in some cases two electrodes are used, one over each arm, while in other devices, three electrodes are used with a grounded electrode in the center between the arms. In either of these configurations, the field can be applied in opposite directions through the waveguides under the electrodes to achieve a push-pull effect on the phase change so tliat the net phase change is $2\Delta\phi$. For

the MZ switch, it can be shown that the output intensity is periodic with minima and maxima occurring at odd and even integer multiples of V_{π}. If the input optical field amplitude is not split exactly equally between the two arms, as is often the case, the minimum power out will be greater than zero, and the switch will not be completely off. The extinction ratio, defined as the ratio of maximum to minimum power outputs in dB, is then not infinite, but can be easily made to be greater than 10 to *20* dB.

2. **Polarization controllers,** Another important class of $LiNbO_3$ devices are those that alter or control the polarization of light beams. For example, TE (TM) to TM (TE) conversion can be accomplished using a single waveguide covered by interdigitated electrodes. The purpose of the alternating electrodes is to periodically change K to produce efficient coupling between modes that are highly mismatched [80]. The coupling of TE into TM, or vice versa, is accomplished by periodically altering K via one of the off-diagonal nonzero electro-optic coefficients such as r_{51}. For example, in x-cut $LiNbO_3$ with propagation in the y direction the TE mode is polarized along the transverse z direction and the TM mode is polarized along the x direction. The interdigitated electrodes lying directly over the waveguide then direct the electric field vertically in the x direction in alternate up-down directions as the light moves along the guide. It is noted that the spatial period of the electrodes is wavelength dependent: at λ = 0.6 pm, the period is 7 mm, while at $\lambda = 1.3\,\mu m$, the period is 18 mm [101]. The dependence on wavelength restricts the applicability of this technique [100,101]. In addition to TE to TM converters, a variety of polarization-selective devices have also been fabricated in $LiNbO_3$. One interesting approach is to take advantage of the fact that the proton exchange process significantly increases n_e, but causes a decrease in n_o [102], Thus, in z-cut $LiNbO_3$ on] y the TM mode is guided, resulting in a polarization selective device. Polarization splitters that spatially separate a mixed TE/TM light beam into pure TE and pure TM beams in two output guides have also been fabricated using Y-branch splitters, intersecting waveguides and directional couplers [80]. The ability to perform polarization separation depends on the fact that the coupling strength, K, is polarization dependent. This comes about because of the fact that the refractive indices for the TE and TM modes are different. Clearly, any radiation-induced changes in refractive index will affect the functionality of this class of modulators.

3. Polarization-insensitive devices. The polarization-selective devices briefly discussed above are necessarily sensitive to polarization so that they can achieve their functionality. However, there are applications where polarization-insensitive devices are also important, Because typical fibers do not preserve. polarization, the functional behavior of $LiNbO_3$ devices can vary as the polarization of the input beam varies. In many systems, this is an unwanted attribute. The variation with polarization arises because the orthogonal TE and TM components of a light beam experience different refractive indices in a birefringent, uniaxial crystal. In addition, the TE and TM polarizations will couple to applied electric fields through different electro-optic coefficients. For example, in y-cut, x-propagating material, the TE mode (z-axis) is sensitive to the extraordinary refractive index, n_e, and couples to the field, E_z, through the r_{33} coefficient, while. the TM mode (y-axis) is sensitive to the ordinary refractive index, no, and couples to E_z through the r_{31} coefficient which is 3 times less than r_{33}. Two approaches have been used to minimize the polarization dependence of switches and modulators [80]. In the first, the coupling strength, K, and/or the propagation difference, $\Delta\beta$, are made insensitive to polarization through appropriate device design. in the second approach, the device is fabricated so that the switch response is insensitive to polarization -induced changes in K or $\Delta\beta$. Using these approaches, several types of polarization-insensitive devices, both interferometers and couplers, have been successful y made [103- 105].

4. **Wavelength filters.** In advanced communication systems, devices that perform functions on the wavelength content and distribution of signal carrying light beams are valuable. A group of $LiNbO_3$ devices that fall in this class are wavelength filters. Important properties of these filters are the center wavelength, the bandwidth, the peak filter efficiency, the magnitude of side lobes and the ability to electrically tune the device [80]. As for other types of switches and modulators, wavelength filters have been fabricated as both couplers and interferometers [106]. Recalling that in a birefringent crystal like $LiNbO_3$ the refractive index of TE and TM modes varies with wavelength, the TE (TM) to TM (TE) mode converter can also be used as a wavelength filter. Since the conversion efficiency for a TE to TM mode converter depends explicitly on wavelength, by varying total lengths of the interdigitated electrodes one can vary the wavelength band pass of the filter. For example, wavelength bandwidths of 50 to 5 Å have been achieved in the visible with electrode lengths between 0.5 and 6 mm [6]. Tuning of the center wavelength of these mode converter wavelength filters is possible by using a third electrode that induces a field in another direction than the field used to achieve mode conversion [107]. Broadband, tunable wavelength filters can also be fabricated from directional couplers [79, 108]. To accomplish the wavelength filter function, the coupler is constructed of two waveguides each with a different width and refractive index, resulting in a different dependence of refractive index on wavelength in each waveguide. The coupler is designed so that at the wavelength of interest, λ_o, the two waveguides have equal refractive indices so that 100% coupling occurs at λ_o. Thus, the light at the center wavelength is coupled into the other waveguidc but other wavelengths are not. By applying a voltage to the electrodes the $n(\lambda)$ dispersion curves can be changed so that the crossover wavelength, λ_o, shifts, resulting in the wavelength tunability of the coupler. Typically, for L = 1.5 cm, $\Delta\lambda$ = 200 Å at $\lambda_o = 0.6\,\mu m$, and $\Delta\lambda$ = 700 Å at λ_o = 1.5pm with a tuning range of approximately 1600 Å[108].

S. **Lasers and** amplifiers. A particularly exciting class of devices that have been developed recently are rare earth doped $LiNbO_3$ waveguide lasers and amplifiers [90,92]. Laser action has been accomplished with Nd [109] and Er [11 O] doping of $Ti:LiNbO_3$, and Cr doping of proton exchanged $LiNbO_3$ [90], These devices are in an early stage of development and work has focused on the methods of incorporating the appropriate dopants at the required concentrations without compromising the waveguide properties of the Ti or PE $LiNbO_3$ [11 1,112]. Various methods of co-doping have been attempted because of the necessity of adding both the laser dopant (Nd or Er) and the waveguide forming dopant (Ti). in addition, it is advantageous to also dope with MgO to reduce photorefractive effects since lasers typically operate at high optical power levels. One fortuitous result of these studies is that diffusion of Er with Ti enhances the slow diffusion rate exhibited by Er alone [112]. An example of laser performance in PE $Nd:MgO:LiNbO_3$ is 14 mW of output power at 1.08 μm with a threshold pump power of 2.7 mW at a pumping wavelength of 0.814 μm [109]. In addition, integrated devices are now appearing that incorporate modulators with the laser structure. For example, a mode locked, 8 ps wide pulse train with a repetition rate of 6 GHz has been produced in a $LiNbO_3$ structure that incorporates a laser and a traveling wave phase modulator [11 3]. One can expect that in the near future there will be a rapid proliferation of this class of devices.

Our brief review of device examples demonstrates the wide variety of devices that have been fabricated in $LiNbO_3$ and $LiTaO_3$. It is important to also note that we have not examined any of the more complex photonic integrated circuits that have been built in recent years. Generally, these sophisticated devices are made up of the basic components we have briefly described above. In any case, a broad array of $LiNbO_3$ devices are available and it will be important to establish radiation hardness assurance for this class of components. We turn now to a review of radiation effects studies in $LiNbO_3$ and $LiTaO_3$.

Radiation Effects in $LiNbO_3$ and $LiTaO_3$

Of the three general material classes we are considering - polymers, insulators and semiconductors -by far the greatest number of radiation effects studies have been performed on modulator structures fabricated from the insulator materials, $LiNbO_3$ and $LiTaO_3$ [1 14-1 59]. We emphasize that this statement is only true if one does not include the large amount of radiation effects work that has been done on related 111-V semiconductor structures like LEDs, lasers, detectors, solar cells and digital devices. As we will see, however, most of the work on radiation effects in $LiNbO_3$ has been on relatively simple structures, basic materials and couplers without electrodes. Thus, much remains to be done in order to build on the present body of work.

Our review of materials and basic device operating characteristics suggests that one should expect that radiation would affect the operating characteristics of $LiNbO_3$ and $LiTaO_3$ devices. The waveguides in these materials are formed, whether by metallic indiffusion or proton exchange, by alteration of the impurity and defect distributions within the guiding region, These distributions should also be susceptible to alteration by the radiation-induced introduction of defects and by the trapping of radiation-generated electrons and holes at color centers in the guiding region, For example, optical radiation can cause changes in waveguide characteristics through the photorefractive effect [116,160], Thus, one would expect similar effects for gamma rays, x-rays, electrons and protons.

It is also apparent that the properties of $LiNbO_3$ are sensitive to external effects through the coupling of the optical properties to other parameters such as temperature (pyroelectric effect) and stress (piezoelectric effect). This general sensitivity of the optical properties of $LiNbO_3$ and $LiTaO_3$ to external parameters suggests that these same optical properties may be susceptible to the effects of radiation.

It is interesting to contrast the potential for radiation effects in $LiNbO_3$ devices with the well-known effects of radiation on Si semiconductor devices, such as CMOS VLSI circuits and Si solar cells. Si CMOS devices, in their unhardened commercial form, are quite sensitive to ionizing radiation, exhibiting degradation at only a few krads. However, Si devices are very pure and highly controlled during the fabrication process. Thus, one expects that a few defects or trapped electrons/holes maybe significant relative to the few defects already present. in contrast, both $LiNbO_3$ and $LiTaO_3$ arc quite impure materials compared with state-of-the-art Si. Impurity levels in $LiNbO_3$ and $LiTaO_3$, whether added intentionally as in Ti indiffusion, added inadvertently during growth and fabrication or merely present in raw material, are much higher, so that radiation-induced defects and trapped charge carriers would not affect $LiNbO_3$ properties until they reach levels comparable with the impurity and defect concentrations present prior to irradiation. As we will note, this is borne out by the total ionizing dose studies of these materials. Thus, while we should not be surprised to see radiation effects in $LiNbO_3$ and $LiTaO_3$, these effects will be observed at radiation levels much higher than is typical for Si-based devices.

Many radiation effects studies have focused attention on the effects of radiation on the absorption spectrum of $LiNbO_3$ [1 14-119,121 -123,131,1 33,135,156,1 59]. Two absorption bands at approximately 387 nm and 480 nm appear to be influenced by ionizing radiation [1 19,131,133,156,159]. The band at 480 nm is associated with the presence of Fe [119,131] and is related to photorefractive effects in $LiNbO_3$. Ionizing radiation causes this band to grow when the doses are above 10^5 rads. The growth is more prominent in Fe-containing crystals, and is absent from crystals doped with Mg, even if the Fe concentration is significant. The 480 nm band is susceptible to both photobleaching and thermal annealing at about 200°C [119]. Doping with Mg reduces the photorefractive effect in $LiNbO_3$, also suggesting a relationship between the 480 nm band and photorefractive effects.

More recently, radiation-induced absorption at 1061 nm in z-cut $LiNbO_3$ and $LiNbO_3$:MgO following a burst of radiation from a pulsed nuclear reactor has been studied [156,159]. It was shown that the effect of neutrons from the radiation pulse, limited to fluence levels less than 1x1013 n/cm^2, was negligible. This is not surprising since it has been shown that fluences of the order of 10^{16} n/cm^2 were required to affect the absorption spectrum [114]. All of the effects observed in these studies were attributed to the prompt gamma dose that was less than 7.5 krads per pulse. As shown in Figure 6, similar to the 480 nm band, the growth of the radiation-induced absorption at 1061 nm with dose was much less in MgO doped $LiNbO_3$. The decay of the radiation-induced absorption was non-exponential and occurred over a broad range in time and appeared to be composed of the decay of a variety of color centers with differing decay constants. This extended decay of radiation-induced absorption was similar to that reported earlier [115] for pulsed electron bombardment of pure $LiNbO_3$, and by Roeske, et al [125] more recently for pulsed electron irradiated Ti:$LiNbO_3$. Thus, we see that prolonged decay of radiation-induced absorption is general] y characteristic of $LiNbO_3$. It is also important to note that while very large doses of steady state ionizing radiation are necessary to produce significant changes in absorption [1 27,129,131 ,133-135,144], pulsed irradiation at levels of a few krads can produce significant transient absorption. Thus, $LiNbO_3$ behaves similarly to optical fibers in the sense that fibers also exhibit strong transient radiation-induced attenuation.

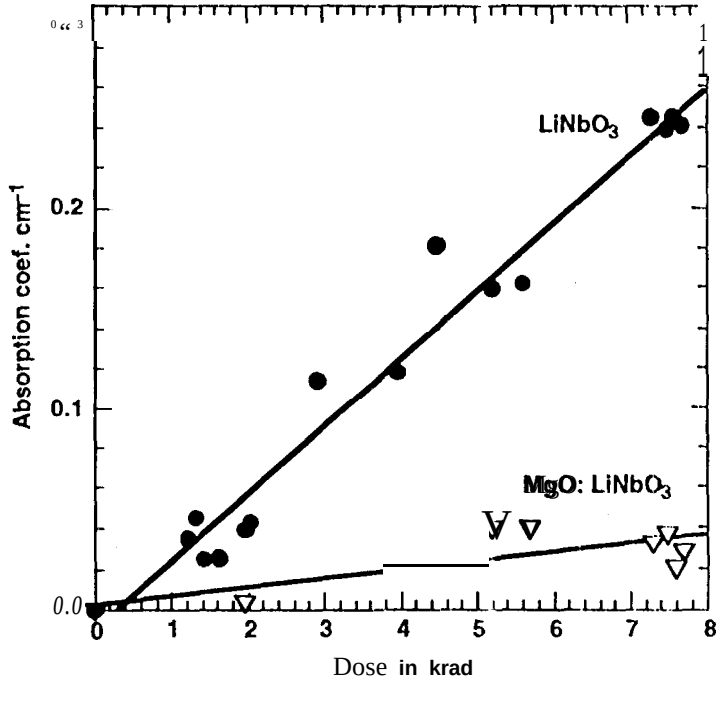

Figure 6. Peak induced absorption coefficient at 1061 nm versus dose from pulsed nuclear reactor exposures for pure and MgO doped $LiNbO_3$ [156].

As part of the extensive work done on radiation effects in $LiNbO_3$ at the Air Force Phillips Laboratory [126,129-131,137-142,146-148, 154, 158], Taylor, et al [60,77] have also examined the decay of radiation-induced attenuation (absorption) in $LiNbO_3$. These measurements, and others we will review, were performed on $LiNbO_3$ waveguides rather than bulk materials as in the studies noted above. Thus, an important difference is that the material is non-uniformly doped either with Ti or by the proton exchange process, and the attenuation observed in a beam exiting a waveguide is influenced not only by color

center absorption, but also by evanescent leakage into the substrate, possibly the result of radiation-induced changes in the refractive index. However, the results in waveguides and bulk materials are similar in the broad sense that attenuation was observed to exhibit a slow recovery extending well beyond the duration of the radiation pulse. Taylor [129-131] used a geminate recombination model to fit attenuation recovery data, which resulted in a $t^{-1/2}$ dependence, similar to Brannon's [156] observations of a $t^{-1/4}$ dependence.

More recent studies by Taylor [137-141,146-148,154] and others [149 -153,1 56,157,1 59] used structures with more than one waveguide even if they only measured the output from one of the guides following irradiation [149-151,153,155,157]. Because of the relative insensitivity of $LiNbO_3$ and $LiTaO_3$ to permanent damage, most of these studies have focused on transient radiation effects. Broadly speaking, the common result observed in all these studies for both $LiNbO_3$ and $LiTaO_3$ was that the waveguide attenuation increased during and immediately following the ionizing radiation pulse, and then recovered relatively slowly, with the induced attenuation lasting milliseconds or longer. Since materials studies, noted above, have shown the same basic result due to color center introduction, it is logical to conclude, as Taylor has done, that at least some portion of the induced waveguide attenuation is due to radiation-induced color center formation and subsequent anneal. In addition to waveguides formed by Ti diffusion into $LiNbO_3$, long lived, radiation-induced attenuation has been observed in proton exchanged $LiTaO_3$ [139,146,1 50,151 ,153,155,157] and proton exchanged $LiNbO_3$ [149,151].

As yet, it is difficult to draw any conclusions about the relative radiation hardness of $LiNbO_3$ vs $LiTaO_3$ because the differences in radiation response of the two materials have not been consistently large and in the same direction. In addition, in two of the studies where both materials were examined [151,157] the wavelengths at which the two materials were examined were different: 850 nm for $LiNbO_3$ and 1300 nm for $LiTaO_3$. Under these conditions, it is not surprising that the $LiNbO_3$ attenuation was greater than that of the $LiTaO_3$ waveguides. However, in a recent study [139] Padden, et al concluded that under the conditions of their testing, $LiTaO_3$ was significantly more radiation resistant than $LiNbO_3$.

Recent work [138- 142,146- 148] by the Phillips Laboratory (PL) Group has focused on the effects of pulsed irradiation on the energy transfer between waveguides (crosstalk) in $LiNbO_3$ and $LiTaO_3$ directional couplers. In the initial phase of this work [138,139,141], results were reported out to a few msec for light intensities exiting from both output waveguides (1300 nm laser light input only to a single waveguide with significant coupling to the crossover waveguide) during and after bombardment by ionizing radiation pulses that delivered 15 krad/pulse to the sample. Foliowing the 15 ns wide pulse of 16 MeV electrons to 15 krads, as shown in Figure 7, there was a large drop in the light intensity exiting from both the throughput and crossover waveguides. The relative magnitude of the decrease depended on the launch conditions and the polarization of the input beam.

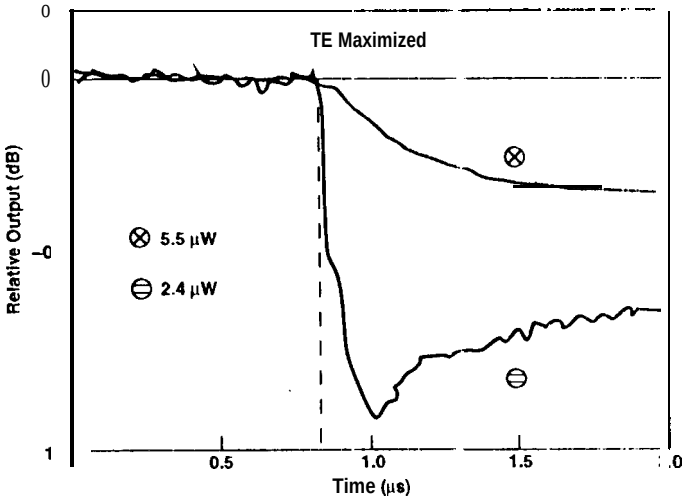

Figure 7. Reduction in directional coupler throughput (lower) and crossover (upper) outputs at 1300 nnr following exposure to 15 krad(Si) of pulsed electron bombardment [137].

In an extension of the above results, the PL Group has shown in later work [139,140,146-148] that one must track the light output for several minutes following the radiation pulse in order to observe a more complete picture of the effects of the irradiation. When this is done the changes observed in the first few microseconds become relatively insignificant. In these later experiments, more intense radiation pulses were employed, and, in most cases, both the TE and TM polarized beam intensities

were monitored. In a typical response, shown in Figure 8, during and immediately following a radiation exposure of 75 krads, there is a small, brief increase in the throughput TM power (pre-inadiation level = 9 mW) followed by a precipitous drop in this power to a minimum of about 1.5 mW at a time after the pulses of approximately 45 sec. The TM throughput power then recovers to a value again greater than the pre-irradiation value at about 85 sec and then decays again. The general envelope of the response is oscillatory with a damping effect in time until the pre-irradiation value is completely recovered at some time longer than the observation time of 200 sec. Thus, the radiation pulses cause significant transfer of energy back and forth between the guides for times extending well beyond the end of the radiation period.'

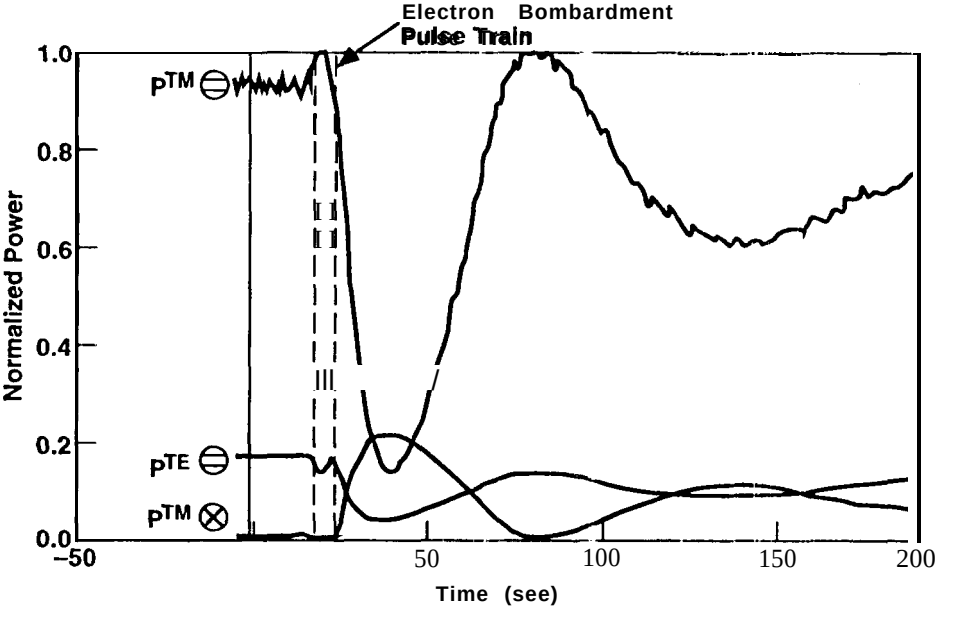

Figure 8. *Effect of* 75 *krad(Si) pulsed electron bombardment on coupling in a* $LiNbO_3$ *directional coupler operating at 1300* ***nrn*** *[148].*

The PL Group has suggested that results such as those shown in Figures 7 and 8 are due in large part to radiation-induced photorefractive effects. The intense, pulsed electron beam creates high densities of electrons and holes throughout the bombarded region of the coupler. Following the pulse train, there will be separation of the electron-hole pairs due to drift of the electrons in internal electric fields, and due to diffusion, because of strong diffusion gradients present. Some of these migrating electrons will undoubtedly be trapped at Fe^{+3} acceptor centers, The presence of these processes strongly suggests that there will be a radiation-induced photorefractive effect, The occurrence of the photorefractive effect depends on the ratio of Fe^{+2} to Fe^{+3} which will surely change during and immediately after exposure to an intense pulse of ionizing, radiation. The iron acceptor, Fe^{+3}, has a large electron capture cross section so that one expects the density of Fe^{+2} to increase following radiation exposure. We have already noted that there is a radiation-induced permanent alteration in the absorption bands associated with the presence of iron. In addition, decay of photorefractive effects are long term, and laser-induced photorefractive effects typically last long after the laser beam is turned off. Thus, the long term residual effects observed after pulsed electron irradiation have a time scale similar to that of photorefractive effects.

We also note that there is precedent for attributing increases in crosstalk between waveguides to photorefractive effects [161]. Schmidt, et al [161] studied optically-induced crosstalk at 633 nm and 1060 nm in reverse-$\Delta\beta$ z-cut, Ti-diffused $LiNbO_3$ couplers. Significant increases in crosstalk were observed under a bias of 25 V and a 633 nm optical power of 20 nW (0.2 W/ cm^2) over a period of 60 min. The crosstalk increased rapidly during the first 5 min and then saturated at a level of about -13 dB. Space charge build up between the illuminated guide and the second guide was attributed to photoconductive motion of carriers under the influence of the applied field. Later work [162] on optical] y-induced photorefractive effects in a Mach-Zender interferometer attributed these effects to photovoltaic (no applied field) effects rather than a photoconductive mechanism.

There are other interesting implications for device behavior during and following an intense pulse which causes a large temporary increase in the concentration of free electrons in the conduction band of the $LiNbO_3$. First, during this brief period, the crystal will be electrically conducting so that if the pulsed irradiation is performed on a device with electrodes and there is an

applied bias present, a photocurrent will flow during the pulse. This condition may alter the optical effects observed during and after the pulse depending on the device configuration and the operating characteristics during and after irradiation. Second, in the case of semiconductors, it is well known [100] that the presence of free electrons and holes can modify the refractive index. The possible implications of this effect on $LiNbO_3$ device behavior during an intense radiation pulse are unknown at this time.

We have discussed radiation-induced color center introduction and photorefractive effects, both of which may influence results such as those shown in Figures 7 and 8. We now wish to briefly examine the. effects of significant changes in the coupling efficiency on the temporal behavior of the light beams in the throughput and crossover guides of couplers. During and immediately following the intense pulse of electron radiation, the refractive indices of the guides in the coupler are reduced and there is greater leakage of the light out of the guides. The evanescent decay length, γ, increases leading to a large increase in the coupling strength, K, because of its exponential dependence on γ (see equation (4)). Following irradiation, the color centers and trapped electrons recover, and the device gradually regains its pre-irradiation characteristics. I)uring the recovery period, y and hence κ decrease toward their pre-irradiation values. As noted earlier, Brannon [156] found a $t^{-\prime\prime}$ dependence of the induced absorption on recovery time following a radiation pulse, while Taylor [130] found a similar $t^{1/2}$ dependence. If one assumes a similar dependence of the recovery of κ, from a large value during and immediately after irradiation to its smaller pre-irradiation value after long recovery times, then the temporal variation of the argument of the $\sin^2$ function in equation (6) will cause η to exhibit an increasing period with time, in agreement with the results shown in Figure 8.1 n addition, the coefficient of the $\sin^2$ function in equation (6) will decrease with time in agreement with the weaker transfer of energy at the second minimum in the throughput power at 145 sec. Thus, the temporal behavior of the throughput and crossover powers in Figure 8 can be explained using equation (6) for the coupling efficiency, η, without invoking a radiation-induced change in the pre-irradiation value of $\Delta\beta$ (the difference in β's between the guides).

Our brief review of the work that has been done on radiation effects in $LiNbO_3$ and $LiTaO_3$ materials and devices suggests that while an excellent start has been made on determining the effects of radiation on these interesting materials, much work remains to be done, especially on full-up devices that employ electrodes to achieve electro-optic performance.

5. SEMICONDUCTOR-BASED MODULATORS

Introduction

A sampling of recent review articles [9,97,163-175] attests to the very rapid growth of the area of semiconductor-based modulator research and development. Indeed, in a recent review article [9], in reference to work on III-V superlattice-based modulators, Jabr states that "there is such a rapidly growing body of research on these materials that it will be hard to give an accurate account thereof". The number and variety of device structures is extremely large, and we shall only touch on representative types of modulators in this Review, Our goal is to discuss those common features and trends in this very large array of devices that are relevant to radiation hardness of semiconductor modulators. In approaching this goal, we will rely heavily on radiation effects studies of other types of semiconductor devices such as Si CMOS, GaAlAs LEDs and laser diodes, and other III-V materials. It is interesting to note that while much radiation effects work has been done in these other semiconductor device types, hardly any radiation effects testing of semiconductor modulators has been performed.

Compared with polymer-based and insulator-based modulator structures, semiconductor modulators have many potential advantages including the following:

1. There is a history of many years of research and development, including the extensive work that has occurred in related III-V device technologies, such as digital GaAs devices, monolithic microwave integrated circuits (MMICs), and conventional photonic devices (LEDs, laser diodes and detectors).

2. While 111-V modulators are not generally commercially available, there is a very large manufacturing base of III-V materials and devices that can easily fabricate and market III-V based modulators. Indeed, much of the research on HI-V modulators has been conducted by groups at facilities that market other types of III-V devices. This established infrastructure will also allow the manufacture of III-V modulators at reasonable cost.

3. A variety of well-established material processing, techniques, in particular, "hand gap engineering", have enabled the development and fabrication of a wide variety of highly complex modulator structures, including structures that are integrated with other photonic devices such as laser diodes.

4. Several electro-optic phenomena have been observed in HI-V materials and devices, particularly in multiple quantum well (MQW) structures, which facilitates the development of EO modulators,

5. III-V modulators are capable of very high speeds with switching times less than 100 ps and frequencies in excess of 50 GHz.
6. Compared with many $LiNbO_3$ modulators, III-V devices arc capable of efficient operation at low voltages and powers.
7. The feature size and physical volume of III-V modulator structures is very smal 1, especially when compared to $LiNbO_3$ devices, facilitating high integration densities.

Disadvantages associated with III-V modulators include the following:

1. Generally, electro-optic effects and their corresponding electro-optic coefficients are significantly weaker in semiconductors than they are in some of the highly sensitive insulator materials like $LiNbO_3$ and $BaTiO_3$ (see Table 1).
2. In the case of GaAs, integration with Si technology is somewhat more difficult than other semiconductor combinations because of the 4.1 % lattice mismatch between GaAs and Si.
3. Commercial III-V modulators are generally not available except as integral parts of sophisticated laser devices.

Materials/Operating Characteristics

An important feature of many types of semiconductor modulators is the requirement for fabrication of optical waveguides. As in the case of polymer and insulator-based devices, this is done by varying the refractive index in a controlled manner. In the III-V semiconductors, there are two methods for achieving the necessary variation in refractive index. The waveguide can be formed using either heterostructures of different materials, or homostructures in which the carrier density is varied in order to alter the refractive index. In the AlGaAs system, layers of varying Al content can be grown in order to fabricate waveguides with varying index. For $Al_xGa_{1-x}As$, the refractive index varies approximately linearly from $n \approx 3.57$ for x = O to $n \approx 3.36$ for x = 0.35 in the near infrared. Thus, a GaAs layer between two AlGaAs layers (double heterostructure) will form a waveguide. The AlGaAs system is particularly well-suited for this "band gap engineering" because GaAs and AlGaAs with moderate Al content have essentially the same lattice constant so that high material quality is maintained in complex layered structures. Similar waveguide structures can be fabricated in other III-V material systems, such as InGaAsP, although the lattice matching requirements are sometimes more restrictive than for AlGaAs.

Waveguides can be constructed in single materials, homostructures, by varying the carrier concentration. The reduction in refractive index, An, due to an increase in carrier concentration, N, is given by [39]

$$\Delta n = -\frac{N\lambda^2 e^2}{8\pi^2 \varepsilon_0 n m^* c^2} \tag{8}$$

where m" is the carrier effective mass. Thus, an undoped GaAs layer grown on a heavily doped GaAs substrate will form an optical waveguide bounded by an air interface on top and the substrate on the bottom. For n-type GaAs at a wavelength of $\lambda = 1$ μm, An = -0.01 when N = 5x1018 electrons/cm³. Therefore, the index changes possible through carrier concentration variation are much less than through heterostructure layer growth. A further problem with homostructures is that large carrier densities can cause significant increases in optical absorption that will result in attenuation of the optical beam if it passes through heavily doped regions of the structure. We also note that radiation-induced displacement damage can reduce the carrier concentration resulting in an increase in An.

With regard to modulators based on semiconductor waveguide structures, there area variety of ways to classify these modulators. These include the following:

1. Material type: AlGaAs, InGaAsP, InP or Si. We will not discuss Si to any extent, and we will also tend to lump the III-Vs together except when there is an important distinction between material types.

2. Bulk or layered structures: while bulk devices are worth noting, the MQW-based modulators are where the real future lies for semiconductor modulators.

3. **Electro-optic or all-optical:** ultimately, the highest speeds and largest densities will be realized with all-optical devices, but at the present time EO devices are important and have impressive performance characteristics. In addition, as we will note, there are interesting combinations of optical and electrical devices.

4. **Basic** operating mechanism: refractive index change (Pockels effect, carrier injection, carrier depletion and quantum well electron transfer), or absorption change (Franz-Keldysh effect and quantum confined Stark effect (QCSE)). In contrast with polymer and insulator modulators, semiconductor modulators also employ optically and electrically-induced variations in the absorption coefficient to achieve modulation of an optical signal. Thus. radiation-induced changes in the absorption coefficient as can occur with neutron irradiated GaAs, may affect these types of modulators.

Before presenting a list of representative semiconductor modulator types, we briefly review the more important basic operating mechanisms given above. It is important to note that in many cases more than one of these mechanisms is simultaneously operative.

Refractive index change

1. Pockels effect. This is the same electro-optic effect that is the basis for modulation in polymer and insulator-based devices. An additional complication that arises with semiconductors, when compared with insulators, is that a carrier-free region must be created in order to support a significant electric field that can alter the refractive index. This usually means constructing *p-n* junctions in lightly doped material so that the electric field extends through a fairly wide depletion layer. This can have significant implications for radiation susceptibility. We also note that the EO coefficients for semiconductors are smaller than for the best insulators like $LiNbO_3$ (see Table 1) so that this technique, by itself, is not widely used to construct modulators in bulk semiconductor materials.

2. **Carrier injection (depletion).** As noted above, the refractive index can be changed by altering the carrier density in the guiding region of the device. Thus, modulation of the optical signal can be achieved by time varying injection of carriers into the guiding region. This can be accomplished by injecting minority carriers with a forward biased *p-n* junction (or removing carriers by applying a reverse bias). The same effect can be realized in an MQW structure by quantum well electron transfer; that is the movement of carriers between quantum wells to change the carrier density in the wells. Carrier injection or depletion allows one to construct a modulator in a material like Si which does not exhibit a linear electro-optic effect. In addition, the carrier-induced change in refractive index can be an order of magnitude larger than the electro-optic effect, as in the case of InGaAsP. However, the applicability of such devices is limited because switching speeds are no faster than the minority carrier lifetime in the device. Interestingly, this is one case where radiation might actually improve device performance because the minority carrier lifetime can be dramatically shortened by irradiation.

Absorption coefficient change

1. Franz-Keldysh effect. In bulk semiconductors the absorption near the band edge is sensitive to electric fields. The electric field-induced shift and broadening of the absorption near the band edge is called the Franz-Keldysh effect. Application of an electric field causes the band edges to tilt which allows the. electron wave function to penetrate into the band gap, effectively lowering the band gap energy. In the case of GaAs, for a light beam with energy 0.01 eV below the band gap energy, E_g, (for GaAs, E_g = 1.4 eV) the absorption coefficient increases by about 1500 cm^{-1} for an electric field of 2×10^5 V/cm [174].

2. **Quantum confined Stark effect (QCSE).** With regard to semiconductor modulators, the QCSE is perhaps the most important mechanism for achieving efficient, high-speed modulation. The basic Stark effect is the change in outer atomic orbits of electrons caused by the application of an electric field. The field causes a splitting in the energy of the outer 2s and 2p orbital states, and there is a corresponding energy shift. When the atoms make up a solid which is composed of multiple quantum wells (MQWs), the Stark effect becomes particularly interesting and useful because of the way in which the field modifies the properties of excitons residing in quantum wells.

In a bulk semiconductor the exciton, a loosely bound electron-hole pair, has a ground state binding energy of about 4.4 meV, determined by the electron effective mass and the material dielectric constant. The small binding energy means that the exciton can dissociate easily due to an increase in temperature (thermal broadening) or to the presence of an electric field (Stark effect). The exciton exhibits a series of hydrogen-like bound states, the energy of which is modified by the dielectric constant of the material in which the exciton is embedded. In a MQW structure, exciton behavior is quite different because the electrons and holes are confined in the wells and there is significantly more overlap between their wave functions. The result is that the exciton is more stable and continues to exhibit its properties even at electric fields 50 times greater than that required to disassociate the exciton in bulk material. The exciton absorption spectrum exhibits resonances corresponding to excitation between hole and

electron ground states (band edge), and between the ground state and higher lying energy levels, the values of which are determined by the well properties. As shown in Figures 9 and 10, when an electric field is applied perpendicular to the quantum well layers, these resonances broaden and shift to lower energies because the bands tilt and the electron and hole wave functions are displaced. The dependence of the absorption edge shift on field in the MQW structure (QCSE) is much stronger than it is in bulk material (Franz-Keldysh effect). We also note that because the absorption coefficient and the refractive index are related through the Kramers-Kronig relationship, the refractive index will also change due to electric field-induced QCSE. Thus, the MQW structure constitutes a sensitive electro-absorption medium that can form the basis for an efficient EO modulator.

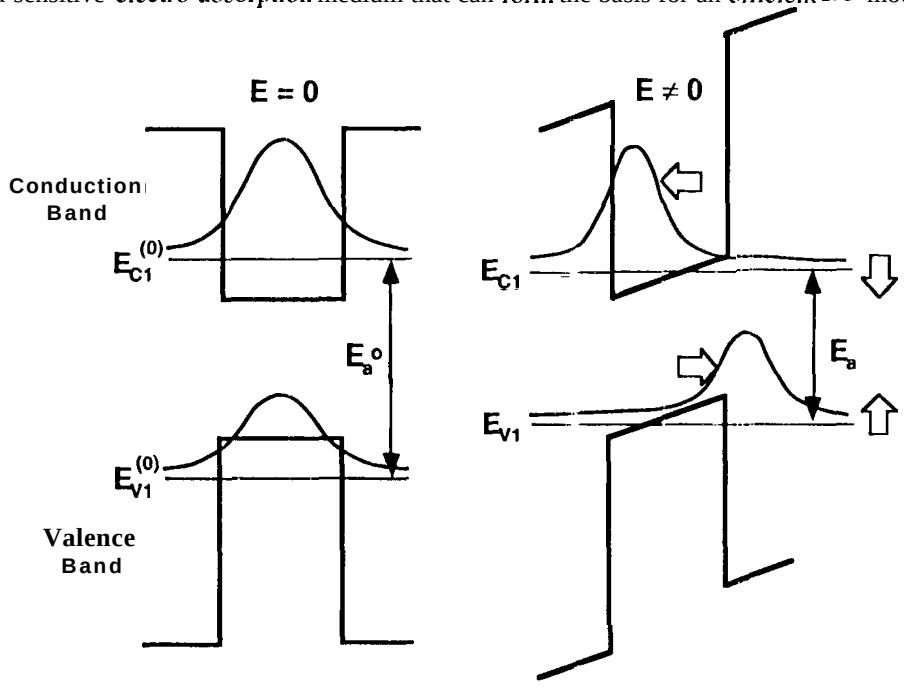

Figure 9. Effect of an electric field, E, on wavefunctions in a AlGaAs/GaAs quantum well [165].

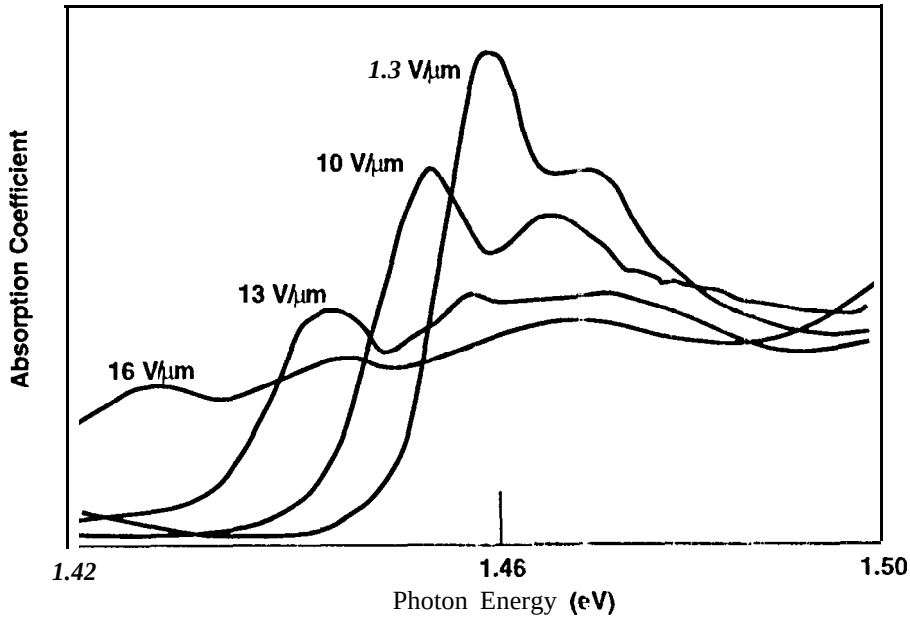

Figure 10. Exciton absorption spectra in AlGaAs/GaAs quantum wells as a function of applied electric field. Note the shift to lower energy corresponding to the changes shown in Figure 9 [1 71].

Representative semiconductor modulator types

1, Transverse electro-absorption modulator [167,169,175], As shown in Figure 11, this device is an AlGaAs/GaAs *p-i-n* diode with the MQW structure embedded in the *i*-region of the diode. The optical signal beam impinges on the top of the modulator, at the right in Figure 11, and passes through the diode in a transverse manner perpendicular to the MQW layers. This configuration makes the device attractive for SLM applications where a matrix of light beams impinge on a grid of such devices. The electric field is applied in the same direction in order to achieve QCSE. With no bias applied the light beam passes through the structure with little attenuation (note 75% transmission with no electrical pulse). Upon the application of bias, the absorption shifts to lower energies so that the light beam is absorbed, achieving the intensity modulation of the beam shown in the transmission curve. These devices are very fast, as shown in Figure 11, because their internal response is limited only by the carrier tunneling times required to remove carriers from the wells, and these times are on the order of 10 to 200 ps, implying possible modulation bandwidths of 50 to 100 GHz. Devices have been reported with impulse responses of 131 ps [176]. The overall response of these modulators is determined by the RC time constant of the circuit in which the modulator is placed. If the capacitance can be limited to a few tenths of a pF, then bandwidths of 10s of GHz are possible..

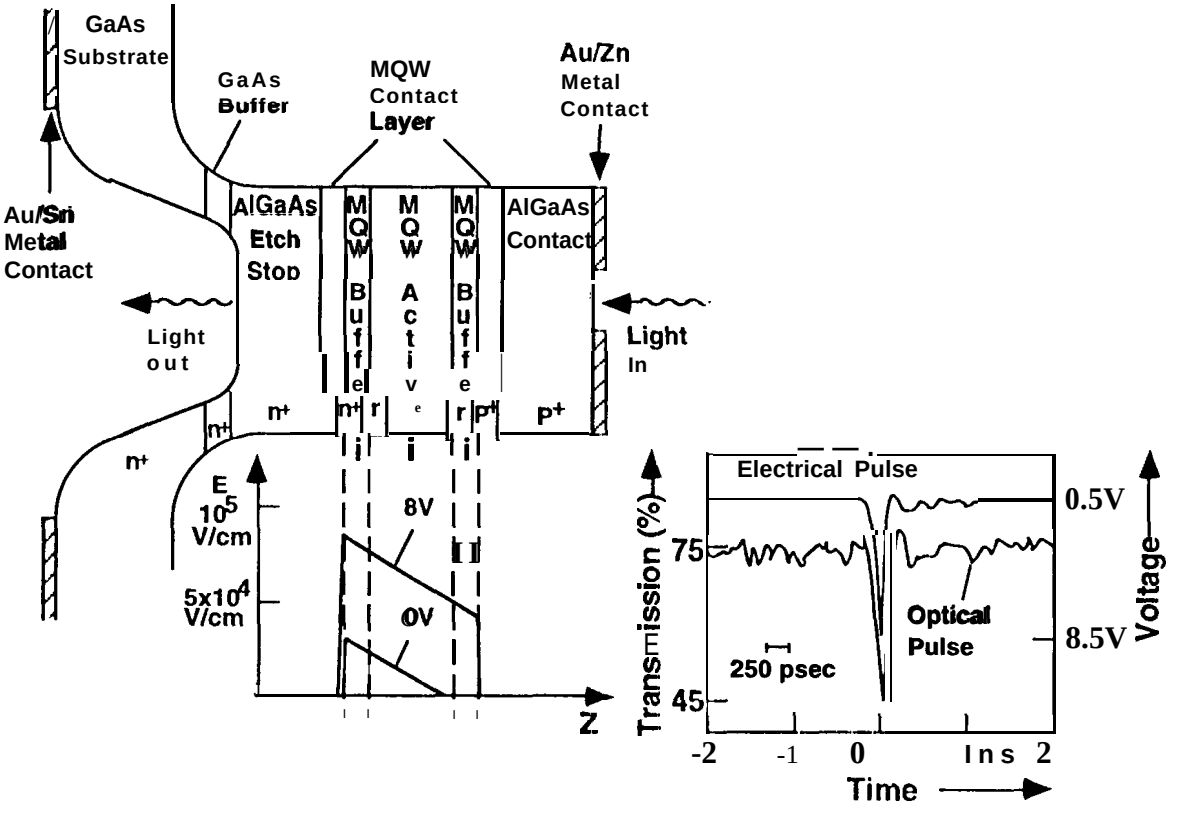

Figure 11. An *MQ* W *transverse electro-absorption modulator [167].*

Another important feature of these modulators is the extinction ratio, or on-off ratio; that is, the ratio of transmitted light beam intensity when the device is on to that when it is off. This ratio depends on the extent of the exciton absorption shift induced by the application of the electric field. This ratio increases rapidly with decreasing temperature as the exciton absorption resonances narrow and become stronger. However, at room temperature it is difficult to achieve a large extinction ratio. One solution to this is to construct the transverse modulator as a reflection modulator so that the beam passes through the MQWS twice. This can be accomplished by depositing a metal reflector at the substrate side of the device, or by using a quarter-wave multilayer dielectric mirror below the MQWS. This structure has the added advantage of not having to remove the substrate, which is required in the non-reflection configuration so that the beam can pass entirely through the device without attenuation in a thick GaAs substrate.

2. **Electro-absorption MQW modulator [165,170,174,17S].** If we change the configuration of the *p-i-n* diode electro-absorption modulator discussed above so that the MQW layers form a waveguide and the light is injected into the waveguide

parallel to the MQW planes, we have an electro-optic modulator that can be coupled to fibers and used in a communication system. In bulk material, the EO effect is small compared with $LiNbO_3$ and other materials. However, if the waveguide is formed from MQWS, then not only the linear EO effect is present, but also the quadratic EO effect due to the QCSE on the refractive index, by way of the Kramers-Kronig relationship. In this type of modulator, the light wavelength must be chosen near the exciton resonances since the QCSE is an excitonic effect. It can be shown that the refractive index depends on the square of the electric field for the QCSE, and this provides the extra sensitivity y that makes these modulators attractive [175]. These devices also operate in the tens of GHz modulation speed range. It has been shown that the electro-optic effect can be enhanced further by introducing strained layer, lattice mismatched quantum wells [175]. With regard to radiation effects, it is important to take into account any type of radiation, such as neutron exposure, that will affect the near-edge absorption spectrum.

A particularly important application of this class of modulators is the external modulation of high speed lasers used in communications systems, Lasers combined with external modulators on the same chip arc available commercially. The use of external modulators avoids the frequency chirping effect exhibited by many lasers when modulated at high frequencies. This chirping effect can significantly reduce the bandwidth of a communication system. The ability to fabricate lasers and modulators on the same chip is due largely to the advent of selective area epitaxial growth techniques in which layers of different thickness and material sequence can be grown on the same substrate. Such techniques are largel y responsible for integration of many types of devices on a single substrate in the III-V materials families.

3. Mach-Zender modulator [177,178]. This popular type of modulator has been constructed in both bulk [177] and MQW [178] forms in the GaAs/AlGaAs system, and also in other II I-V material systems. The Mach-Zender modulator is a particular implementation of the waveguide modulator discussed above in 2. Growth techniques such as selective area epitaxy must be used that allow the patterning and routing of MQW waveguides in order to Fabricate Mach-finder modulators and other complex waveguide structures. By applying the electric field to one arm of the modulator, a phase shift is introduced that modulates the intensity of the recombined output beam of the device when viewed through an analyzer and/or polarizer. Because these devices can be easily operated in the 10s of GHz range they lend themselves to microwave applications more easily than $LiNbO_3$-based modulators. In addition, high speed 111-V modulator structures such as the Mach-Zender device, can be integrated on a single substrate with III-V monolithic microwave integrated circuits (MMICs).

4. **Total reflection switch/modulator [165,1 74].** In this device, two intersecting waveguides made up of MQWS allow total internal reflection to occur at the intersection of the waveguides in such a manner that the light beam can be switched from one output waveguide to the other. The electric field-induced QCSE is used to control the. reflectivity of the intersecting planes so that total internal reflection occurs at a certain applied bias, but not at zero bias where the light beam passes straight through the device in the waveguide in which it was launched. A particularly important feature of this device is that its operation is independent of the polarization of the input beam so that polarization fluctuations often seen in fiber transmission do not affect its operation. The total reflection switch is relatively simple to construct and matrix switch arrays are easily fabricated.

5. **Directional coupler switch/modulator [165,168,1 74].** Directional couplers similar to those discussed earlier fabricated from $LiNbO_3$ have also been reported in a variety of 111-V materials. Most of the devices reported were made in bulk heterostructures rather than MQW waveguides. While these devices are not as sensitive as $LiNbO_3$ couplers, because of the smaller EO coefficients, they have the significant advantage of being easily integrated with other photonic devices on III-V substrates. More recently, vertical MQW directional couplers have been fabricated in both GaAs/AlGaAs and GaInAs/InP materials structures [179]. In these devices the waveguides actually lie on top of each other so that coupling occurs vertically between the guides. The increased sensitivity due to the QCSE allowed the use of very short device lengths, approximately 170 μm.

6. **All-optical modulators [167,180,181].** In GaAs/AlGaAs structures it is possible to achieve refractive index changes by optically altering the carrier density in a waveguide [1 80], or by altering a built-in electric field that exists in a waveguide [181]. Optical excitation of electrons from the valence band to the conduction band fills the lower states in the conduction band minima, a process termed band filling, and results in a change in the near- band edge. absorption coefficient. Thus, it is also possible to optically alter the absorption of the signal beam by modifying the absorption in the waveguide. Using these optically induced effects, one can construct an all-optical modulator using a signal beam and a second control beam that changes the refractive index in the signal beam optical path. The control beam can be orthogonal to the signal beam [180], or be parallel to it with a different polarization in order to keep the beams separate. Modulation depths greater than 8 dB have been observed using a control beam in the mW range [180]. As in other carrier-induced modulation schemes, the speed of these modulators is

limited by the minority carrier lifetime. It is interesting to note that ion implantation has been used to purposely reduce the lifetime to the picosecond range so that the resultant modulator has greater bandwidth [182]. Thus, as we noted earlier, one might anticipate that radiation would actually improve the operation of these devices.

7. **Transverse Fabry-Perot reflection modulators [165,183,184].** One can advance the reflection modulator discussed above to a more efficient level by placing the MQW active structure between two Fabry-Perot cavities, each made up of quarter wave composite stacks of multilayer mirrors composed of heterolayers of GaAs and AlGaAs. The large number of reflections has resulted in observed extinction ratios of 20 dB at only a few volts. In addition, these devices can be very fast: operation at 40 GHz has been reported recently [183]. Because the power dissipation in these devices and other electro-absorption modulators, is mainly due to the absorbed optical energy, it is beneficial to suppress the responsivity, especially in Fabry-Perot modulators where the beam experiences repeated internal reflections and thus has a long path length in the material. It is interesting to note that proton bombardment has recently been successfully used to suppress responsivity and improve the performance of Fabry-Perot modulators [184]. As in the case of shortening the minority carrier lifetime, this is another example of radiation exposure improving device operation.

8. **Delta-doped MQW lateral field modulator [185].** This device is similar to the transverse electro-absorption modulator discussed in 1. above except that the electric field is applied in the lateral direction parallel to the MQW layer planes. Thus, the field is applied orthogonal to the direction of the light beam. In addition, a doping technique used to construct high electron mobility transistors (HEMTs) is used in these modulators. Delta or modulation doping is accomplished in MQW layers by heavily doping the alternate wide band gap layers, but growing undoped small band gap layers in between the heavily doped layers. The band gap offset between layers in the GaInAs/InP heterostructure is such that the electrons end up residing in the lower energy wells of the undoped narrow band gap GaInAs wells. In H EMT structures this configuration is advantageous because the electrons have very high mobility since there are no ionized dopant atoms to cause carrier scattering in the wells in which the electrons move, thus producing a very high speed transistor. Light of the proper wavelength will pass through the wide band gap InP layers in the MQW, and when no electric field is applied, it will also not be absorbed in the small band gap GaInAs layers because the subband states in the wells where the electrons reside are all filled, reducing the absorption coefficient at the light beam wavelength. This is then similar to the band filling effect mentioned above. Upon application of the lateral electric field, the electrons are drawn out of the center of the Gain As wells over to that side of the device where the positive bias is applied, and accumulate near the positive contact. The result is that the subband states in the GaInAs wells in the center of the device, where the light beam passes, are empty and available to accept electrons excited from the valence band in the GaInAs well. Thus, the absorption coefficient increases markedly. These devices are expected to be very fast and to show good extinction ratios.

Although these modulators are just being developed [185], we mention them because their use of modulation doping raises interesting issues concerning radiation effects. The undoped, high mobility small band gap wells may be especially susceptible to radiation-induced degradation of carrier properties such as mobility.

9. **Self electro-optic effect devices (SEEDS) [171,173,175,186-1 90].** The class of devices called self electro-optic effect devices (SEEDS) has received a great deal of attention and there are now many variants of SEEDS. The earliest SEEDS were very similar to the transverse electro-absorption modulator described in 1. above, essentially a *p-i-n* diode containing a MQW structure in the *i* region, along with a resistor in series with the power supply across the diode. The key to operation of these devices is to use the photodetection capability of the reverse biased MQW diode itself, or to use the modulator in conjunction with an external photodetector (although the detector may be. fabricated on the same chip). The inclusion of the resistor in series with the constant reverse bias supply allows the photocurrent detected by the *p-MQWi-n* structure (as a photodetector) to modify the electric field across the MQW region, which, in turn, alters the absorption characteristics that the light beam experiences in the *p-MQWi-n* (as a modulator). This feedback circuit introduces a negative differential resistance (NDR) into the photocurrent vs. bias curve of the device. Although the bias supply is constant, the device characteristic can move along this curve because the variation in photocurrent causes a variation in voltage drop across the resistor resulting in a bias variation across the *p-MQWi-n* diode. We also note that the SEED is a combination between an electro-optical and "all-optical" device: a constant bias is applied to the device, but the modulation is caused by the optical beam itself.

The basic resistor-SEED acts as a bistable switch that can also exhibit oscillations because of the NDR. The bistability can be seen by noting that at very low light levels all the voltage drop is across the MQW diode. As the optical input power is increased, the photocurrent caused by absorption in the MQW diode causes a voltage drop to appear across the resistor that results in a decrease in voltage across the MQW diode. If the device is operated at a wavelength where a decrease in voltage

causes an increase in absorption, then there will be a further increase in photocurrent and an additional decrease in diode bias, and this process will continue to build until the diode bias approaches zero and the diode approaches forward bias. The net result is that the diode switches abruptly from a high voltage to a low voltage; hence, the bistability.

The next variation in the SEED employed a separate photodiode as a load device rather than a resistor. The separate photodiode acted as a variable resistor whose value was determined by a control beam. Both the photodiode and the MQW diode can be stacked as different heterolayers on the same substrate with the photodiode on top, if the photodiode control beam is at a short wavelength, and the signal beam is long wavelength so that it passes through the photodiode unchanged. The use of a photodiode rather than a resistor allowed the device to have a much wider dynamic range. The device could also be used as a volatile optical memory.

While the resistor and photodiode SEEDs are attractive bistable switches, their use in large scale optical processing applications is problematical. These SEEDS are t wo terminal devices that] equire precise control of power supply voltages, and in the case of the photodiode SEED, precise control of the optical bias beam power. in addition, these SEEDS can exhibit unwanted reflections of the optical beams back into the system and the onset of oscillations. These detrimental features have led to the development of symmetric SEEDS, or S-SEEDS, perhaps the most important variation of the SEED technology.

As **shown** in Figure 12, the S-SEED is made up of two *p-MQWi-n* diodes fabricated side by side on the same GaAs substrate (QW reflector stacks reflect the output beam back out the top of the device). The two diodes are biased in series by a power supply and each has its own optical input/output beams. One diode acts as the load for the other, and vice versa. As in the case of the resistor and photodiode SEEDS, the S-SEED is still an optical bistable device, but its bistability and switched state depends on the ratio of optical beams, Therefore, if the two input beams are derived from the same source, the S-SEED is insensitive to fluctuations in the optical power. Another interesting feature of the S-SEED is that it has what has been termed time sequential gain; that is, the state of the device can be set with low power input beams, and subsequently read out with high power optical beams. This allows the S-SEED to have good input-output isolation since the high output readout does not coincide in time with the low power input. Thus, the S-SEED does not require close control of biasing, and it has all the features of a three terminal device.

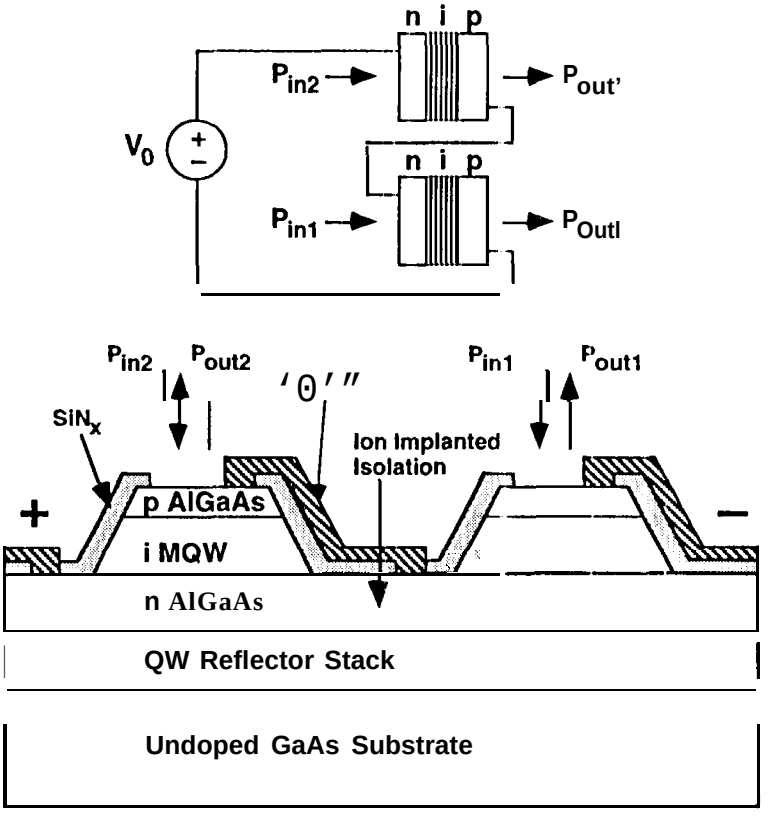

Figure 12. Schematic circuit diagram of symmetric SEED and corresponding heterolayer structure [190].

Under actual operation, each diode in the pair has a signal beam and a clock beam input (not shown in Figure 12). The bistable state of the device is first set with the two signal beams, the difference in power of which forces the S-SEED into one of its two possible states. A contrast ratio of 2:1 between the two input signal beams is more than sufficient to allow possible selection of either state. Since the bistable state is determined by the ratio of the two signal beams, fluctuations in optical power are not important as long as the signal beams have a single source.

The second set of two beams have equal powers and are the clock beams used for read out. The two clock beams which impinge on the device after the signal beams, must be approximately equal in power so that they merely read the state of the device and do not change it. The time sequential gain comes about because of the differences in power between signal and clock beams. The state of the device is set by a low power beam, but it is read later by a high power beam. We note that the gain analogy here is not with an optical amplifier where the input beam itself is amplified, but with a traditional bipolar transistor where a very small base current controls the output of a strong collector current. Timing between input beams and read beams is not critical because the device can retain its bistable state in the dark for a period of time much longer than typical clock frequencies. A key feature of these S-SEEDS is that their switching times can be very fast; switching times as fast as 33 ps have been measured recently [191].

The development of the basic S-SEED technology has proliferated dramatically, and there are now many variations of this device. Monolithic arrays of S-SEEDS have been made with 32,768 elements [192], and commercial arrays are available with 2048 elements. In addition, basic logic functions have been implemented, as have memory functions. Using multiple SEEDS (M-SEEDS, more than two *p-MQWi-n* diodes in series), a tri-state output bus has been demonstrated [193]. Recently, S-SEEDS have been implemented with transistors, so-called T-SEEDs, so that there is gain between the photodetector and the modulator. One can have a phototransistor in series with the *p-MQWi-n* modulator, or a FET-SEED, a modulator in a circuit with a MESFET and a quantum well photodiode, or a heterojunction bipolar transistor (HBT)-based device in which the MQW structure is embedded in the base-collector region. In the HBT-SEED, the HBT and the modulator can be physically separated even though they have been grown on the same substrate. After selective etching down to the. n^+ substrate between the modulator and HBT, the emitter region is selectively etched off of the modulator leaving a p^+-*MQWi*-n^+ modulator and an *n*-p^+-*MQWi*-n^+ HBT. The control light beam then impinges on the HBT and the information signal is directed at the modulator portion. Principally due to the inherent gain of the HBT-SEED, this device has several interesting applications that have been discussed by Bhattacharya [175].

Radiation Effects

Although 111-V semiconductor modulator structures present an interesting challenge with regard to radiation effects, we note that essentially no radiation effects studies have been performed directly on these types of devices. Three features of III-V modulators suggest that these devices will have a broader, more varied response to irradiation than polymer or insulator-based modulators. First, as we have noted, III-V modulator structures take advantage of the variation of the absorption edge with electric field, in particular the absorption governed by exciton behavior in quantum wells. It is well known that irradiation can affect the absorption edge of III-V materials. Second, in many of these structures we find a diode structure with an *i* region that has an electric field across it. Such a structure will be particularly sensitive to transient upset caused by large radiation-induced photocurrent pulses. Third, many semiconductor modulator structures contain some type of transistor, such as an HBT phototransistor, that increases the gain of the device. These devices will be sensitive to permanent damage of the type that affects the minority carrier lifetime. Thus, it should not be surprising if the response of II I-V semiconductor modulators to radiation reveals several interesting and significant effects.

Fortunately, there have been a variety of radiation effects studies of other types of111-V electronic and photonic devices and materials. It should be possible, at least in part, to infer the effects of rad iation on modulator structures based on these studies of 111-V materials and other device types. In the recent literature, these include radiation effects in GaAs MESFETs [194-199], GaAs MMICs [200], HIITs and HEMTs [201-204], GaAs diodes [205,206], solar cells [207-209], electrical properties of GaAs [210-21 2], optical properties of GaAs and GaP [213-215], and various photonic devices (photodiodes, lasers, quantum well lasers and LEDs) [216-2251. Certain general comments can be made that a1 e derived from this body of work which are relevant to the issue of radiation effects in semiconductor modulators. These comments include the. following:

Neutron irradiation studies [201] of high electron mobility transistors (HEMTs) have revealed that these devices are surprisingly resistant to irradiation. Although a neutron fluence of approximately 1014 n/cm^2 causes a significant reduction in

electron mobility (about a factor of 4), the transconductance of the HEMT does not decrease much because the carriers are in velocity saturation. Thus, although the undoped GaAs wells in which the electrons move are relatively pristine because of a lack of dopant atoms that can act as scattering centers, these devices are not particularly susceptible to displacement damage. Therefore, the delta-doped MQW lateral field modulator mentioned above will be more resistant to irradiation than one might expect.

It has been known for some time that neutron-induced displacement damage in GaAs and AlGaAs has unique features compared with point defects generated by electrons and protons [226,227]. In particular, as shown in Figure 13, neutron irradiation causes a broad smearing of the absorption edge with significantly greater absorption at photon energies well below the band gap energy. This general result suggests that modulators that depend on electric field-induced changes in exciton absorption (QCSE), as shown in Figure 10, to achieve modulation maybe strongly affected by neutron irradiation. These effects would be accentuated in those modulators constructed so that the light beam makes multiple passes through the MQW region (Fabry-Perot and reflection modulators).

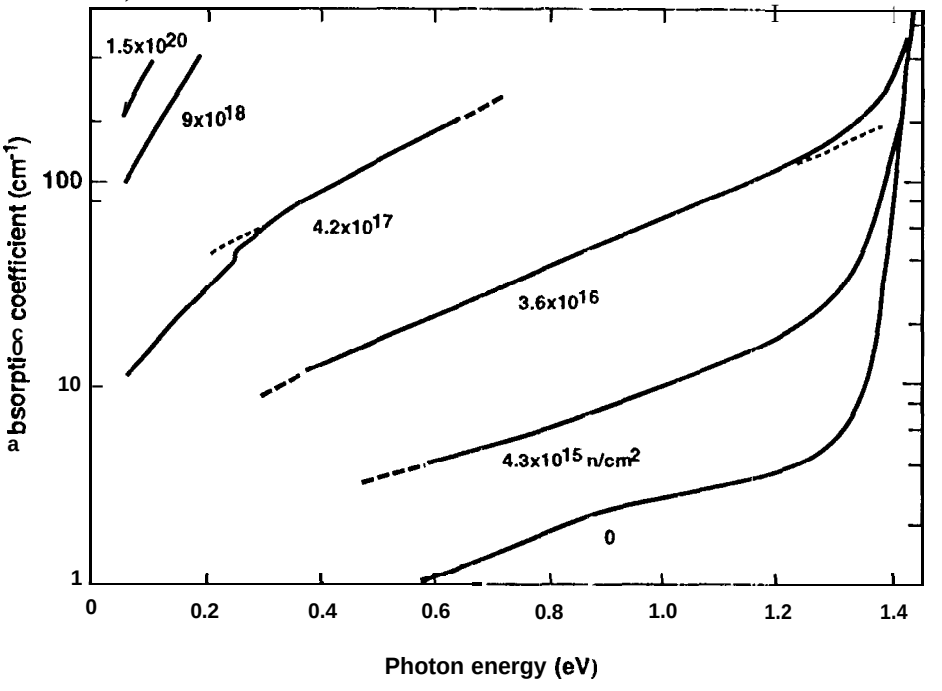

Figure 1.?. The effect offast neutron irradiation on the absorption spectrum of GaAs [227].

With regard to ionizing radiation effects (total ionizing dose: TID) in GaAs, this material is much more resistant than standard Si CMOS circuits. This is because the SiO_2 gate and field oxides in Si devices are very susceptible to ionization-induced changes caused by trapping of holes and interface state creation at SiO_2/Si interfaces. Essentially, there is no analogous effect in GaAs/AlGaAs devices and TID effects are not usually a problem in 111-V devices. Thus, in photonic systems total dose effects arc usually considered only for the optical fiber portion and any Si digital or analog signal processing electronics in the system.

Since the minority carrier lifetime in GaAs is typically short (10s of nanoseconds compared to 10s to 100s of microseconds in Si), displacement damage-induced reductions in minority carrier lifetime are not as much of a problem in GaAs devices, such as LEDs, laser diodes, solar cells and bipolar transistors, that depend on minority carrier lifetime for their successful operation (this is why GaAs solar cells resist irradiation much better than Si solar cells). However, many studies [220-225,228-232] have shown that LEDs and laser diodes can experience significant degradation in light output at neutron fluences below 10^{14} n/cm^2. Thus, in T-SEED modulators, for example, that contain phototransistors that provide. gain, device degradation may occur at neutron (or proton) fluences that are near or below military requirements. In contrast, as we have noted above, in those modulators whose switching time is limited by carrier lifetime, irradiation may actually improve device performance.

Many of the representative modulators reviewed above contain biased i-regions as part of a diode structure. These diodes, as well as the photodetector portions of SEED devices, will be susceptible to transient upset and survivability require-

ments. These structures are designed to collect photocurrent generated by 1 ight signals, and they will perform this same function with transient ionizing radiation pulses. In addition, if modulator structures are grown on semi-insulating GaAs substrates, photocurrents generated in the substrate can last well beyond the pulse width of the ionizing radiation due to deep traps in the substrate material.

Neutron or proton-induced displacement damage can affect the performance of photodetectors by increasing the dark current and decreasing the responsivity of the devices [229,230]. These effects may also be seen in the photodetector controlled SEEDs discussed above.

Single event effects (SEE) occur in GaAs digital integrated circuits, such as static RAMs, just as they do in Si digital devices. There are differences in SEE response between Si and GaAs, such as less effect of diffusion in GaAs, but these are relatively subtle. SEE effects may be important for modulators in two cases: first, when the modulator is used as a storage element, and second, when the current transient induced by a single ion is large enough to affect device behavior. The SEED optical memory may be upsettable by a single ion, and if an ion impacts a SEED device between write and read operations, it would probably induce an error. In those modulator types that contain biased diodes with i-regions, single ion-induced photocurrents may well temporarily disrupt modulator function. In more traditional fiberoptic systems, recent data [233] on a MIL-STD 1773 fiber optic data bus onboard a Goddard SFC spacecraft has demonstrated that single ions interacting with the Si photodiode in the receiver have caused many current transients. Error correction circuitry and soft ware were used to force bus retries whenever these photocurrent pulses were detected.

Earlier we noted that the refractive index of a semiconductor material is dependent on carrier density and decreases with increasing carrier concentrations (see equation (8)). Displacement damage-induced carrier removal caused by protons, electrons and neutrons could result in an increase in refractive index in modulators with waveguides fabricated by variations in carrier concentration. However, because of the inverse dependence of refractive index on carrier density, this may be a positive effect. Recall that we mentioned a lightly doped GaAs region with a high index between an air interface and a heavily doped AlGaAs layer as one example of a waveguide structure. Radiation-induced carrier removal at moderate fluences will be more influential in the lightly doped GaAs than it will in the heavily doped AlGaAs. Thus, there may be a greater refractive index differential between the two regions after irradiation, which would increase light signal confinement in the waveguide.

At this point, we wish to briefly discuss one other issue involving semiconductor modulators that is related to radiation effects; that is, the use of these modulators as electromagnetic field sensors [234,235]. For some time the Navy has worked on the development of shipboard electromagnetic environment (EME) monitoring techniques utilizing electro-optic and fiber optic techniques. Because a significant portion of this emission from various sources is at high frequencies (above 10 GHz), the monitoring system must have high bandwidth. The key element in this system is an antenna coupled external modulator in which the EME modulates an input light beam from a laser diode coupled to the modulator via a polarization maintaining fiber. The modulated signal is then detected by a high speed photodetector. Both InGaAsP Franz-Keldysh and MQW QCSE InGaAs/InP modulators were compared with a $LiNbO_3$ Mach-Zender modulator in the EME sensor link. It was found that at lower frequencies (less than 20 GHz), the three modulator types performed equally we] 1, but above 20 GHz the semiconductor modulators were superior in performance.

A somewhat related radiation effects problem, although not one that should affect shipboard EME monitoring, is the observation of broad band electromagnetic damage in GaAs MESFETs [236]. Exposure of SiN_2 - passivated GaAs MESFETs to large pulses of electromagnetic radiation caused physical damage to the SiN_2 passivation layer and eventually led to gate-source metallization failure resulting in device failure. This type of radiation-induced physical failure, similar to high power laser damage to optic elements, is very different from the general subject of this review, and will only be important for application of photonic elements in SDI-like beam weapon scenarios.

6. SPATIAL LIGHT MODULATORS

Introduction

Spatial light modulators (SLMs) area diverse and complex class of devices that have in common the property that they provide a controlled and high speed method of changing the direction of a light beam, and also a method of spatially storing information. In this Section we depart somewhat from our format of the previous three Sections and include all materials used to fabricate devices in this class. We begin with a brief review of the operating characteristics of the various types of SLMS.

Operating Characteristics

Acousto-Optic Devices, Bragg Cells

Acousto-optic (AO) devices, including AO Bragg gratings, are an important class of SLM devices that are fabricated in a variety of materials **[39,40,237-241].** The AO effect occurs in photoelastic materials like $LiNbO_3$ and TeO_2, and is one form of stress-induced birefringence that is exhibited by these materials. When an acoustic wave, which can be either a longitudinal or transverse traveling wave, passes through a photoelastic material it causes a traveling wave of refractive index variations whose maxima and minima correspond with the peaks and troughs in the acoustic wave. These variations can be used to diffract an optical beam, the basis of operation for Bragg cells. An acoustic wave can also propagate as a surface acoustic wave (SAW) confined to a near-surface region like an optical waveguide. These longitudinal and transverse SAW modes are an important class of acoustic waves because they can interact efficiently with waveguided optical beams.

For a given power density in the acoustic wave, P_a, one can estimate the expected change in refractive index [39,40]. The maximum change in refractive index, Δn_{max}, is given by

$$An_{max} = \sqrt{\frac{P_a M_2}{2}}, \qquad M_2 = \frac{2 p^6}{\rho v} \tag{9}$$

where M_2 is an AO figure of merit, p is the photoelastic tensor or acousto-optic interaction coefficient, similar to the EO tensor or Pockels coefficient, r_{ij}, p is the material density and v is the acoustic velocity. Typical M_2 values are 6.95×10^{-15} s^3/kg for $LiNbO_3$ and 104×10^{-15} s^3/kg for GaAs. For an acoustic beam power of 1 W/mm^2, the value. of Δn_{max} is approximately 6x10-5 for $LiNbO_3$ [39]. While this change in refractive index is small, the. overall d infraction effect can be quite significant because the diffraction effects are accumulated constructively (or destructively) if proper phase matching is done. Note also the very strong dependence of M_2 on the magnitude of the refractive index, which favors materials such as $LiNbO_3$ that have large values of n. This strong dependence also suggests that small radiation-induced changes in the refractive index will lead to noticeable alterations in the AO effect and the functionality of these devices.

The optical-acoustic interaction in the Bragg cell or Bragg type modulator is similar to the volume diffraction of x-rays by multiple atomic planes in a crystal, termed the Bragg effect. For the proper acousto-optic effect to take place, the interaction length between the optical and acoustic beams must be relatively long. Multiple diffraction of the beam will then occur and a single diffraction lobe will be observed in the far field pattern. For maxii num interaction in the Bragg modulator, the optical beam should beat an input angle equal to the Bragg angle, θ_B, given by

$$\sin\theta_B = \frac{\lambda}{2\Lambda} \tag{10}$$

where A is the acoustic wavelength. The input angle is measured between the optical propagation direction and the perpendicular to the propagation direction of the acoustic beam. The first order diffracted output optical beam emerges from the modulator at an angle of $2\theta_B$ with the undiffracted Oth order beam. It can be shown [40] that the modulation depth, referred to as the modulation index, η_B, is given by

$$\eta_B = \frac{I_0 - I}{I_0} = \sin^2\left(\frac{\Delta\phi}{2}\right) = \sin^2\left[\frac{\pi}{\lambda}\sqrt{\frac{P_a M_2 l_i}{2a}}\right] \tag{11}$$

where I_0 is the transmitted intensity in the absence of the acoustic beam, I is the Oth order intensity with the acoustic beam present, $\Delta\phi$ is the phase shift experienced by the optical beam as it passes through the modulator, 1, is the interaction length between the optical and acoustic beams and a is the thickness of the acoustic beam. Of the terms in equation (11), only the AO figure of merit, M_2, should be susceptible to radiation through radiation-induced changes in the reflective index and the photoelastic tensor. In a SAW device where both the optical and acoustic beams are confined to narrow regions, one can also expect an indirect effect of radiation through a loss of optical waveguiding that will change the strength of overlap and interaction of the optical and acoustic beams.

Bragg modulators have been fabricated in a variety of materials and structures. For the highest efficiency it is appropriate to use a hybrid structure. For example, a modulation index of η_B=93% was obtained with an As_2S_3 film deposited on $LiNbO_3$ at λ = 1.15 μm and an acoustic surface wave frequency of 200 MHz [242.]. Later work has focused on monolithic devices but this is difficult because the materials with the best AO efficiencies - $LiNbO_3$, GaP, GaAs, TeO_2, $PbMoO_4$, α-quartz, $CaMoO_4$, Tl_3AsSe_3 - do not lend themselves easily to monolithic integration (with the exception of GaAs) with other types of electronic devices and fabrication techniques. $LiNbO_3$, GaAs and GaP are more appropriate for high frequency applications in the GHz range.

A wide variety of devices have been fabricated using the basic AO Bragg grating technique. These include beam deflectors, switches, spectrum analyzers, tunable filters and frequency shifters. These types of devices are usually used in laser systems to control the intensity and position of the laser beam. One example is a beam scanning system for a laser printer. The wide variety of Bragg cell devices is an outgrowth of the advantages of the AO Bragg grating, which are as follows:

1. One does not have to usc a mechanically produced grating.
2. The gratings can be finely spaced and close to each other.
3. The period of the grating can be varied by changing the acoustic frequency to easily produce filtering.
4. Several acoustic frequencies can be combined to generate gratings of different periods to produce multiple diffraction effects.
5. Compared with an EO modulator, AO modulators can operate with unpolarized light, and with relatively low voltage power supplies.

Photorefractive Devices, Holography

In our discussion of $LiNbO_3$ and $LiTaO_3$ modulators, the photorefractive effect was discussed and characterized as a detrimental effect that reduced the functionality of these modulators. However, the photorefractive effect is also responsible for an important number of photonic devices including certain types of holograres. Feinberg [243] has noted that laser beams can produce spectacular visual effects in strongly photorefractive crystals like $BaTiO_3$. Indeed, at the beginning of a recent Scientific American article on the photorefractive effect [244], the authors state that the "photorefractive effect maybe the key to developing computers that exploit light instead of electricity". Since we have already established that radiation can alter and/or induce photorefractive effects, it is important to consider these devices in this review.

As we have noted earlier, the photorefractive effect is due to a redistribution of charge in a nonlinear electro-optic crystal containing impurities that act as trapping centers. When a light beam with spatially varying intensity impinges on a photorefractive crystal, electrons in the regions of intense light become mobile and migrate to dark regions where they are trapped, leaving behind regions of fixed positive charge. This separation of charge sets up internal electric fields that vary spatially in the same manner as the intensity of the light beam. As a result of the electro-optic effect, the spatially varying electric field causes a corresponding spatial variation in the refractive index of the material. Thus, for a light beam with periodic spatial variation, one can create a grating, similar to the acousto-optic induced gratings mentioned above, without doing anything mechanical to the crystal. This effect has been exploited to produce interesting and useful photonic structures and devices such as real time holograms.

One way of obtaining periodic, spatially varying light within a photorefractive crystal is to use two laser beams which experience constructive and destructive interference with each other. The resulting sinusoidal variation of light produces a refractive index grating, also termed a refractive index volume hologram. The electric field and the corresponding spatially varying refractive index grating have the same periodicity as the interacting light beams, but they have a 90^0 phase shift with respect to the light beams. The phase shift is responsible for the phenomenon of two beam coupling which is unique to photorefractive crystals. In this effect, the grating deflects the light beams, and because of the phase difference, the two deflected beams interfere constructively and destructively with the two incoming beams. Depending on the crystal and its orientation with respect to the input beams, one of the beams gains energy from the other beam and emerges more intense than the input beam. Thus, this effect can be used in applications requiring transfer of energy between input beams, such as the manipulation of parallel analog input signals.

The interactions between coherent laser beams in photorefractive crystals has also lead to the phenomenon of phase conjugation and the many applications derived from this effect [237]. Initially, phase conjugation was observed as the result of

four wave mixing experiments. In these experiments, two laser beams impinge on a photorefractive crystal creating a volume hologram. One of the input beams contains an image and the other is a coherent reference beam so that the hologram contains the image information, A laser read beam directed opposite to the reference beam at the Bragg angle is used to reconstruct the diffracted image beam. The reconstructed image beam has the fascinating property of being the time-reversed or phase conjugate of the input image beam. Thus, even if the input beam has been purposely distorted, the phase conjugate beam will accurately reconstruct the image as long as it is passed back through the distorter. It is also possible for the reconstructed image beam to be more intense than the input image beam since it can derive energy from the other input beams. Notice that there are four beams involved in this process, thus the term four wave mixing. This phase conjugation effect is the basis for the phase conjugate mirror, a device with many potential applications in the fields of optical communications, high power laser control, reconfigurable optical interconnections and optical computing.

Phase conjugation can also be achieved more simply through the self-pumped phase conjugation effect [245]. In this scheme the two pump beams (reference and read beams in four wave mixing) are eliminated and the input image beam creates its own phase conjugate beam. This phenomenon occurs in part because of beam fanning - the scattering of the beam by defects which allows the scattered light to set up grating effects that accomplish the phase conjugation. It is also possible to construct phase conjugate mirrors from many types of nonlinear optical materials, but photorefractive crystals have important advantages, one of which is the ability to produce self-pumped phase conjugation. In addition, phase conjugation can be achieved in photorefractive crystals at relatively low laser power levels. Also, electrical contacts can be applied to the device and additional control can be exercised over optical processing by applied electrical signals.

Many photorefractive materials have been used to create energy coupling and steering, holography and phase conjugation. Examples are $BaTiO_3$, $LiNbO_3$, $KNbO_3$, InP, CdTe, GaAs and many other complex materials [246], including insulators, organics and semiconductors. Of these materials, GaAs is important because of the advanced state of III-V device processing, including the ability to perform band gap engineering, and the ability to integrate several types of functions on one substrate,

Other Spatial Light Modulators

In addition to the device types discussed above, there area large variety of other spatial light modulators (SLMs) that have been developed or are under investigation and development [241,247-259]. As early as 1985, Fisher [260] in a survey of SLMS tabulated 45 SLM device types in eighteen major categories. Considering that this field has grown very rapidly in the last ten years, one must conclude that there are a very large number of SLM device types under investigation and development. In this brief review, we will merely touch on a few of the major SLM types.

SLMS are a key component in many types of optical systems. In particular, they are critical for parallel optical and neural computing architectures. Very broadly, they consist of components that allow one to spatially modulate optical fields, usually in the form of a matrix or grid of parallel optical signals. SLMS consist of an addressing material and a material whose optical properties can be modulated so that the read beam can be altered by the properties of this material. Important properties of an SLM are high spatial resolution (greater than 100 line pairs/mm), large size (1000x 1000 pixels or more), high speed (MHz frame rates), high extinction ratios (greater than 1000: 1), gray level capability, low power and low cost. As in any complex electronic device, it is difficult to achieve all of these desirable properties in one device, and compromises are necessary depending on the specific application.

There are many ways one could categorize SLMS; for example, by function or basic material t ype. SLMS of one type or another have been fabricated in all three of the materials categories we have discussed for modulators: polymers, organics [252], insulators [24 1,255,256], **and semiconductors [24 1,257]. One might also classify SLMS according to whether they are all-optical addressable or electrically addressable. At this point in time the electrically addressable SLMS dominate because of their greater** speed and flexibility. Electrically addressable devices may be electron beam scanned [255] or driven by an active semiconductor device back plane [259], and are serial access devices whose resolutions are limited by pixel size. It is noted that as SLMS grow in size and performance demands, a point will be reached when all optical S1 .Ms will be superior.

Another way of categorizing SLMS is according to whether they contain a solid EO material or a liquid crystal for light modulation. Liquid crystal-based SLMS require only low voltages relative to the requirements for solid crystals like $LiNbO_3$, but have relatively low resolution and low frame rates. However, these characteristics are rapidly improving as extensive research continues to take place. For example, NTT has recently reported [261] an optically addressed ferroelectric liquid crystal light valve (LCLV) with a frame speed of 2000 frames/see. Some of the important types of SLMS are as follows:

1. Liquid crystal light valves (LCLVs) [247,250]. This optically addressable device, an example of which is shown in Figure 14, typically consists of a complex sandwich of thin film layers made up of glass or fiber optic face plates, transparent conductors, a photoconductor to allow optical addressing (writing) (CdS or amorphous Si, for example), a light blocking layer so that the writing light is blocked from the read side, a dielectric mirror to reflect the read beam back out, and the twisted nematic liquid crystal (LC) through which the read light passes on its way to and from the mirror, With no write beam-induced voltage from the photoconducting material (off state), the LC molecules, which are rodlike and have a birefringence related to the molecular orientation, are all oriented parallel to the surface of the conductor plates, and the read beam does not experience any polarization change passing through the LC. The write beam reduces the resistivity of the CdS photoconductor so that a voltage appears across the LC resulting in a twisting of the molecules toward the direction perpendicular to the plate surface. The molecular birefringence then causes a change in polarization of the read beam as it passes through the LC into and out of the structure. Polarizers and analyzers can be used to provide intensity or phase modulation of the altered read beam. A typical LCLV has a resolution of 40 to 60 line pairs/mm, a contrast ratio greater than 100:1, and a response time of 15 to 50 ms, limited by the time response of the nematic LC.

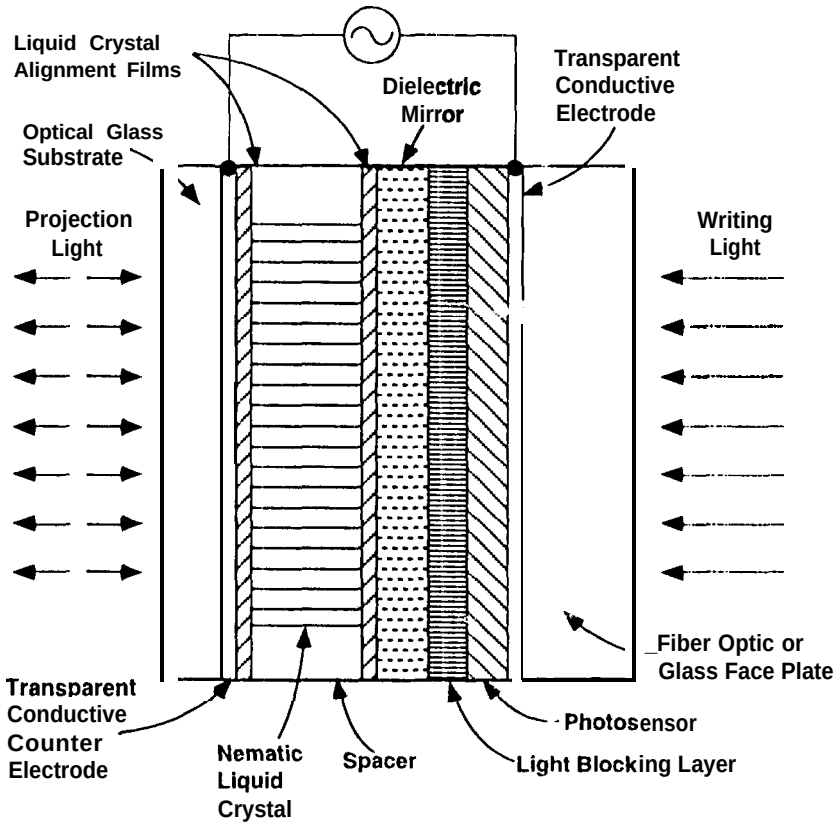

Figure 14. An example of a liquid crystal light valve (LCLV) spatial light modulator (SLM) [247].

2. Liquid crystal television (LCTV). The LCTV is a 90° twisted nematic liquid crystal sandwiched between two parallel polarizers. When no electric field is applied, the plane of polarization for linearly polarized light is rotated through 90° by the twisted LC molecules, and no light is transmitted through the second polarizer. Under an applied electric field, the twist of the liquid crystal molecules is altered, resulting in a greater fraction of the light maintaining the initial polarization direction and thus passing through the second polarizer. The primary advantage of typical commercial LCTVs is their low cost. However, the light transmission efficiency is only about 4% and the maximum contrast is about 10, precluding their use in certain photonic applications.

3. Silicon-based spatial light modulators (SLMs) [248,259]. Future high speed, parallel architecture computing systems will take advantage of the attributes of both optical signal processing and Si-based digital signal processing. Toward that end, work has been going on to integrate SLMS with Si CMOS technology. The principal challenge is mating the various technologies on a single substrate so that one obtains a high performance SLM integrated with digital processing elements. Various schemes have been proposed and attempted using both hybrid and monolithic concepts to integrate light modulators

with light detection and logic processing circuits. For those devices that propose using an EO modulator with standard photonic devices, such as laser diodes and detectors, our discussion of radiation effects in modulators and other photonic devices can be referred to for relevant information. Other schemes involve more esoteric techniques using ferroelectric liquid crystals imbedded in a Si substrate, and these applications must be considered in this section.

4. Magneto-optic (MO) SLMS [256]. These commercially available SLMS consist of a 2-dimensional array of MO shutter elements made up of epitaxial layers of magnetic garnet on a nonmagnetic substrate. In the presence of a strong magnetic field the shutter magnetic domains orient themselves along this field. When a linearly polarized light beam traverses the magneto-optic element, its polarization direction changes due to the Faraday effect. The polarization modulation of the light beam is transformed to a light intensity modulation or to a phase modulation by a polarizer/analyzer combination placed on the two sides of the SLM. These devices do not transmit a large fraction of the light beam even in the on-state. However, they are relatively fast, and 128x 128 commercial MO SLMS have been run at 350 frames/second.

5. **Microchannel SLM [258].** The MSLM is an optically addressed SLM consisting of a photocathode as an addressing material and an EO crystal such as $LiNbO_3$ as a modulating device in a vacuum sealed tube. The photocathode is used as a 2-dimensional photoelectric converter and a microchannel plate is used to multiply the 2-dimensional photoelectric signal that impinges on the $LiNbO_3$ for EO modulation. The MSLM can operate at very low writing light levels, but with a high readout light intensity at the same wavelength. The MSLM can perform image addition, subtraction, thresholding and memory retention.

6. **Electron beam addressed SLM [255].** In this device the electrical addressing device is the electron gun. The electron beam, whose intensity is proportional to the electrical input signal, bombards an EO crystal such as $LiNbO_3$ and modifies its optical properties so that the $LiNbO_3$ can modulate a read light beam in proportion to the input electrical signal.

7. **Electrically addressed ferroelectric liquid crystal (FLC) SLM [241,250].** This SLM contains a thin layer of FLC between two closely spaced glass electrodes. The FLC layer has two optical axis orientations, both parallel to the electrode plates but different in direction. These two optical axis states can be selected by voltages of opposite sign applied to the electrodes. If the polarization of the normally incident light is parallel to one of the optic axes, the beam will be transmitted through the FLC unaffected. Application of the opposite voltage switches the FLC optic axis so that as the incident beam passes through the FLC, its polarization is rotated through 90^0. Polarizers and/or analyzers can then be used to produce an intensity or phase modulated output beam. The advantages of the FLC SLM are small pixel size (17 mm x 17 mm) and high switching speed (switching times as low as 20 ns).

While the above list represents a cross section of SLM types, there are many variations of SLMS, and the literature on this subject has become enormous. In spite of this, however, our brief review does allow us to draw some insights about the effects of radiation on SLMS.

Radiation Effects on SLMS

It is not surprising that very little work has been done on radiation effects on SLMS. These devices represent a new field of research and device development, and most SLMS are quite complex devices, as illustrated in Figure 14. Their complexity and variety make it difficult to perform definitive radiation effects studies, and to interpret the results of such studies in a manner that can be generalized and applied to a variety of SLMs. The following discussion reviews the work in the literature on radiation effects on SLMS, and discusses the radiation effects implications of the operating characteristics and structure of SLMS.

Early studies [262-264] of radiation effects on quartz, and $LiNbO_3$ surface acoustic wave (SAW) delay lines investigated displacement damage from neutrons, CO-60 gamma ray effects and transient ionizing radiation effects. The results of these studies indicated that the delay lines were essentially immune to permanent radiation effects, but that some devices exhibited a response to high dose rate transient radiation bombardment. While the immunity of these devices to irradiation is encouraging, one cannot conclude that state-of-the-art SAW devices would behave similarly because of the improved quality of more recent devices, and because these were relatively simple delay lines rather than narrow band devices such as resonators or filters.

More recently, Hines, et al [265] examined various types of quartz SAW resonators for total dose effects using a variety of radiation sources. Several device characteristics were measured as a function of dose and no parameter showed any change

below 100 krads. Swept quartz substrate devices showed a negative shift in frequency at which a certain insertion loss is measured relative to a control device. However, these changes were small, even at 10 Megarads. The non-swept quartz devices showed much stronger positive frequency shifts to as much as 1 ?0 ppm at 10 Megarad of 40 MeV electron dose. While this is a larger change than the swept quartz devices, it is still much less than is typically exhibited by Si CMOS integrated circuits, even those with relatively good radiation hardness. The authors suggested that the frequency shifts were due to radiation-induced changes in the quartz surface material where the surface acoustic waves pr opagate through the crystal.

Recently, Taylor, et al [142,147,266] have examined radiation effects on $PbMoO_4$ AO devices, and found in the first study [266] that a transient x-ray pulse delivering 366 rad in 20 ns (1.8x 101" rad/see) caused an induced attenuation of about 2.5 dB for the optical signal traversing the AO grating device. Exposures at relatively low total dose levels near 9 krads at low dose rates did not alter the properties of this AO grating.

Later studies [147,266] detected the pulsed radiation-induced shift in the Bragg diffracted optical beam from AO Bragg grating devices fabricated from $PbMoO_4$, $Te0_2$ and InP. As shown in Figure 15, exposure. of a $PbMoO_4$ AO Bragg grating device to pulse trains of 15 MeV electrons from a LINAC demonstrated that the position of the diffracted optical beam shifts more and more with dose (15 to 386 krads) away from the pre-irradiation beam position. These shifts were attributed to radiation induced temperature increases in the active regions of the AO Bragg grating since measurements demonstrated that there was a significant temperature rise following the pulse train. Interestingly, the authors checked for temperature-induced changes in the Bragg angle, but found none. The authors also observed a decrease in diffraction efficiency with increasing dose and this was attributed to the introduction of color centers.

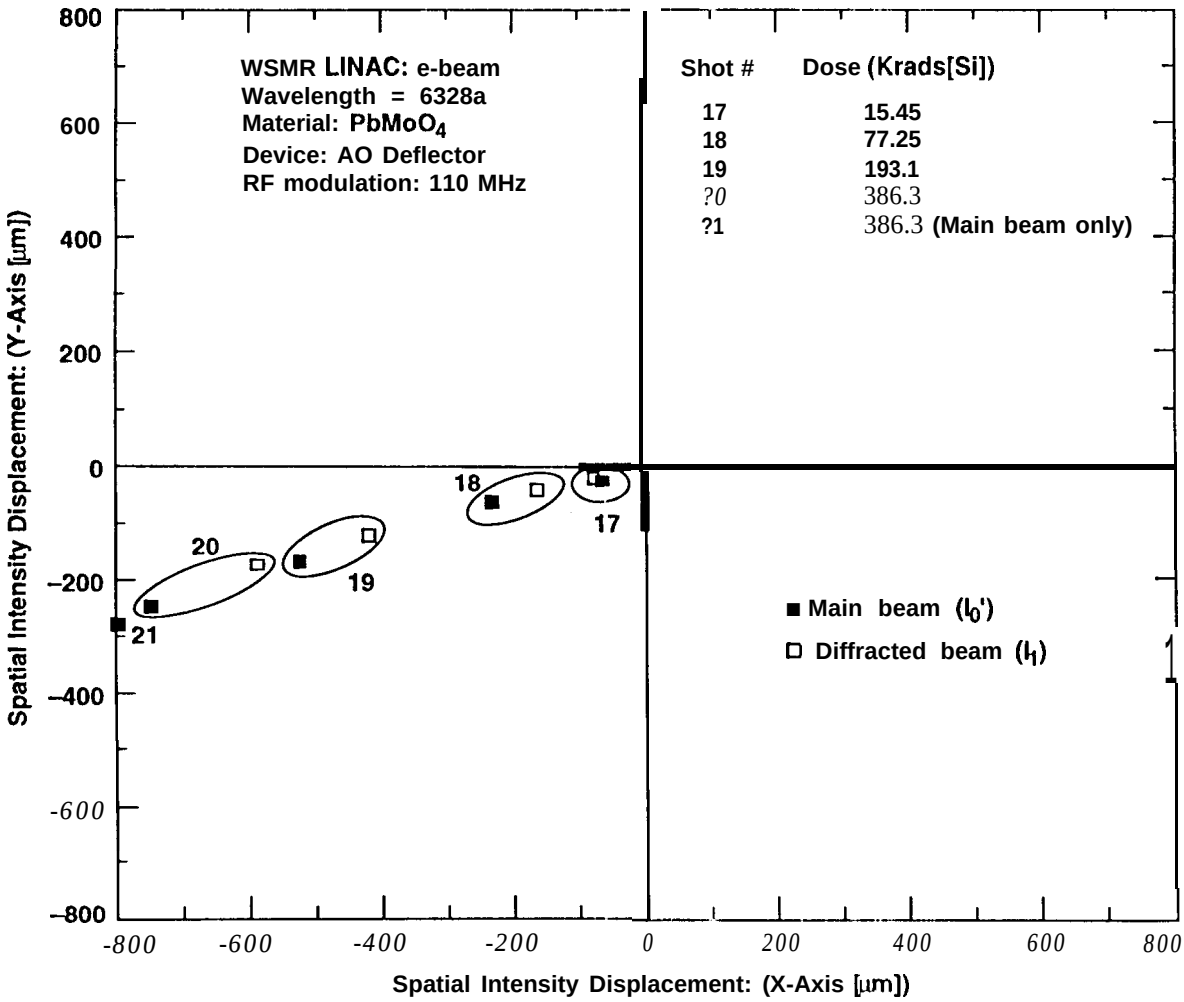

Figure 15. Peak radiation-induced spatial displacements of the AO deflector main and diffracted beams [266],

Taylor, et al *[267]* recently examined the effects of pulsed 15 MeV electrons and Co-60 gamma rays on a ferroelectric liquid crystal (FLC) light valve. This device was made up of glass cover plates enclosing the thin FLC layer. Transparent conducting coatings of indiurn-tin-oxide (ITO) were used as electrical conductors on the glass plates. Exposure of these FLC light valves to CO-60 irradiation up to a level of 67 krad showed no changes in characteristics of the FLC device. In contrast with these results, for electron exposure, permanent attenuation was observed at doses above 66 krad. No explanation was given for the difference in response to CO-60 and 15 MeV electrons. It was also noted that because the light valve 'could not be disassembled for radiation studies, the authors were not able to tell in which part of the device the radiation-induced attenuation occurred. The attenuation may have been due to darkening of the glass cover plates, since onc does not expect changes in organic based liquid crystal materials at doses as low as 100 krad. This is supported by recent electron irradiation studies of dispersions of nematic liquid crystals in polymers [268].

7. CONCLUSIONS AND RECOMMENDATIONS

In this Section we summarize our conclusions and recommendations for establishing radiation hardness assurance (RHA) for optical modulators, based on the technology assessment provided in previous Sections of this Review. We divide this Section in the same manner as the earlier Sections, and begin with our recommendations for polymer-based modulators.

One general comment regarding all modulator categories is appropriate: as work progresses in the qualification of modulators for application in radiation environments, there should be a clear separation between natural space environment applications and requirements, and applications intended for nuclear weapons-related environments. This is necessary because the latter environment will clearly be more difficult to satisfy. Dose rate and survivability requirements at very high dose rate levels may be difficult to meet for all modulator types, while the natural space environment does not include these highly stressing requirements. Thus, many more materials and devices may be appropriate for the natural space environment than for the weapons-related environment.

Polymer-based modulators

We strongly recommend that extensive radiation characterization of polymer materials and devices be undertaken for three principal reasons. First, as we noted earlier, polymer-based waveguides and modulators have many attractive features, not the least of which is an excellent compatibility with semiconductor processing technologies. Thus, one can anticipate that polymer-based devices will find broad usage in future photonic systems, Second, in spite of their positive attributes, before these devices can be employed in hardened systems their radiation response characteristics must bc thoroughly explored and defined. We have emphasized that many of the properties of polymers in general, and NLO-active polymers in particular, are susceptible to radiation effects. Third, the development of polymer waveguides and modulators is an emerging technology that still remains to be fully matured. One aspect of this early stage of evolution is that there have been only a very few studies of the effects of radiation on the material and device properties of polymer-based photonic devices, Another is that timely studies of radiation effects can provide guidance for further development of the technology in those directions that will lead to hardened, high reliability materials and devices. More specific recommendations are as follows:

1. Polymer-based materials, waveguides and modulators selected for radiation characterization should be restricted to those materials that have the highest reliability. In particular, EO devices that have the most stable poled state are the most desirable. Generally, this implies that materials with high glass transition temperatures, T_g, should be selected for study. Of the materials that we have mentioned in this review, polyamides presently come closest to satisfying this requirement.

2. As the technology is developed, alternative means, other than poling a polymer, for establishing permanent, strong EO activity maybe developed, such as insertion of dopant molecules directly in the polymer structure in such a manner that the resulting material is noncentrosymmetric. Any material that avoids the requirement of a highly stabilized poled state should be seriously considered for radiation study.

3. Other things being equal, like the stability of the poled state, polymer hosts should be chosen for radiation study that are most compatible with Si process technology. Here again, polyimides are desirable materials because they are already used in advanced Si process technologies such as the fabrication of stacked, multichip module structures.

4. The very limited number of radiation effects studies [41,42] of polymer-based waveguides and modulators indicates that fairly basic studies must bc performed that emphasize the discovery and elucidation of the basic mechanisms of the effects

of radiation. As we have noted in this Review, the refractive index and the electro-optic coefficient are critical material parameters whose response to irradiation must be established.

S. Our Review suggests that there may be polymer EO structures that will actually improve with exposure to ionizing radiation. We have seen that radiation can increase the refractive index of a polymer, and that greater stability of the poled state can be achieved by radiation exposure following poling. Such possibilities should clearly be borne in mind as materials and fabrication techniques are selected for radiation study.

6. A particularly attractive area for the application of polymer-based modulators is the modulation of microwave signals. As we have noted, polymers are well-suited for these applications because the optical and microwave refractive indices are essentially equal. As a result, successful modulation at several tens of GHz has been achieved. Polymer-based microwave traveling wave modulators and related test structures should be subjected to radiation with the intent of measuring the effects of radiation on the devices and also on the optical and microwave refractive indices. If these two indices are affected at different rates by radiation, either high dose rate or total dose, then there may be an observed reduction in the maximum frequency at which modulation can be achieved.

7. A radiation effects study should be carried out that focuses on the investigation of the response of various poling parameters to radiation. A matrix of parameters should be selected, such as method of dopant incorporation, poling field, atmosphere and temperature, post-poling treatment, and extent of post-poling crosslinking. Then, the effects of radiation on a set of EO-active samples in which these parameters are intentionally varied should be determined,

8. Once the radiation effects responses of polymer-based EO devices are well-characterized and established, then RHA guidelines and device specifications should be developed for this important class of photonic devices.

9. Lastly, we conclude that in spite of the fact that this technology is not fully matured, it holds very exciting prospects for applications in high reliability, hardened systems. The polymer-based modulator technology has many advantages, and while susceptible to various types of radiation effects, generally large radiation doses arc required to cause significant changes. Certainly, most of these radiation effects will occur at doses above typical natural space environment mission requirements. In addition, we have seen that radiation is often used as a tool to improve the performance and quality of these materials and devices. It should be emphasized also that the radiation effects community must pay particular attention to the reliability aspects of this technology so that hardness assurance and high reliability can be simultaneously achieved.

Insulator-based modulators

Before listing specific recommendations based on our review of radiation effects in $LiNbO_3$ and $LiTaO_3$, we wish to make two general recommendations. First, the very rapid recent progress and intense level of effort on the development of EO devices in polymers and semiconductors suggests that these material classes may surpass $LiNbO_3$ and $LiTaO_3$, even though the latter materials enjoy a greater commercial availability at the present time. As we have already pointed out, there are inherent advantages in using polymers and semiconductors compared with $LiNbO_3$ and $LiTaO_3$ devices. Thus, the polymer and semiconductor EO technologies may "leapfrog" those of $LiNbO_3$ and $LiTaO_3$. In addition, if $LiNbO_3$ and $LiTaO_3$ are rapidly surpassed by polymers and/or semiconductors in quality and capability, then their commercial availability may actually be significantly less in the future. Thus, an effort should be made to determine as precisely as possible what the projected future of these devices is and what role they will play in military and space systems. It is also important to note that the availability of these devices for military applications will be influenced by the general commercial availability, which will be driven in turn by their attractiveness relative to polymer and semiconductor EO devices. An examination of the future general commercial viability of $LiNbO_3$ and $LiTaO_3$ EO devices is outside the scope of this Review, but there is enough uncertainty in future directions to warrant undertaking such an assessment before committing significant resources to hardening efforts on $LiNbO_3$ and $LiTaO_3$ EO devices.

Second, with regard to an RHA effort in $LiNbO_3$ and $LiTaO_3$ EO materials and devices, we recommend two broad parallel efforts that will build on the work that has been done previously: 1) studies of the basic mechanisms of radiation effects, including effects of various dopants and waveguide fabrication techniques, and 2) studies of radiation effects on state-of-the-art EO devices. These efforts can be carried out simultaneously, and the results of the basic mechanisms studies should feed into process modifications that will produce EO devices with greater radiation hardness assurance.

Specific recommendations are as follows:

1. Except for applications with extremely high radiation requirements, our review indicates that the primary problem in these materials is transient ionizing radiation effects that cause long lasting detrimental effects following the radiation pulse. From this perspective, $LiNbO_3$ and $LiTa0_3EO$ devices are similar to fibers which also exhibit severe, long lasting transient effects. We emphasize, however, that as material quality improves, these devices could become more sensitive to permanent ionizing radiation effects so that observed total dose failure levels may become more of an issue.

2. In order to determine the effects of various dopants and fabrication techniques on radiation susceptibility in $LiNbO_3$ and $LiTaO_3EO$ devices, studies should be carried out on high quality materials that have reproducible, consistent properties, This requirement strongly argues for a teaming effort between a materials/device vendor and a radiation effects laboratory. The test vehicle for conducting these studies should be sophisticated enough to examine several relevant properties, but simple and straightforward enough to have some prospect of sorting out and interpreting the various observations. We recommend either a directional coupler with electrodes or a Mach-Zender interferometer, or better yet, both types of structures. It has been shown [162] that Mach-finder structures provide a definitive measure of photorefractive effects. We note that the activities at Phillips Laboratory are in this direction, and we look forward to further progress from the PL Group.

3. Of particular importance in the basic radiation effects studies will be the effect of MgO and the comparison of $LiNbO_3$ with $LiTaO_3$. We have pointed out that MgO minimizes the photorefractive effect and seems to prevent the introduction of at least some of the radiation-induced absorption bands in $LiNbO_3$ [156]. While several papers have compared $LiNbO_3$ and $LiTaO_3$, for various reasons noted above, it is still not clear which material is the least sensitive to ionizing radiation, although one might anticipate that $LiTaO_3$ is harder because it is more immune to photorefractive effects.

4. It is also not clear whether Ti-diffused or proton-exchanged (PE) $LiNbO_3$ is inherently the least susceptible to radiation effects. Interesting comparisons should be possible by examining radiation effects in devices with waveguides fabricated with these two techniques. It is imperative that the starting material for both types of devices be the same in order to eliminate other possible differences. Recall that in PE $LiNbO_3$, the ordinary refractive index, n_o, actually decreases so that there will be no waveguiding effect using this refractive index. For example, in z-cut material only the TM mode will be guided in a PE-produced waveguide. Differences that are observed between the radiation responses of these. two types of waveguides should allow one to more clearly identify radiation effects mechanisms.

5. It is imperative that radiation effects studies include the effects of bias on the response of the device to irradiation, whether permanent or transient exposures are used. As we have pointed out, as yet there has been essentially no work done on the effects of bias on radiation susceptibility. Although the exposure levels and dose rates in recent investigations are probably higher than most practical program radiation requirements, the observation, that dramatic oscillations in waveguide output can persist for minutes after a large radiation pulse warrants further attention. As in the case of fibers, a strong transient response that lasts only as long as the radiation pulse, as in the case of photoluminescence, for example, is not nearly as detrimental as very long term effects that linger after exposure to a pulse of radiation.

We have noted that electrodes are used to allow the degree of transfer of light from one guide to another to be selectable. In the reverse-$\Delta\beta$ switched coupler, bias can be applied to cause either no switching or 100% switching. This ability to "clamp" the amount of light transfer between guides may have. significant implications for quickly removing the extended oscillations that have been observed after pulsed irradiation. In addition, it may be possible do design a feedback circuit in which detected radiation-induced variations in light output are used to modify the voltage in order to hold the energy transfer constant and independent of time following the radiation pulse.

6. We noted earlier the important new class of devices that employ rare earth dopants to achieve laser action within the $LiNbO_3$ material. Because of their potential usefulness, these devices should be examined for radiation effects vulnerability.

7. Although not specifically reviewed herein, there are many types of very sophisticated and specialized $LiNbO_3$ EO devices being developed at various research laboratories and commercial vendors. Representative devices of this caliber should be selected for radiation effects evaluation. Permanent total dose effects should be checked to be sure that these effects are only observed at very high dose levels. Attention should then be given to transient effects in these devices. These tests will be complex and should be conducted by a team of device developers and radiation efi ects experts. Device functionality in typical circuit

applications should be checked as well as parametric measurements to detect degradation in important parameters, both as a function of dose and as a function of time after a radiation pulse,

8. **With regard to the issue of other types of radiation** exposure, in particular, neutron, proton or electron bombardment, we do not see the need for studying permanent displacement damage effects due to neutrons or protons. As we have pointed out, $LiNbO_3$ and $LiTaO_3$ are not pure materials with perfect lattice structures. Significant lattice damage effects due to neutrons will only be observed at neutron fluence levels well above any conceivable program requirements. There also is no evidence to suggest that one form of ionizing radiation is more appropriate than another. For example, as long as dosimetry is properly done and charge yield is taken into account for proton irradiation, it should be possible to equilibrate proton and ^{60}Co irradiations to determine the effects of ionizing radiation. The device does not know the history of the deposited ionizing energy that creates excess electron-hole pairs.

9. Although we have not discussed SiO_2-based waveguides and IO devices at any length, they pose interesting contrasts with regard to radiation hardness assurance. On the one hand, they are particularly attractive from an integration point of view because of the well-established technology of CMOS Si devices. However, it is also well-known that the Si/SiO_2 interface is very susceptible to ionizing radiation damage. For waveguides located near such interfaces, one can expect that the waveguide properties will be perturbed by the sensitivity of this interface to radiation effects. However, we do recommend that the effect of radiation on such waveguides be examined in order to determine whether they are in fact as sensitive as one might expect them to be.

Semiconductor-based modulators

Our recommendations for radiation effects testing efforts in the area of III-V semiconductor modulators are based primarily on our earlier comments relating previous radiation effects in III-V materials and devices to issues concerning modulators. These recommendations are as follows:

1. Of paramount importance will be the determination of the effects of neutron and proton-induced displacement damage on the QCSE, and modulators that depend on the QCSE for functionality. Relatively simple structures should be used so that the various possible effects of displacement damage can be sorted out. We recommend using something similar to the transverse electro-absorption modulator described earlier (see Figure 11). In addition a structure should be used that would allow recording of absorption spectra as a function of fluence. The ability of the device to modulate an optical signal, including measurement of the extinction ratio, should be studied as a function of bias and fluence. The reverse bias electrical characteristics of the *p-MQWi-n* diode should also be monitored as a function of fluence in order to detect changes in dark current.

2. For those modulator structures that contain biased *p-i-n* diodes, it will be important to perform transient upset testing to determine the response of the modulator to this environment, One can expect that large photocurrent pulses will be generated in the *p-i-n* diodes by the transient ionizing radiation. In the various SEEDS, for example, the radiation pulse will produce the same result as an intense controller light beam - large current flow will reduce the bias across the modulator portion of the device. Because the SEED depends on feedback for its operation, it maybe possible. to design an error detection and correction (EDAC) circuit in which the photodiode detects the pulse and initiates a circumvention and correction procedure.

3. Similar to 2. above, we recommend single event testing of modulators containing biased *p-i-n* diodes. As in the case of the 1773 fiber optic link [233] containing Si detectors, current pulses generated by single ions may produce false signals in the optical information bit stream. EDAC techniques should also be applicable to this case.

We note that a more attractive and fundamental solution to the general issue of the sensitivity of photodetectors, and modulators containing these devices, to transient ionizing radiation is to avoid first window (820 -900 nm) photonics that employ Si detectors. Because Si is an indirect bandgap material, wide *i* regions are required in *p-i-n* photodiodes in order to achieve satisfactory responsivity to light signals. However, in direct band gap materials like GaAs and InGaAsP, sufficient responsivity can be realized with much thinner active regions, which minimizes the sensitivity to ionizing radiation pulses. Thus, for radiation environments second (1300 nm) and third (1550 nm) window photonic systems that use III-V detectors are more appropriate [269,270]. An added benefit is that most fibers are less sensitive. to total dose at these longer wavelengths. Fortunately, in the case of modulators, all of the photodetector structures we have mentioned above are, in fact, built in III-V materials.

4. When integrated photonic circuits that contain modulators together with other photonic devices on a single Si substrate, along with Si analog and digital electronics, become available, it will be important to perform total dose testing to determine if oxide-related effects in SiO_2 regions cause detrimental effects to overall circuit performance.

5. A fundamental study should be conducted of the effects of displacement damage on the refractive index in relevant III-V material families like GaAs, AlGaAs, InGaAsP and InGaAs. In addition, absorption spectra over relevant wavelength ranges should be measured. The fact that absorption effects and index effects are interrelated suggests that subtle and complex results may be obtained that may have been difficult to predict. These results will also be affected by radiation-induced carrier removal.

6. We have noted above that displacement damage causes a reduction in minority carrier lifetime, and that, in spite of the fact that lifetimes in most III-Vs are much shorter than in Si, LED and laser diode degradation can be observed at relatively low neutron (and proton) fluences. This effect is particularly strong in amphoterically Si doped (where Si is the dopant in both *p* and *n* regions) GaAs devices because of the long minority carrier lifetime, approaching that of some Si devices, in these materials. Therefore, modulator structures that contain phototransistors or other bipolar devices, should be avoided, or at least, radiation effects testing should be done on such modulators.

Spatial light modulators

1. With regard to radiation effects, two general attributes we can ascribe to SLMS are that these are complex devices, making it difficult to sort out radiation effects mechanisms, and very little work has been done as yet on radiation effects in SLMS. The complexity and variety of SLMS suggests that radiation effects studies will have to be done on a case-by-case basis, and that it will be extremely difficult to derive general characteristics about radiation response that will be widely applicable to many SLM types.

2. Many of the components that make up SLMS are similar to the modulator structures we have already discussed. These materials and devices, and also liquid crystals, should be relatively hard to total dose ionizing radiation effects since they are relatively imperfect materials.

3. An exception to the above statement is the class of SLMS that are based on Si substrates, and contain Si devices of one sort or another. If in the process of integrating various types of device structures on a Si substrate, SiO_2 oxide isolation techniques are used, then one should take care to detect oxide-related total dose effects which are well known to occur at relatively low doses in commercial Si integrated circuits.

4. Perhaps the most susceptible radiation scenario is the exposure of an SLM to an intense transient pulse of ionizing radiation while the device is being addressed or read. For those applications with a transient upset requirement, it would be appropriate to study SLM behavior during and after exposure to a radiation pulse during which addressing and/or reading of the SLM is taking place. Intense ionization may well distort the addressing and reading processes.

5. Along the same lines, those SLMS, such as real time holograms, that are used for storing information, even temporarily, should be exposed to transient pulses to determine if the information contents of the storage elements are affected by intense ionization.

6. It should be possible to study twisted liquid crystals as a function of radiation exposure. Does ionizing radiation alter the physical configuration of these materials and the ability of bias to change the physical arrangement of the molecules? These are questions that are relevant but probably only to applications with transient pulse requirements and/or very high total dose requirements.

7. SLMS containing GaAs components may be affected by neutron and/or proton-induced displacement damage effects. This would also be true of SLMS that contain standard photonic elements such as microdot lasers or photodiodes.

8. Those SLMS that depend on Si photodiodes for their operation will be sensitive to pulsed ionizing radiation and should be checked for these effects.

9. In the case of acousto-optic devices, test structures should be designed that allow one to determine the effect of

irradiation on the elastic and acoustic properties of the material without the interfering effects of radiation-induced changes in optical properties. Certainly, one would expect the elastic properties of materials to be temporarily altered by intense transient pulses of ionizing radiation. Care must be taken to insure that the observed effects are not clue to changes in some other external parameter such as temperature.

10. Radiation effects tests of SLMS will be complicated to conduct and difficult to interpret. They should be carried out with special attention to closely controlling all external parameters such as temperature and bias. Such studies should be conducted by teams of SLM experts from the SLM vendor, and radiation effects experts.

8. ACKNOWLEDGMENTS

The authors wish to acknowledge partial support of this work by the Jet Propulsion Laboratory, operated by the California Institute of Technology under contract to NASA, and by the Defense Nuclear Agency.

9. REFERENCES

1. T. Findakly, C.C. Teng and L. Walpita, "Wideband NLO organic external modulators", *SPIE Proc.* **1476**, *14* (1991).

2. R.T. Chen, "Polymer-based photonic integrated circuits", *Optics and Laser Tech, 25,347 (1993).*

3. R.T. Chen, "Polymer-based passive and active guided wave devices and their applications" in *integrated Optics and Optoelectronics,* K. Wong and M. Razeghi, Editors, *SPIE Proc. CR45, 198 (1993).*

4. C.C. Teng, M.G. Scaturo and T.K. Findakly, "Very high speed polymeric external modulator with more than 40 GHz of 3-dB electrical bandwidth and low drive voltage", *Integrated Photonics Research* **10**, *196(1 992).*

5. G.F. Lipscomb, R. Lytel, S. Ermer, J.F. Valley, T.E. Van Eck, D.G. Girton and A.J. Ticknor, "organic electro-optic devices for optical interconnection", *SPIE Proc.* **1774**, *76(1993).*

6. D. K. Paul, B. Markey, R. Hefele and B. Pontano, "Organic polymer integrated optical channel waveguide devices", *SPIE Proc.* **1849**, 342(1993).

7. A. Beuhler, D. Wargowski, T. Kowalczyk and K. Singer, "Optical polyamides for single mode waveguides", *SPIE Proc.* **1849**, *92 (1993).*

8. T. Van Eck, D. Girton, J. Valley, S. Enner, A. Ticknor, G. Lipscomb and R. Lytel, "Chip-to-chip interconnects using poled polymer integrated optic transmitter networks", *SPIE Proc.* **1849**, *27 (199?).*

9. S. Jabr, "The economics and technology of integrated optical modulators: 1969-1999" p. 180 in in *Integrated Optics and Optoelectronics, SPIE Critical Reviews of Optical Science and Technology* **CR45**, K. Wong and M. Razeghi, Editors (1993).

10. R. Lytel, "Applications of electro-optic polymers to integrated optics", *SPIE Proc. L216,30(1990).*

11. H. Lee, R. Hughes, Jr., J. Davis, C. McConaghy, A. Hamza and M. Balooch, "Feasibility of high speed all-optical switching with fullerene thin films", *AFCEA '94, 215 (1994).*

12. H. Takahara, s. Koikc, S. Yamaguchi and H. Tomimuro, "Optical waveguide interconnections for optoelectronic multichip modules", *SPIE Pmt.* **1849**, *70 (1993).*

13. D. Burland, R. Miller, R. Twieg, W. Volksen and C. Walsh, "Assessment of polymeric materials for second harmonic generation and optoelectronic applications", *SPIE Proc.* **1852**, 186 (1993).

14. W. Horsthuis, J. Heideman and M. Klein-Koerkamp, "Recent developments in polymeric devices", *POF* '93 *Proc., Second Inter. Conf. on Plastic Optical Fibers and Applications,* p. *20 (1992).*

15. J. Frechet, J. Beecher, T. Durst and A. Godt, "Preparation of stable photopatternable polymeric materials for non-linear optics", Cornell University Report No. TR-12, (1993).

16. J. Chen, S. Najafi and S. Honkanen, "Polymer glass waveguide all-optical switches", *SPIE Proc.* **1794**, 388 (1992).

17. K. Rajasekharan, C. Ober and N. Johnen, "Photoimageable polymer waveguides for optoelectronic applications", p. 464 in *LEOS '93 Conf. Proc. (1993).*

18. G. Bjorklund and D. Burland, "Prospects for electro-optic polymer devices", p. 466 in *LEOS* '93 *Conf. Proc.* (1993).

19. P. Prasad and D, Williams, *Introduction to Nonlinear Optical Effects in Molecules and Polymers,* John Wiley & Sons (1991).

20. S. Bethke and S. Grubb, "Atmospheric effects on corona poling, of nonlinear optical doped polymer films", *SPIE Proc.* **1216**, *260 (1990).*

21, K. Beeson, M. McFarland, W. Pender, J. Shari, C. Wu and J. Yardley, "Laser written polymeric optical waveguides for integrated optical device applications", *SPIE Proc.* **1794**, 397 (1992).

22. P. Cahill, C. Seager, M. Meinhardt, A. Beuhler and D. Wargowski, "Polyimide-based electro-optic materials", Sandia National Laboratories Report No. SAND-93 -0336C, 1993.

23, C. Feger, "Evaluating polyamides as lightguide materials", *Appl. Optics, 27,* 21 (1 988).

24. J. Salley, T. Miwa and C. Frank, "Intramolecular charge transfer in aromatic polyamides", Mat. *Res, Soc. Proc.* **227**, 117 (1991).

25. W. holland, M. Kuzyk, K. Singer and J. Sohn, "Non-linear optical polymer films", p. 300 in *Tech. Digest, 14th European Conf. on Optical Comm. (1988).*

26. S. Ermer, J. Valley, R. Lytel, G. Lipscomb, T. Van Eck and D. Girton, "DCM polyimide system for triple track poled polymer electro-optic devices", *Appl. Physics Lett.* **61**, *2272 (1992).*

27. K. Chakravorty, "Ultraviolet defined selective in-diffusion of organic dyes in polyimide for applications in optical interconnect technology", *Appl. Phys. Lett. (ii,* 1163 (1992).

28. C. Sullivan, "Optical waveguide circuits for printed wire board interconnections", *SPIE Proc.* **994**, *92 (1988).*

29. D. Hewak, F. Picard and H. Jin, "Optical waveguides in polyimide by direct laser writing utilizing thermal curing", p. 265 in *Proceedings of the First International Workshop on Photonic Networks, Components and Applications (* 1991).

30. Y. Chen, R. Jeng, L. Li, X. Zhu and J. Kumar, "Stable second order nonlinear optical epoxy-based polymer", *Molecular Crystal Liquid Crystal Science and Technology Section B: Nonlinear Optics* **4**, *71 (1993).*

3]. G, Meredith, J. VanDusen and D. Williams, *Macromolecules* **15**, 1385 *(* **1982).**

32. C. Ye, N. Minarni, T. Marks, J. Yang and G. Wong, "Persistent, efficient frequency doubling by poled annealed films of a chromophore-functionalized poly(p-hydroxystyrene)", *Macromolecules* **21**, 2899 *(1988).*

33. H. Hampsch, G. Wong, J. Torkelson, S. Bethke and S. Grubb, "Second harmonic generation in corona poled polymer films as a function of processing atmosphere and corona polarity", *SPIE Proc.* **1104,** 268 (1989)..

34. D. Haas, H. Yoon, H. Man, G. Cross, S. Mann and N. Parsons, "Polymeric electro-optic waveguide modulator: materials and fabrication", *SPIE Proc. ill,* 222(1989).

35. D. Jungbauer, B. Reck, R. Twieg, D. Yoon, C. Wilson and J. Swalen, "Highly efficient and stable nonlinear optical polymers

via chemical cross-linking under electric field", *Appl. Phys. Lett.* **56**, 2610 (1990).

36. M. Eich, B. Reck, D. Yoon, C. Wilson and G. Bjorklund, "Novel second-order nonlinear optical polymers via chemical cross-linking-induced vitrification under electric field", *Jour. Appl. Phys.* **66**, *3241 (1 989).*

37. C. Willand and D. Williams, *Ber. Buns. Gs. Phys. Chem.* **91**, *1304 (1987),*

38. Y. Chen, R. Jeng, L. Li, X. Zhu and J. Kumar, "Stable second order nonlinear optical epoxy-based polymer", *Molecular Crystal Liquid Crystal Science and Tech. Section B: Nonlinear Opticsg,71 (1993).*

39. R. Syms and J. Cozens, *Optical Guided Waves and Devices,* McGraw-Hill, New York, NY (1992).

40. R. Hunsperger, *Integrated Optics: Theory and Technology,* Springer-Verlag, New York, NY (1984),

41. A. Kanofsky and W. Herman, "Radiation effects on polymer waveguides", *SPIE Proc.* **1794**, *234 (1992).*

42. W. Herman and A. Kanofsky, "Radiation effects on polymer waveguides: accelerated aging tests", *SPIE Proc.* **2074**, *192* (1994).

43. G. Pettit and R. Sauerbrey, "Pulsed ultraviolet laser ablation", *Appl. Phys. A* **A56**, 51 (1993).

44. A. Brezini and N. Zekri, "X-ray photoelectron spectroscopy analysis of polyimide films modified by ultraviolet pulsed laser radiation at 193 rim", *Jour. Appl. Phys.* **75**, *2015 (1994).*

45. E. Arenholz, J. Heitz, M. Wagner, D. Bauerle, H. Hibst and A. Hagemeyer, "Laser-induced surface modification and structure formation of polymers", *Appl. Surface Science 69, 16(1993).*

46. E. Eremeeva, M. Votinov, A. Dokukina, V. Ovchinnikov and Z. Smirnova, "Effect of low molecular weight additives on the radiation strength of transparent polymers", Sov. *Jour. Optical Tech.* **53**, 361 *(1986).*

47. P. Demkovich, M. Kotlyar, V. Kulagin and K. Sonin, "Modification of the optical properties and dynamics of laser ultraviolet ablation of polyamide", Sov. *Jour. Quantum Elec.* **22**, *400 (1992).*

48. A. Aleshin and A. Suvorov, "Inversion of the type of conduction in ion irradiated polyimide films", Sov. *Phys. - Solid State* **35**, *364 (1993).*

49. R, Jeng, Y. Chen, B. Mandal, J. Kumar and S. Tripathy, "UV-curable epoxy based second order nonlinear optical material", *Proc. of Electrical, Optical and Magnetic Properties of Organic Solid State Materials Symposium, 111 (1992).*

50. P. Cahill, C. Seager, M. Meinhardt, A. Beuhler and D. Wargowski, "Polyimide based electrooptic materials", *Sandia National Labs. Report No. SAND-93 -0336C (1 993).*

51. J. Chen, R. Moody, Y. Chen, J. Lee, S. Sengupta, J. Kumar and S. Tripathy, "Dielectric study of a photocrosslinkable nonlinear optical polymer", *Pmt. of Electrical, Optical and Magnetic Properties of Organic Solid State Materials Symposium, 223 (1992).*

52. K. Chakravorty, "Photogeneration of refractive index patterns in doped polyimide films", *Appl. Optics* **32**, *2331* (1993).

53. R. Rye, "Spectroscopic evidence for radiation-induced crosslinking of poly(tetrafluoro-ethylene)", *Jour. Polymer Sci.* **31**, *357 (1993).*

54. R. Jones, G. Salmon and I. Ward, "Radiation-induced crosslinking of polyethylene in the presence of acetylene: a gel fraction, UV-visible, and ESR spectroscopy study", *Jour. Polymer Sci.* **31**, *807 (1993).*

55. Y. Zhao, D. Poirier and R. Pechman, "Electron stimulated polymerization of solid C_{60}", *Appl. Phys. Lett. 64,577* (1993).

56. D. McHerron and G. Wilkes, "Electron irradiation of polystyrene-poly (vinyl methyl ether) blends", *Polymer* **34**, 3976 (1993).

57. N. Betz, E. Balanzat, A. Le Moel and J. Duraud, "Grafting of polymers after swift heavy ion irradiation", *Radiation Effects in Solids* **126**, *221* (1993).

58. C. Hoyle, D. Creed, P. Subramanian, R. Nagarajan and C. Pandey, "Photodegradation of polyamides: effect of donor-acceptor groups on the photooxidative stability of polyimides and model compounds", *Univ. Southern Mississippi Tech. Report No. 19, (1993).*

59. R. Clough and K. Gillen, "Oxidative degradation of polymers induced by ionizing radiation", *Sandia National Laboratories Report Nol SAND- 92-0236C, (1992).*

60. G. George, D. Hill, J. Odonnell, P. Pomery and F. Rasoul, "Study of the UV and VUV degradation of fluorinated ethylene propylene", p. 967 in *LDEF: 69 Months in Space: Second Post-Retrieval Symposium (* 1993).

61. Y. Qi, L. Limin and L. Changjiang, "Radiation-induced variations of electrical conduct ivity in polyaniline", *Chinese Phys. Lett.* **11**, 113 *(1994).*

62. M. Kassem, N. Madi, N. Rehire and W. Taleb, "Radiation and field-induced effects on the electrical and optical properties of polyvinylidene fluoride", *Materials Lett.* **19**, *87 (1994).*

63. S. Rabie, S. Moharram, A. Daghistani and M. Moharram, "Effect of gamma irradiation on electrical conductivity of metal chloride treated polyacrylamide", *Polymer Plastics Tech. and Eng.* **32**, *39-/ (1993).*

64. F. Soliman and H. Ashry, "Radiation effects on non-linear resistances", *Jour. Mat. Sri.: Materials* in *Electronics* **4**, *293 (1993).*

65. J. Davenas, V. Massardier and T. Van Hoang, "Relation between optical and electrical properties of ion implanted PPV", *Nuclear Instruments & Methods in Phys. Res.* **B83**, *189(1993).*

66. B. Bennamane, J. Decossas, C. Gagnadre and J. Vareille, "Optical waveguide fabrication by ion beams in the PADC polymer", *Nuclear instruments & Methods in Phys. Res.* **B62**, *103 (1991).*

67. M. Lewis, E. Lee, L. Mansur and W. Coghlan, "Homogeneous reaction rate model for hydrogen production from ion irradiated polymers", *Jour.* Nut. *Materials* **208**, *61 (1994).*

68. J. Kaschny, L. Amaral, D. Fink and M. Behar, "Radiation-induced diffusion of Xe in a pol ymer film", *Radiation Effects and Defects in Solids* **125**, *289 (1993).*

69. E. Laue, "Accelerated simulation of near earth orbit polymer degradation", p. 253 in *Proc. of NASA Goddard Space Flight Center Seventeenth Space Simulation Conference* (1993).

70. N. Suleman, "Characterization of radiation-induced damage in high performance polymers by electron paramagnetic resonance imaging spectroscopy", p. 185 in *Hampton Univ. Report of The NASA/American Society for Eng. Education Summer Faculty Fellowship Program (1992).*

71. B. Jang, "Space environmental effects on polymers and composites", p. 5 in *Auburn Univ. Report of The NASA/American Society for Eng. Education Summer Faculty Fellowship Program (1992).*

72. J. Connell, E. Siochi and C. Croall, "The effect of high energy electron radiation on poly(arylene ether) s", *High Performance Polymers* **5**, 1 (1993).

73. B. Yates and D. Shinozaki, "Radiation degradation of poly(methyl methacrylate) in the soft x-ray region", *Jour. Polymer Sci.* **31**, *1779 (1993).*

74. N. Genkina and E. Shitova, "Optical properties of p-xylylene films", *Jour. Appl. Spectroscopy* **32**, 185 (1990).

75. A. Suzuki, "Light-induced phase transition of poly(n-isoprpylacrylamide-co-chlorophyllin) gels", *Jour. intelligent Material Systems and Structures* **5**, 112 (1 *994).*

76. D. McHerron and G. Wilkes, "Apparent reversal of physical ageing in amorphous glassy polymers by electron beam irradiation", Polymer **34**, 915 (1993).

77. J. Laghari, "Complex electrical, thermal and radiation aging of dielectric films", *IEEE Trans. on Elec. insulation* **28**, *777 (1993).*

78. L. McCaughan, "Critical materials issues in the performance and manufacturability of $LiNbO_3$ integrated optics", p. 15 in *Integrated Optics and Optoelectronics, SPIE Critical Reviews of Optical Science and Technology* **CR45**, K. Wong and M. Razeghi, Editors (1 993).

79. F. Yu and S. Yin, "Specially doped (Ce:Fe:)$LiNbO_3$ based crystal holography", *SPIE Proc.* **2051**, 342 (1993).

80. R. Alferness, "Titanium-diffused lithium niobate waveguide devices", p. 145 in *Guided Wave Optoelectronics,* T. Tamir, Editor, Springer-Verlag (1 988).

81. S. Korotky and R. Alferness, "Ti:$LiNbO_3$ integrated optic technology: fundamentals, design considerations and capabilities", p. 169 in *integrated Optical Circuits and Components,* L. Hutcheson, Editor, Marcel Dekker (1987).

82. M. Minakata, S. Saito, M. Shibata and S. Miyazawa, "Precise determination of refractive index changes in Ti-diffused $LiNbO_3$ optical waveguides", *Jour. Appl. Phys.* **49**, *4677* (1 *978).*

83. J. Ctyroky, M. Hofman, J. Janta and J. Schrofel, "3-D analysis of $LiNbO_3$:Ti channel waveguides and directional couplers", *IEEE Jour. Quantum Electron.* **QE-20**, *400(1984).*

84. A. Rauber, "Chemistry and physics of $LiNbO_3$", p. 46 in *Current Topics in Materials Science 1,* E. Kaldis, cd., North Holland Publishing Co., Amsterdam (1978).

85. S. Kwiatkowski and A. Mickelson, "Characterization of lithium outdiffused slab waveguides in $LiNbO_3$ as a function of fabrication conditions", p. 151 in *LEOS* '93 *Conf. Proc. (1993).*

86. D. Bryan, R. Gerson and H. Tomaschke, "Increased optical damage resistance in lithium niobate", *Appl. Phys. Lett* **44**, *847* (1984).

87. J. Jackel, C. Rice and J. Veselka, "Proton exchange for high index waveguides in $LiNbO_3$", *Appl. Phys. Lett 41,607* (1 982).

88. R. Becker, "Comparison of guided wave interferometric modulators fabricated on $LiNbO_3$ via Ti indiffusion and proton exchange", *Appl. Phys. Lett* **43**, *131* (1983).

89. R. Davies, "Acousto-optic Bragg diffraction in proton-exchanged waveguides", *SPIE Proc.* **517**, 74 (1984),

90. R. De LaRue, F. Zhou, P. jiang, C. Ironside, T. Han, A. Ferguson and B. Henderson, "Active. guided wave optical devices in lithium niobate and lithium tantalate", *SPIE Proc.* 1794, 318 (1992).

91. A. Yi-Yan, "Index instabilities in proton-exchanged $LiNbO_3$ waveguides", *Appl. Phys. Lett* **43**, *633 (1983).*

92. E. Pun, "Proton exchange technology for integrated optics application", p. 15 in *Integrated Optics and Optoelectronics, SPIE Critical Reviews of Optical Science and Technology* **CR45**, K. Wong and M. Razeghi, Editors (1993).

93. T. Fujiwara, X. Cao, R. Srivastava and R. Ramaswamy, "Photorefractive effect in annealed proton exchanged $LiNbO_3$ waveguides", *Appl. Phys. Lett 61, 743 (1992).*

94. R. Alferness, "Waveguide electro-optic modulators", *IEEE Trans. Microwave Theory and Tech.* **MTT-30, 1221 (1982).**

95. R. Simons, *"Optical Control of Microwave Devices"*, Artech House, Boston (1990).

96. R. Alferness, R. Schmidt and E. Turner, "Characteristics of Ti-diffused lithium niobate optical directional couplers", *Appl. Optics* **18**, *4012 (1979).*

97. A. Billings, *Optics, Optoelectronics and Photonics, Engineering Principles and Applications,* Prentice Hall, New York, NY (1993).

98. G. Bogert, E. Murphy and R. Ku, "Low crosstalk 4x4 Ti:$LiNbO_3$ optical switch with permanently attached polarization maintaining **fiber array"**, *IEEE Jour. Lightwave Tech.* **LT-4**, 1542 (1986).

99. F. Auracher, D Schiketanz and K. Zeitler, "High speed $\Delta\beta$ - reversal directional coupler modulator with low insertion loss for 1.3 μm in $LiNbO_3$", *Jour. Optics Commun.* **5**, *7 (1984).*

100. S. Miller, "Some theory and applications of periodically coupled waves", *Bell System Tech. Jour.* **48**, 2189 (1969),

101. R. Alferness, "Efficient waveguide electro-optic TE-TM mode converter/wavelength filter", *Appl. Phys. Lett.* **36**, *513* (1980).

102. J. Veselka, "Low insertion loss channel waveguides in $LiNbO_3$ fabricated by proton exchange", *Elect. Lett.* **23**, 265 (1987).

103. W. Burns, T. Giallorenzi, R. Moeller and E. West, "Interferometric waveguide modulator with polarization-independent operation", *Appl. Phys. Lett.* **33**, *944 (1978).*

104. R. Alferness, **"Polarization-independent optical directional coupler switch** using weighted coupling", *Appl. Phys. Lett.* **35**, *748 (1979).*

105, J. Watson, M. Milbrodt and T. Rice, "A polarization-independent lx] 6 guided wave optical switch integrated on lithium niobate", *IEEE Jour. Lightwave Tech.* **LT-4**, *1717* (1986).

106. A. Neyer, "Integrated optical multichannel wavelength multiplexer for monomode systems", *Elect. Lett.* **20**, 744 (1984).

107. R. Alferness and L. Buhl, "Tunable electro-optic waveguide TE-TM converter/wavelength filter", *Appl. Phys. Lett. 40,861 (1982),*

108. R, Al ferness and J. Veselka, "Simultaneous modulation and wavelength multiplexing with a tunable Ti :$LiNbO_3$ directional coupler filter", *Elect. Lett.* **21**, 466(1985).

109. E. Lallier, J. Pocholle, M. Papuchon, M. DeMicheli, M. Ii, Q. He, D. Ostrowsky, C. Grezes-Besset and E. Pelletier, "Efficient Nd:MgO:$LiNbO_3$ waveguide laser", *Elect. Lett.* **26**, 927 (1990).

110. R. Brinkmann, W. Sohler and H. Suche, "Continuous wave Er diffused $LiNbO_3$ waveguide laser", Elect. *Lett.* **27**, 415 (1991).

111. Ch. Buchal and S. Mohr, "Ion implantation, diffusion and volubility of Nd and Er in $LiNbO_3$", *Jour. Materials Res.* **6**, *134 (1991).*

112. D. Gill, A. Judy, L. McCaughan and J. Wright, "Method for the local incorporation of Er into $LiNbO_3$ guided wave optic devices by Ti co-diffusion", *Appl. Phys. Lett.* **60**, *1067 (1992).*

113. E. Lallier, J. Pocholle, M. Papuchon, M. DeMicheli, Q. He, D. Ostrowsky, C. Grezes-Besset and E. Pelletier, **"Integrated** Nd:MgO:$LiNbO_3$ FM mode locked waveguide laser", *Elect. Lett.* **27**, *936(1991).*

114. V. Antonov, P. Arsenev, B. Baranov, N. Barinova, E. Kustov and I. Linde, "Radiation defects research in single crystals of lithium niobate", *Crystal Res. And Tech.* **9**, **1403 (1974).**

115. L. Karaseva, G. Bondarenko and V. Gromov, "Investigation of optical active centers of the irradiated lithium niobate", *Radiation Phys. & Chem.* **10**, *241 (1977).*

116. R. Schmidt, R. Cross and A. Glass, "Optically induced cross-talk in $LiNbO_3$ waveguide switches", *Jour. Appl. Phys.* **51**, 90 (1980).

117. J. Rosa, K. Polak and J. Kubatova, "ESR and optical studies of impurity centers in gamma and x-irradiated $LiNbO_3$", *Physics Status Solidi B* **B111**, *K85 (1 982).*

118. R. Pareja, R. Gonzalez and M. Pedrosa, "Study of thermo-chemically reduced **and electron irradiated** $LiNbO_3$ single crystals by positron annihilation and optical absorption measurements", *Physica Status Solidi A* **A84**, *179(1984).*

119. L.. Arizmendi, J. Cabrera and F. Agullo-Lopez, "Defects induced in pure and doped $LiNbO_3$", *Jour. Phys. C: Solid State Phys. 17,* 515 *(1984).*

120. E. Vartanyan, R. Ovsepyan, A. Pogosyam and A, Timofeev, "Influence of gamma irradiation on the photorefractive and photoelectric properties of lithium niobate crystals", *Sov. Phys. - Tech. Phys. 26,* 1464 (1984),

121. G. Abgaryan, A. Matviichuk and G. Kholodar, "Radiation-stimulated rotation of the axis of unipolar properties in lithium niobate crystals", *Sov. Phys. - Tech. Phys.* **30**, *1423 (1985).*

122, E. Hodgson and F. Agullo-Lopez, "Oxygen vacancy centers induced by electron irradiation in $LiNbO_3$", *Solid State Commun.* **64**, 965 (1987).

123. T. Volk, **M.** Ivanov, **M.** Meilman **and N.** Rubinina, **"interpretation of radiation** optical effects in lithium niobate", *Sov. Phys. - Solid State* **26**, *497 (1987).*

124. T. Volk, S. Shramchenko, M. Ivanov, M. Meilman, N. Rubinina and I. Shuvalov, "X-irradiation influence on some optical properties of lithium niobate crystals", *Ferroelectrics* **73**, *367* (1 *987).*

125. F. Rocske, D. Jander, G. Lancaster, M. Lowry, G. McWright, R. Peterson and W. Tindall, "Preliminary radiation hardness testing of $LiNbO_3$:Ti optical directional coupler modulators operatingat810 rim", *SPIE Proc.* **787**, *36(1987).*

126. E. Taylor, "Overview of Air Force radiation effects programs in fiber optics", *Inter. Jour. Of Optical Sensors* **2**, 201 *(1987).*

127. E. Drummond, "Resistance of $Ti:LiNbO_3$ devices to ionising radiation", *Elect. Lett. 2.3, 1214* (1 987).

128. E. Hodgson and F. Agullo-Lopez, "Displacement damage in $LiNbO_3$", Nut. *Instr. & Methods in Phys. Res., Section B* **B32**, *42 (1988).*

129. E. Taylor, V. Wilson, A. Sanchez, M. Coughenour and S. Chapman, "A comparison of integrated and fiber optic responses in the presence of nuclear fields", *SPIE Proc.* **898**, *42 (1988).*

130. E. Taylor, "Geminate recombination behavior of a x-ray irradiated single mode $LiNbO_3$:Ti waveguide operating at 1300 nm", *Jour. Optical Commun.* **9**, *64 (1988).*

131. E. Taylor, "Integrated optic response to nuclear irradiations", *SPIE Proc.* **836**, *2 (1987).*

132. R. Volk and N. Rubinina, "X-ray and UV influence on the optical absorption spectra of the non-photorefractive lithium niobate", *Phys. Status Solidi A* **108**, *437 (1988).*

133. A. Kanofsky, C. Jack, W. Minford, J. Watson, W. Herman and W. Rosen, "Radiation effects on $LiNbO_3$ devices", *SPIE Proc.* **1174 263 (1989).**

134. B. Evans, "Radiation induced attenuation in integrated optic materials", *SPIE Proc.* **1177**, 280 (1989).

135. C. Jack and A. Kanofsky, "Radiation damage of titanium diffused lithium niobate Devices", *SPIE Proc.* **1177**, *274 (1989).*

136. B. Ped'ko, V. Rudyak and A. Shabalin, "Influence of metallic impurities and gamma radiation on the optical properties of lithium niobate single crystals", *Bull. Academy of Sci. Of USSR, Phys. Set.* **54**, *142 (1990,).*

137. E. Taylor, "Behaviour of coupled waveguide devices in adverse environments", *SPIE Proc.* **1314**, *155 (1990)*

138. E. Taylor, V. Wilson, A. Sanchez, S. DeWalt, S. Chapman, M. Vigil and R. Padden, "Nuclear-induced refractive index effects observed in typical guided wave devices", *SPIE Pmt.* **1177**, *287 (1 989).*

139. R. Padden, E. Taylor, A. Sanchez, J. Berry, S. Chapman, S. DeWalt and K. Wong, "$LiTaO_3$ and $LiNbO_3$:Ti responses to ionizing radiation", *SPIE Proc.* **1474**, 148 (1991).

140. E. Taylor, R. Padden, A. Sanchez, S. Chapman, J. Berry and S. DeWalt, "Radiation-induced crosstalk in guided wave devices", *SPIE Proc.* **1474**, 126 (1991).

141. E. Taylor, "Ionization-induced refractive index and polarization effects in $LiNbO_3$:Ti directional coupler waveguides", *IEEE Jour. Lightwave Tech.* **9**, *335 (1991).*

142. E. Taylor, A. Sanchez and S. DeWalt, "Radiation effects in photonic technology devices", p. 29 in *Conf. Proc., Second Biennial Dept. Of Defense Fiber Optics and Photonics Conf.* McLean, VA (1992),

143. K. McCammon, M. Lowry, C. West, C. McConaghy and C. Yuanhann, "High sensitivity external modulator data link for high energy particle detector diagnostics", *Annual Conf. On Electronics for Future Colliders,* Dept. Of Energy Report no. UCRL-JC-11125 (1 992).

144. F. Brioschi, A. Caridi, E. Cereda, G. Marcazzan and E. Zanzottera, "Radiation effects on laser crystals for space applications", Nut. *Instr. & Methods in Phys. Res., Section B,* **B66**, *357 (1992).*

145. T. Tsang and V. Radeka, "Progress in the optoelectronic analog signal transfer for high energy particle detectors", *Annual Conf. On Electronics for Future Colliders,* Dept. Of Energy Report no. BNL-47904 (1992).

146. E. Taylor, "On the measurement of radiation induced crosstalk in polarization preserving optical fibers and directional coupler waveguides", p. 391 1 n *Conf. Proc.: First European Conf. On Radiations and Their Effects on Devices and System (RADECS 91)(* 1992).

147. E. Taylor, "Radiation effects observed in selected guided wave devices", p. 299 in *Critical* **Reviews** *of Optical Science and Technology, SPIE Proc. CR-45,* K. Wong and M. Razeghi, editors (1993).

148. E. Taylor, "Radiation effects in guided wave devices", *SPIE Proc.* **1794**, 54 (1992).

149. A. Kanofsky and W. Minford, "Radiation effects on proton exchange waveguides", *SPIE Proc.* **1794**, 62 (1992).

150. H. Henschel, O. Kohn and H. Schmidt, "Radiation-induced transmission loss of integrated optic waveguide devices", *SPIE Proc. 1794, 79 (1992).*

151. D. Smith, K. Hugenberg, J. Flatley and H. Garrett, "Transient radiation effects in annealed proton exchange $LiNbO_3$ and $LiTaO_3$ waveguides", *SPIE Proc.* **1794**, *70 (1 993).*

152. W. Callen and T. Gaylord, "Holographic data storage crystals for the LDEF", p. 1403 in *Second Post-Retrieval Symp.*

Proc.: NASA Langley Res. Center; LDEF: 69 Months in Space: Part 4 (1993).

153. R. West and S. Dowling, "Radiation effects on a lithium tantalate optical waveguide structure", Elect. *Lett.* **29**, 97(I (1993).

154. E. Taylor, "Overview of photonic components for space applications: radiation and temperature responses", *SPIE Proc.* **1953**, *7 (1993).*

155. R. West and S. Dowling, "Effects in a lithium tantalate waveguide structure exposed to radiation from a flash x-ray source", p. 239 in *Second European Conf. On Radiation and Its Effects on Components and Systems (RADECS 93) (1993).*

156. P. Brannon, "Transient radiation-induced absorption at 1061 nm in $LiNbO_3$ and $MgO:LiNbO_3$", *IEEE Trans. Nut. Sci. 41, 642 (1994).*

157. A. Johan and P. Charre, "Pulsed x-ray induced attenuation measurements of single mode optical fibers and coupler materials", p. 251 in *Second European Conf. On Radiation and Its Effects on Components and Systems (RADECS 93) (1993).*

158. E. Taylor, "Dual use of photonic components in radiation environments", *SPIE Proc.* **2215**, 10 *(1994).*

159. P. Brannon, "Transient radiation-induced absorption in laser materials", *SPIE Proc.* **2119**, *142* (1994).

160. G. Harvey, G. Astfalk, A. Feldblum and B. Kassahun, "The photorefractive effect in Ti-diffused $LiNbO_3$ optical directional couplers at 1.3 mm", *IEEE Jour. Quantum Electron.* **QE-22**, *939 (1986).*

161. R. Schmidt, R. Cross and A. Glass, "Optically induced cross-talk in $LiNbO_3$ waveguide switches", *Jour. Appl. Phys.* **51**, *90 (1980).*

162. R. Becker and R. Williamson, "Photorefractive effects in $LiNbO_3$ channel waveguides: model and experimental verification", *Appl. Phys. Lett.* **47**, ***1024 (1985).***

163. R. De La Rue and J. Marsh, "Integration technologies for III-V semiconductor optoelectronics based on quantum well waveguides", p. 259 in *integrated Optics and Optoelectronics, SPIE Critical* ***Reviews*** *of Optical Science and Technology* **CR45**, K. Wong and M. Razeghi, Editors (1993).

164. N. Shaw and A. Carter, "Optoelectronic integrated circuits for microwave optical systems", p. 90 in *Microwave Journal,* October, 1993.

165. K. Shimomura and S. Arai, "Semiconductor waveguide optical switches and modulators", *Fiber and Integrated Optics* **13**, *65* (1992).

166, T. Drabik, "Devices for optoelectronic integrated systems", *SPIE Proc.* **1562**, *194* (1991).

167. K. Ebeling, *Integrated Optoelectronics,* Springer-Verlag, New York, NY (1993),

168. F. Leonberger and J. Donnelly, "Semiconductor integrated optic devices", p. 317 in *Guided Wave Optoelectronics,* T. **Tamir, Editor, Springer-Verlag (1988).**

169. C. Chang and F. Kai, ***GaAs High Speed Devices,*** John Wiley & Sons, New York, NY (1994).

170. K. Kawano, "High speed Ti :$LiNbO_3$ and semiconductor optical modulators", *IEICE Trans.* ***Electron. 1176-C, 183 (1993).***

171. A. Lentine, "Self f-electro-optic effect devices for optical information processing", p. 45 in *Optical Computing Hardware,* J. Jahns and S. Lee, Edit., Academic Press, Boston, MA (1994).

172. A. Selvarajan, K. Shenai and V. Tripathi, *Optoelectronics: Technologies and Applications,* SPIE Press (1993).

173. E. Li and B. Weiss, "Bandgap engineering and quantum wells in optoelectronic devices", p. 63 in *Electronics and Commun. Eng.* J. April, 1991.

174. Y. Suematsu and A. Adams, *Handbook of Semiconductor Liners and Photonic Integrated Circuits,* Chapman & Hall, London, UK (1994).

175. P. Bhattacharya, *Semiconductor Optoelectronic Devices,* Prentice-Hall, New York, NY (1 994).

176. T. Wood, C. Burrus, D. Miller, D. Chemla, T. Damen, A. Gossard and W. Wiegmann, "131 ps Optical modulation in semiconductor multiple quantum wells (MQWs)", *IEEE J. Quantum Electron.* **QE-21**, *117* (1 *985).*

177. R. Walker, "Broadband (6 GHz) GaAs/AlGaAs electro-optic modulator with low drive power", *Appl. Phys. Lett.* **54**, 1613 (1989).

178. J. Cites and P. Ashley, "High performance Mach-Zender modulators in multiple quantum well GaAs/AlGaAs", *J. Lightwave Tech.* **12**, 1167 (1994).

179. M. Kohtoku, S. Baba, S. Arai and Y. Suematsu, "Switching operation in a GaInAs/InP MQW integrated twin guide (ITG) optical switch", *IEEE Photo. Tech. Lett.* **3**, *225 (1991).*

180. R. Chen, D. Robinson and R. Shih, "Single mode optically activated phase modulator on GaAs/AlGaAs compound semiconductor channel waveguides", *SPIE Proc.* **1794**, 101 *(1992).*

181. C. Thirstrup, P. Robson, P. Kam Wa, M. Pate, C. Button and J. Roberts, "Optical nonlinearities in GaAs/AlGaAs multiple quantum well hetero-*nipi* waveguides", *IEEE J. Quantum Electron.* **QE-28**, *864 (1992).*

182. M. Johnson and T. McGill, "Carrier lifetimes in ion-damaged GaAs" *Appl. Phys. Lett.* **54**, *2424(1989).*

183. C. Barron, C. Mahon, B. Thibeault, G. Wang, J. Karin, L. Coldren and J. Bowers, "High speed III-V asymmetric Fabry-Perot modulators", p. 658 in *LEOS '93 Conf. Proc. (1993).*

184. T. Woodward, B. Tell, W. Knox, M. Asom and J. Stark, "Low responsivity GaAs/AlAs asymmetric Fabry-Perot modulators", *OSA Pmt. on Photonics in Switching 16, 99(1993).*

185, S. Vernon, "Monolithic high speed electro-optic modulator using delta doped multi-quantum wells and lateral electric field-induced absorption", *Defense Nuclear Agency Tech. Report DNA-TR-94-Ill* (1995).

186. D. Miller, "SEEDS and other MQW nonlinear optical devices", *Digital Optical Computing, SPIE Critical Reviews Series CR-35 (1990).*

187. M. Prise, "Optical computing using self-electro-optic devices", *Digital Optical Computing, SPIE Critical Reviews Series* **CR-35, 3 (1990).**

188. R. Morgan, "Improvements in self-electro-optic devices: toward system implemental ion", *SPIE Proc.* **1562**, *213 (1991).*

189. L. Chirovsky, "Massive connectivity and SEEDS", *SPIE Proc.* **1562**, *228 (1991).*

190. A. Lentine and D. Miller, "Evolution of the SEED technology: bistable logic gates to optoelectronic smart pixels", *IEEE J. of Quantum Electronics* **29**, *655 (1993).*

191. G. Boyd, A. Fox, D. Miller, L. Chirovsky, L. D'Asaro, J. Kuo, R. Kopf and A. 1 entine, "33 ps optical switching of symmetric self-electro-optic effect devices" *Appl. Phys. Lett.* **57**, 1843 *(1990)).*

192. L. Chirovsky, M. Focht, J. Freund, G. Guth, R. Leibenguth, G. Przybylek, L. Smith, L. D'Asaro, A. Lentine, R. Novotny and D. Buchholz, p. 56 in *Proc. of the OSA Topical Meeting on Photonic Switching (199* 1).

193. A. Lentine, S. Hinterlong, T. Cloonan, F. McCormick, D. Miller, L. Chirovsky, L. D'Asaro, R. Kopf and J. Kuo, "Quantum well optical tri-state devices" *Appl. Optics* **29**, 1157 (1990).

194. T. Weatherford, L. Tran, W. Stapor, E. Petersen, J. Langworthy, D. McMorrow, W. Abdel-Kader and P. McNulty, "Proton and heavy ion upsets in GaAs MESFET devices", *IEEE Trans. Nut. Sci.* **38**, *1450(1991).*

195. D. McMorrow, T. Weatherford, A. Knudson, L. Tran, J. Melinger and A. Campbell, "Single event dynamics of high performance HBTs and GaAs MESFETs", *IEEE Trans. Nut. Sci.* **40**, *1858 (1993).*

196. T. Weatherford, D. McMorrow, W. Curtice, A. Knudson and A. Campbell, "Single event induced charge transport modeling of GaAs MESFETs", *IEEE Trans. Nut. Sci.* **40**, *1867 (1993).*

197. N. Islam, J. Howard, O, Fageeha and R. Block, "A model for the bipolar-like response of GaAs MESFETs to a high dose rate environment", *IEEE Trans. Nut. Sci.* **41**, *2494 (1994).*

198. G. Shaw, M. Xapsos, B. Weaver and G. Summers, "Low temperature irradiation of GaAs MESFETS", *IEEE Trans. Nut. Sci. 40, 1300 (J993).*

199. G. Messenger and M. Ash, *The Effects of Radiation on Electronic Systems*, Van Nostrand Reinhold, New York, NY (1992).

200. W. Anderson, J. Gerdes and J. Roussos, "Temperature dependent GaAs MMIC radiation effects", *IEEE Trans. Nut. Sci. 40, 1735 (1993).*

201. E. Dupont-Nivet and M. Pasquali, "Neutron effects on HEMT devices", p. 189 in *First European Conf. On Radiation and Its Effects on Components and Systems (RADECS 91) (1992).*

202. B. Hughlock, A. Johnston, T. Williams and J. Harrang, "A Comparison of charge collection effects between GaAs MESFETS and III-V HFETs", *IEEE Trans. Nut. Sci.* **39**, 1642 (1992).

203. S. Saito, "Reliability of low noise HEMTs under gamma ray irradiation" *IEICE Trans. Elect. 1376-C,* 1379 (1993).

204. S. Witmer, S. Mittleman, D. Lehy, F. Ren, T. Fullowan, R. Kopf, C. Abernathy, S. Pearton, D. Humphrey, R. Montgomery, P. Smith, J. Kreskovsky and H. Grubin, "The effects of ionizing radiation on GaAs/AlGaAs and InGaAs/AlInAs heterojunction bipolar transistors", *Mat. Sci. & Eng. B* **B20**, 280 (1993).

205. M. Kearney, N. Couch, M. Edwards and I. Dale, "Neutron radiation effects in GaAs planar doped barrier diodes", *IEEE Trans. Nut. Sci.* **40**, *102(1993).*

206. F. Soliman and S. Kamh, "Radiation damage in negative differential resistance devices", *J. Mat. Sci.: Materials in Electronics* **5**, *30 (J994).*

207. R. Walters, S. Messenger, G. Summers, E. Burke and C. Keavney, "Space radiation effects in InP solar cells", *IEEE Trans. Nut. Sci.* **38**, *1153* **(1991).**

208. G. Summers, E. Burke, P. Shapiro, S. Messenger and R. Walters, "Damage con elations in semiconductors exposed to gamma, electron and proton radiations", *IEEE Trans. Nut. Sci.* **40**, 1372 **(1993).**

209. R. Jain, I. Weinberg and D. Flood, "Diffusion length variation and proton damage coefficients for InP/$In_xGa_{1-x}As$/GaAs solar cells", *J. Appl. Phys. 74, 2948 (1993).*

210. F. Auret, S. Goodman, G. Myburg and W. Meyer, "Electrical characterization of defects introduced in *n*-GaAs by alpha and beta irradiation from radionuclides", *Appl. Phys. A* **A56**, *547 (1 993).*

211. S. Goodman, F. Auret, M. hayes, G. Myburg and W. Meyer, "Electrical defect characterization of n-type GaAs irradiated

with alpha particles using a Van de Graff accelerator and an Am-241 radionuclide source" *Phys. Stat. Solidi A* **140**, 381 (1993).

2]2. A. Jorio, M. Parenteau, M. Aubin, C. Carlone, S. Khanna and J. Gerdes Jr., "A mobility study of the radiation induced order effect in GaAs", *IEEE Trans. Nut. Sci.* **41**, *1937 (1994).*

213. W. Wesch, E. Wilk and K. Hehl, "Radiation damage and near edge optical properties of nitrogen implanted GaAs", *Phys. Stat. Solidi A* **70** *243 (1982).*

214, E. Wendler, W. Wesch and G. Gotz, "Radiation damage and optical properties of Ar+ implanted GaP", *J. Appl. Phys.* **70**, *144* **(1991).**

215. C. Carlone, **M.** Parenteau, **C.** Actik, **S. Khanna, N.** Rowell and J. Gerdes Jr., "Radiation effects on heavily doped *n*-GaAs", p. 183 in *First European Conf. On Radiation and Its Effects on Components and Systems (RADECS 91) (1992).*

216. B. Evans, H. Hager and B. Hughlock, "5.5 MeV proton irradiation of' a strained quantum well laser diode and a multiple quantum well broad band LED", *IEEE Trans. Nuc. Sci.* **40**, 1645 (1993).

217. G. Shaw, R. Walters, S. Messenger and G. Summers, "Time dependence of radiation induced generation currents in irradiated InGaAs photodiodes", *J. Appl. Phys.* **74**, 1629 (1993).

218. J. Camparo, S. Delcamp, and R. Frueholz, "AlGaAs diode laser blue shift resulting from fast neutron irradiation", The Aerospace Corp. Report No. TR-0091 (6925- 13)-2, Nov., 1992.

219. S. Hava and N. Kopeika, "Space as an adverse environment: vacuum surface gamma ray irradiation effects on LEDs and photodiodes", *SPIE Proc.* **721**, 2 (1 987).

220. H. Lischka, H. Henschel, W. Lennartz and H. Schmidt, "Radiation sensitivity of light emitting diodes (LEDs), laser diodes (LDs) **and photodiodes (PDs)" p. 404 in** *First European Conf. On Radiation and Its Effects on Components and Systems (RADECS 91) (1992).*

221. H. Lischka, H. Henschel, O. Kohn, W. Lerrrrartz and H. Schmidt, "Radiation effects in light emitting diodes, laser diodes, photodiodes and optocouplers", p. 226 in *Second European Conf. On Radiation and Its Effects on Components and Systems (RADECS 93)(1 994).*

222. E. Friebele, P. Marshall, G. Summers, Y. Chen, A. Campbell and J. Langworthy, "Fiber optic data bus radiation effects study", Naval Research Laboratory Report No. NRL/MR/46 13-92-6982, Sept., 1992.

223. P. Marshall and C. Dale, "Space radiation effects on optoelectronic materials and components for a 1300 nm fiber optic data bus", *IEEE Trans.* Nut. *Sci.* **39**, 1982 (1992).

224. P. Marshall, C. Dale, E. Friebele and K. LaBe], "Survivable fiber based data links for satellite radiation environments", p. in *SPIE Critical Review Series* **CRSO (1993).**

225. A. Holmes-Siedle and L. Adams, *Handbook of Radiation Effects*, Oxford University Press, Oxford, UK (1993).

226. C. Barnes, T. Zipperian and L. Dawson, "Neutron-induced trapping levels in aluminum gallium arsenide", *J. Elec. Mat.* **14**, *95 (1985).*

227. R. Coates and E. Mitchell, "A model for the damage produced by fast neutrons in gallium arsenide", p. 96 in *Proc. of the International Conf. on* Radiation *Damage and Defects in Semiconductors,* Reading, UK, July, 1972, The Institute of Physics, London, UK (1973).

228. C. Barnes, "The effects of neutron irradiation on the high temperature operation of injection laser diodes", *SPIE Proc.* **506**, *218 (1984).*

229. C. Barnes and J. Wiczer, "Radiation effects in optoelectronic devices", *Sandia National Laboratories Report No. SAND84-0771 (1984).*

230. C. Barnes, "Radiation effects on light sources and detectors", *SPIE Proc.* 541, *138 (1985),*

231, C. Barnes, "Radiation hardened optoelectronic components: sources", *SPIE Proc.* 616, 248 (1986).

232. R. Carson and W. Chow, "Neutron effects in high power GaAs laser diodes", *IEEE Trans. Nut. Sci.* 36, 2076(1989).

233. K. LaBel, M. Flanegan, P. Marshall and C. Dale, "Spaceflight experiences and lessons learned with NASA's first fiber optic data bus", p. 221 in *Second European Conf. On Radiation and Its Effects on Components and Systems (RADECS 93) (1994).*

234. S. Pappert, S. Lin, R. Orazi, M. McLandrich, P. Yu and S. Li, "Broadband electromagnetic environment monitoring using semiconductor electroabsorption modulators", *SPIE Proc.* 1476, *282 (1991).*

235. S. Pappert, M. Berry, S. Hart, R. Orazi and S. Li, "Remote multi-octave electromagnetic field measurements using analog fiber optic links", *Digest of IEEE Antennas and Propagation Society International Symposium* 2, *718 (1992).*

236. J. McAdoo, W. Bollen, W. Catoe and R. Kaul, "Broad band electromagnetic radiation damage in GaAs MESFETs", *Digest of IEEE MTT-S International Microwave Symposium* 2, *1067* (1992).

237. C. Yeh, *Applied Photonics*, Academic Press, New York, NY (1990).

238. J. Xu and R. Stroud, *Acousto-Optic Devices: Principles, Design, and Applications,* John Wiley & Sons, New York, NY (1992).

239. C. Tsai, "Guided wave magnetooptic and acoustooptic Bragg cells for RF signal processing", *SPIE Proc.* 1562, *55 (1991).*

240. C. Garvin and B. Sadler, "Surface acoustic wave acousto-optic devices for wide bandwidth signal processing and switching applications", *SPIE Proc.* 1562, *303 (1991).*

241. See also papers in *Applied Optics* 31, *3876-4041* (1992).

242. Y. Omachi, *J. Appl. Phys. 44, 3928 (1973).*

243. J. Feinberg, "Photorefractive nonlinear optics", *Physics Today* 41, *46 (1988).*

244. D. Pepper, J. Feinberg and N. Kukhtarev, "The photorefractive effect", *Sci. American,* p. 62 in October, 1990 issue,

245. J. Feinberg, "Self-pumped continuous wave conjugator using internal reflection", *Optics Lett.* 7, *486 (1982).*

246. R. Neurgaonkar, W. Cory, J. Oliver, E. Sharp, M. Miller, G. Wood, W. Clark, A. Mott, G. Salamo and B. Monson, "Photorefractive tungsten bronze materials and applications", *SPIE Pmt. JMJ,2(1989).*

247. M. Karim, *Electro-Optical Devices and Systems,* PWS-Kent, Boston, MA (1992).

248. S. Esener, "Silicon based smart spatial light modulators: technology and applications to parallel computers" in *Digital Optical Computing,* R. Athale, Edit., *SPIE Critical Reviews of Optical Science and* Technology CR35, 100 (1990).

249. T. Hall, "Optical information processing", p. 461 in *Principles of Modern Optical Systems,* I. Andonovic and D. Uttamchandani, Edit., Artech House, Norwood, MA (1989).

250. H. Arsenault and Y, Sheng, *An Introduction to Optics in Computers,* SPIE Press, Vol. TT8, Bellingham, WA (1992),

251. S. Desmond and A. Walker, "Technologies for free space optical systems demonstrators", *SPIE Proc.* 1807, *210* (1992).

252. Q. Wang Song, C. Zhang, R. Blumer, R. Gross, Z. Chen and R, Birge, "Chemically enhanced bacteriorhodopsin thin film spatial light modulator", *SPIE Proc.* **2051**, *77 (1993).*

253. S. Perlmutter, D. Doroski, B. Landreth, A. Gabor, P. Barbier and G. Moddel, "Tradeoffs in the design and operation of optically addressed spatial light modulators", *SPIE Proc.* **1562**, *74 (1991),*

254. I. Underwood, D. Vass R. Sillitto, G. Bradford, M. Birch, W. Crossland and A. Sparks, "A high performance spatial light modulator", ***SPIE Pmt. 1562, 107*** *(1991).*

255. R. Hillman, Jr., G. Melnik, T. Tsakiris, F. Leard, R. Jurgilewicz and C. Warde, "Electron beam addressed lithium niobate spatial light modulator", *SPIE Proc.* **1562**, 136 *(1991).*

256. W. Ross and D. Lambeth, "Advanced magneto-optical spatial light modulator device development", *SPIE Proc.* **1562**, *93* (1991).

257. J. Maserjian and A. Larsson, "Low power optically addressed spatial light modulators (O-SLMs) using MBE-grown III-V structures", *SPIE Proc.* **1562**, 85 (1991).

258. Y. Suzuki, "Spatial light modulators and applications", *SPIE Proc.* **2321**, *665* (1993).

259. K. Johnson, D. McKnight and I. Underwood, "Smart spatial light modulators using liquid crystals on silicon" *IEEE J. Quantum Elect.* **29**, ***699 (1993).***

260. A. Fisher, "A review of spatial light modulators", *OSA Meeting on Optical* **Computing,** Lake Tahoe, CA, paper Tu Cl (1985).

261. NTT, "High speed image processor works in optical domain", p. 56 in *Laser Focus World,* June, 1990.

262. N. Berg and J. Speulstra, "The operation of acoustic surface wave delay lines in a nuclear environment", *Trans. Nucl. Sci. NS-20, 137 (1973).*

263. N. Berg and J. Udelson, "Nuclear radiation effects on surface wave devices", *Trans. Nucl. Sci.* **NS-21**, *141 (1974).*

264. N. Berg and J. Udelson, "The effects of pulsed ionizing radiation on the operation of surface acoustic wave amplifiers and convolves", ***Trans. Nucl. Sci. NS-22, 2503 (1974).***

265. J. Hines, C. Dale and W, Stapor, "Ionizing space radiation effects on surface acoustic wave resonators", *SPIE Proc.* **1784**, 206 (1992).

266. E. Taylor, A. Sanchez, S. DeWalt, R. Padden, S. Chapman, T. Monarski, D. Craig and D. Page, "Radiation-induced effects in acousto-optic devices", *SPIE Proc. ~,217* (1992).

267. E. Taylor, A. Sanchez, S. DeWalt, D. Craig, M. Kelly, S. Chapman and M. Mitcham, "Radiation effects observed in a spatial light modulator", p. 17 in *Conf. Proc., DoD Fiber Optics* '94, McLean, VA (1994).

268. G. Nosov and E. Generalova, "Effect of electron irradiation on the electro-optical properties of nematic dispersions in a polymer matrix", Sov. *Tech. Phys. Lett.* **18**, *78 (1992).*

269. J. Wiczer, C. Barnes, T. Fischer, L. Dawson and T. Zipperian, "AlGaAs/GaAs radiation hardened photodiodes", *SPIE Proc.* **506**, *224 (1984).*

270. J. Wiczer and C. Barnes, "Optoelectronic data link designed for applications in a radiation environment", *IEEE Trans. Nut. Sci.* **NS-32**, *4046 (1985).*